Derivation of Parameters and Calibration of Modified Cam Clay Constitutive Soil Model for Airfield Matting

Thesis

Submitted to

The School of Engineering of the

UNIVERSITY OF DAYTON

In Partial Fulfillment of the Requirements for

The Degree

Master of Science in Civil Engineering

by

Bradley M. Doudican

UNIVERSITY OF DAYTON

Dayton, Ohio

December, 2006

Derivation of Parameters and Calibration of Modified Cam Clay Constitutive Soil Model for Airfield Matting

By Brad Doudican

APPROVED BY:

ABSTRACT

Derivation of Parameters and Calibration of Modified Cam Clay Constitutive Soil Model for Airfield Matting

Doudican, Bradley M
University of Dayton

Advisor: Dr. M. Zoghi

The United States Armed Services seeks to develop next-generation airfield matting, made of fiber reinforced polymer (FRP) composite materials to reduce the panel weight and improve upon installation difficulties of the current AM-2 aluminum matting system. Finite element analyses of prototypical systems are being developed to evaluate the alternatives. In accordance with the directives of the Army Corp of Engineers, this study seeks to provide an effective and economical constitutive soil model of Vicksburg Buckshot Clay at a California Bearing Ratio (CBR) of 6 for use in modeling the matting subgrade. Based on a thorough literature review and the investigation of existing constitutive soil models, an extended version of the Modified Cam Clay model was selected as the most appropriate soil model for this study. A series of laboratory tests consisting of soil classification, one-dimensional consolidation, California Bearing Ratio, and consolidated-undrained triaxial testing were performed to correlate the test results from this study with existing Buckshot clay material property data and

to append to the existing laboratory database as required to derive input parameters for the Modified Cam Clay model. Input values for the model parameters were derived from the combined data. These parameters were refined by calibration in a first iteration to mirror the ASTM Standard CBR 6 curve in a finite element model of the laboratory CBR testing apparatus. Field testing of the prototype airfield matting was performed by others and pressure cell measurements were obtained. A second iteration of calibration was undertaken using a finite element model of the field arrangement of matting and subgrade to refine the first-iteration model parameters. A final set of Modified Cam Clay constitutive soil model parameters was developed for use in current and future research.

ACKNOWLEDGEMENTS

This work has been completed in remembrance of my grandfather and fellow U.D. engineering alum Charles Doudican (Class of 1932). He was an engineer and Commanding Officer in World War II on the islands in the Pacific where the original airfield matting systems were first employed. It has been an honor as his grandson to have a role in the research and development of the next generation of airfield matting systems.

First and foremost, I want to thank my beautiful wife for her patience and serving heart through the completion of my graduate degree. I could not have completed this work without her support.

I'd like to thank Dr. Manoochehr Zoghi for his mentorship, encouragement, patience, and friendship through the last seven years of undergraduate and graduate schooling. He has invested countless hours in me personally, and his role has been significant in my development as a young engineer and as a person.

A special thanks to TesTech, Inc. and especially Mrs. Sheila Sennet for her help with components of the laboratory testing. In addition to providing highest-caliber

materials testing, Mrs. Sennett provided a wealth of input regarding testing procedures and far exceeded expectations on scope of deliverables.

Many thanks to Dean Foster for overseeing the project and for facilitating the financial support of Wright Patterson Air Force Base. Thanks to Dr. Geoff Frank and Dr. Robert Brockman of UDRI for the support, guidance, and lab space throughout the project. And thanks to the engineering staff at the Waterways Experiment Station in Vicksburg, Mississippi for the data and project assistance.

And as any good son would do, I'd like to say Thanks Mom and Dad. I owe it all to you.

TABLE OF CONTENTS

LIST OF FIGURES

LIST OF TABLES

CHAPTER 1 – INTRODUCTION

1.1 Problem Statement

1.1.1 Project Background

The United States Armed Services is charged with the task of providing a quick and sustained response to events across the globe. The front-line response teams from all branches of the U.S. Armed Services rely heavily on a complex support infrastructure to maintain and supplement equipment and personnel during activities in any theater. Often the Armed Services are required to respond in geographies that do not immediately provide the required infrastructure for proper support. Accordingly, the Armed Services often must be prepared to airlift all required support to the theater of operation. The airfields in these locations, as demonstrated repeatedly by history, are often ill-suited in their existing conditions to accommodate the rapid change in usage. The speed at which an Armed Services' response can be mobilized is often a function of the condition and size of the receiving theater airfield.

According to Foster and Anderson (2003), a major consideration in the evaluation of an airfield's capacity is the space available for aircraft parking,

referred to as Maximum on Ground, or MOG. As an example, over 200,000 square feet of parking apron are required for a squadron of fighter aircraft (Foster and Anderson, 2003). Typically the soil subgrade at these remote airfields is incapable of adequately supporting the wheel loads from aircraft without pavement or matting. Accordingly, portable airfield matting technologies have been developed by various branches of the Armed Services to bridge the weak subgrade and allow rapid expansion of an airfield.

The first portable airfield matting systems were developed during World War II for use in the Pacific Theater "island-hopping," allowing the Armed Services to rapidly establish air power at subsequent islands with the use of aircraft carriers (Naval Air Engineering Station – Lakehurst, 2006). Advances in technology produced heavier aircraft with greater wheel loads. The original matting technology was improved upon by the U.S. Navy in the creation of the AM-2 aluminum Airfield Matting System during the Vietnam War in 1961. According to the Naval Air Engineering Station – Lakehurst (2006), "over 10 million square feet of AM2 mat was used by both the Air Force and the Marine Corps throughout Vietnam" for use in both aircraft and helicopter airfields. Recently, the AM-2 Matting System has been employed abroad in Operation Desert Storm in Iraq, Operation Restore Hope in Somolia, Operation Enduring Freedom in Afghanistan, and Operation Iraqi Freedom in Iraq (Naval Air Engineering Station – Lakehurst, 2006).

The AM-2 Matting System is composed of 1.5-inch thick aluminum panels weighing over six pounds per square foot that are connected into the required configuration using a series of key locks, connector bars, locking bars, and other hardware as shown in Figure 1 Foster and Anderson (2003). Assembly of the system typically requires a 16-person crew. To provide enough taxiway and parking space to support a fighter squadron, 480 pallets of matting with a volume of 39,066 cubic feet and a weight of 1,274,316 pounds are required. This system requires 48 C-130 transport aircraft and a crew working 12 hours per day approximately five days to install, excluding additional subgrade treatments.

The AM-2 Matting System has been successfully implemented over the last 40 years, but drawbacks exist. Fisher, Hartzer, and Pratt (2005, 10) reveal that the AM-2 is "heavy, cumbersome, slow to install, difficult to repair, and has very poor air-transportability characteristics." Additionally, Foster and Anderson (2003, 18) found the joints between panels to be "complicated, requiring many additional parts, and ... not allow[ing] for individual panel removal for repair or placement. Its joint also acts as a hinge, flexing in- and out-of-plane, and do not transfer load across panels." In an effort to improve upon the existing system and employ modern technologies, the Air Force Headquarters Air Combat Command Installations and Mission Support Readiness Division has sponsored research to develop a replacement (Fisher, Hartzer, and Pratt 2005, 10). Preliminary studies by a joint-services effort of the Army Engineer Research & Development Center, the Naval Air Engineering Station – Lakehurst, and the Air Force Research

Laboratory have concluded that a composite materials alternative will be most advantageous (Fisher, Hartzer, and Pratt 2005, 10). More rigid joint connections have been proposed to limit panel edge rotation and improve transfer of shear forces at the matting edges (Foster and Anderson 2003, 20).

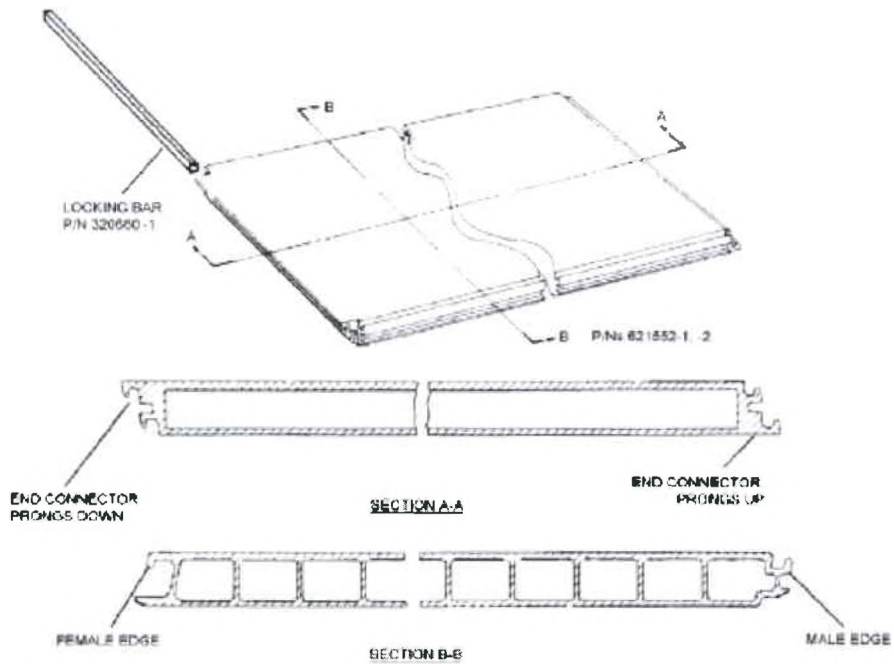

Figure 1 - Original AM2 Aluminum Airfield Matting (Source: Naval Air Engineering 2003)

Currently two private contractors are working with the Air Force Research Laboratory to develop and fabricate test specimens of the AM-2 replacement composite matting (Foster and Anderson 2003, 19).

The Structural Materials Branch of the Air Force Research Laboratory's Materials and Manufacturing Directorate (AFRL/MLBC) has contracted with the University

of Dayton Research Institute (UDRI) to employ the finite element method to study concept alternatives and systems designs to replace the current AM-2 Matting System. The present study considers the panel loading to be modeled by the equivalent pressure of the main landing gear of an F-15 fighter jet acting through the mat supported by a low strength subgrade. Future evaluations will consider loads representing a C-17 aircraft over various subgrades (Foster and Anderson 2003, 21). This pressure induced by an F-15 wheel is equivalent to an applied pressure of 350 pounds per square inch (psi) over a 100.9 square inch tire footprint (Johnson and Frank 2006, 8) as shown in Figure 2.

One goal of the aforementioned study was to investigate the various proposed alternatives via finite element analysis. The finite element analysis was intended to model the transfer of the wheel load through the panels and into the subgrade below. Several configurations of panels and panel joints were modeled. An example of a typical finite element model is shown in Figure 3.

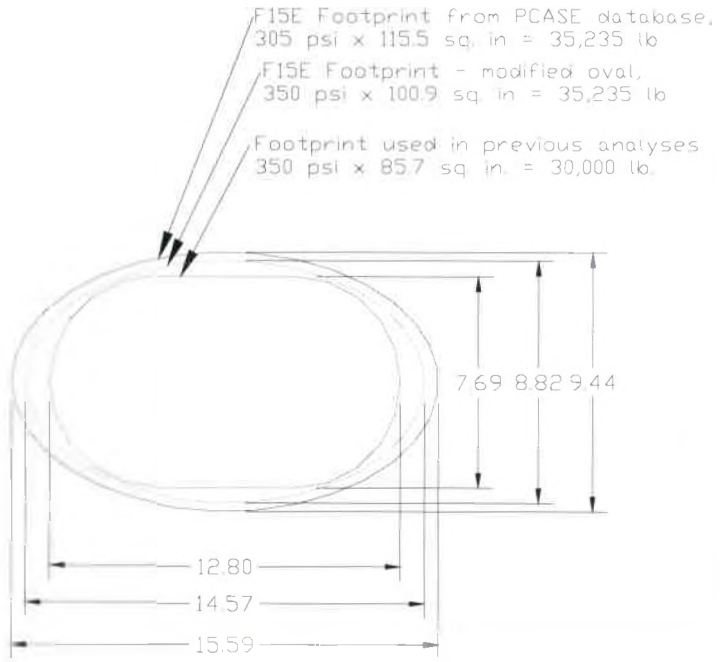

Figure 2 - F-15 Main Gear Footprint Alternatives (Source: Johnson and Frank 2006, 8)

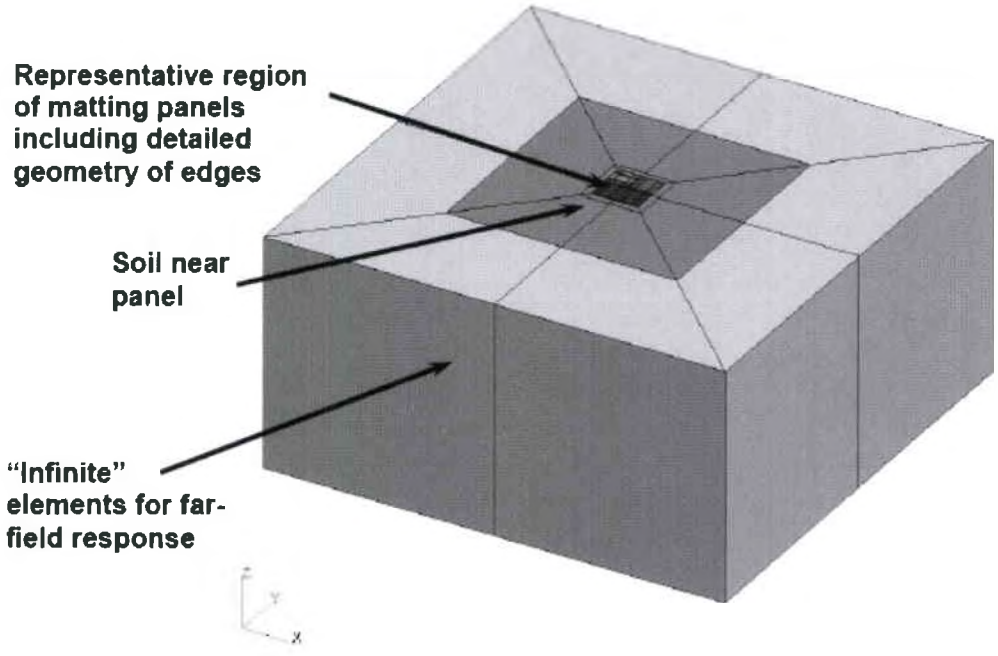

Figure 3 - Isometric Representation of a Typical Finite Element Loading Model (Source: Whitney and Frank 2005, 4)

The Air Force design directive for the subgrade soil was to represent repeated loading on a soil with a California Bearing Ratio (CBR) of 6. The Vicksburg "Buckshot" clay, a high-plasticity moisture-sensitive clay, was identified as the soil type to be utilized in this study for both finite element analysis as well as field testing. Earlier finite element models by Whitney and Frank (2005, 5-6) employed simplified empirical correlations between the CBR and elastic resilient modulus (*E*) to characterize the soil. They used two correlations, vis-à-vis, one by Heukelom and Foster (1960) who proposed:

$$E = 1500 \times CBR \qquad \text{(Eq. 1)}$$

and a second by the American Association of State Highway and Transportation Officials (AASHTO 1993):

$$E = 2555 \times CBR^{0.64} \qquad \text{(Eq. 2)}$$

These correlations estimated the resilient moduli varying between 9,000 and 8,043 psi corresponding to a CBR of 6 in accordance with the Heukelom and Foster (1960) relation and the AASHTO relation (1993), respectively. Initial finite element analysis of the structural panels suggested that the soils would experience strains on the order of one to eight percent. Johnson and Frank (2006, 9) extracted the secant moduli at each of these strains from the standard CBR 100 plot and scaled the values to a CBR 6 soil to establish a spectrum of

anticipated soil secant moduli. The values varied from 4,500 psi at one percent strain to 1,500 psi at eight percent strain. In the Whitney and Frank (2005) report, the soils were modeled as linear elastic isotropic solids with E = 1,500 psi and Poisson's ratio of 0.33. This is a conservative approach with the resilient modulus lower than that predicted by the literature correlations and at the low end of the interpolated range, forcing the matting panels to sustain higher bending stresses under various loading scenarios. Noting these limitations, a more accurate soil model was desired to aid in the appropriate comparison of structural panel alternatives.

1.1.2 Objectives

The primary objective of this study is to evaluate the soil material properties of Buckshot clay in order to develop pertinent input parameters for an accurate and economical constitutive soil model. This soil model will supplement the isotropic linear elastic correlation employed in previous finite element analysis of the alternative structural matting systems to improve the accuracy of the findings. More specifically, a model that represents a non-linear elastic-plastic hardening response typical of wet, normally consolidated, soils is desired. Additionally, economic consideration must be maintained in evaluating alternatives. While it may be desirable to create a new finite element constitutive soil model compatible with the finite element software specifically to simulate the response of this specific soil type and moisture condition, the costs associated with

laboratory work, engineering time, and algorithm derivation would far exceed the value of the model obtained. The more appropriate solution is to adapt an existing compatible soil model to reflect the pertinent response characteristics of the soil and evaluate potential sources of error.

1.2 Overview of Constitutive Soil Modeling

The mathematical modeling of traditional construction materials such as concrete and steel are simplified by the fact that these material are typically isotropic and homogeneous, implying that the stress-strain response of each is predictable, replicable, and independent of direction of load application. Soils, on the other hand, are both anisotropic and heterogenous. Additional consideration must be given in establishing mathematical models for soils as opposed to other homogenous isotropic materials. Brinkgreve (2005, 71) describes seven aspects of real soil behavior that must be considered, paraphrased as follows:

- Influence of water on the behavior of soil. Two key hydraulic components of soil stress response are the effective stress and pore water pressure. Effective stress is determined by considering the buoyancy effect of the pore fluids in the soil. The mechanical response of soil to changing conditions is substantially controlled by the current effective stress state. For example, a saturated highly impermeable soil subjected to rapid loading will respond with increased pore pressures and a slow

consolidation response, while the same load applied to a saturated permeable specimen will result in little flux in pore pressure and a rapid consolidation response.

- Lack of consistency in soil stiffness. The stiffness of soil will vary depending upon the state condition of any of the following variables: stress level, stress path, strain level, time duration, density, water/permeability, over-consolidation state, and direction of load.
- Irreversible deformation. Most soils have a very limited elastic region, and will therefore exhibit mainly irreversible deformation (plastic deformation).
- Lack of consistency in soil strength. The shear strength response of a soil will vary as a function of loading speed, time duration, density, undrained behavior, over-consolidation state, and direction of load.
- Time-dependent responses. Depending on drainage conditions the pore pressure stress in low permeability soils can dissipate over time, resulting in changes in consolidation characteristics over time such as creep. Additionally, dissipation of tensile stresses within a soil mass may permit swelling.
- Compaction and dilatency. Loose soils under shear loading may compact, while dense soils under the same loading may expand. This is a result of the individual interactions between soil particles as they move against one another during shearing. Crushing of calcareous soils may occur as well.
- Memory of pre-consolidation stress. A soil that has previously been subjected to a higher stress than its current in-situ state is considered

over-consolidated. Under loading, cohesive soil will exhibit a stiffer response up to the previous maximum stress state. Beyond this state it will exhibit a softer response to load.

In theory, it might be possible to derive mathematical models of soils by modeling the interaction of each individual soil particle as governed by an algorithm of responses based upon the aforementioned seven conditions. However, given the random distribution of soil particle shapes and sizes and the mathematical complexity required of such a model, this type of model has had negligible impact on the development of current constitutive models (Prevost and Popescu 1996, 3).

To meet the needs of a simpler mathematical soil model, continuum constitutive models (hereafter "constitutive models") have been employed. A constitutive model considers the global response characteristics of a given volume of material in response to a change of state. In constitutive soil modeling, the response characteristics of a mass of soil particles is modeled, as opposed to the interaction of individual particles. Constitutive models typically consist of elastic and plastic stress-strain responses. Given the multitude of parameters that influence soil behavior, the individual mathematical models are typically tailored not only to a specific soil classification, but also to a given set of conditions. For example, a constitutive soil model for normally-consolidated saturated cohesive soils at strains of less than 20 percent (typical for settlement analyses) should not

be used to model the response of highly-overconsolidated partially-saturated soils at high strain (typical for some slope stability analyses).

1.3 Brief History of Constitutive Soil Models

Scientists and engineers have been developing relationships to model the stress-strain response of materials for many years. Even a simple log laid over a river to serve as a bridge was observed to have some capacity and deflection response to load. In regards to soil stress-strain response, Coulomb (1776) published the famous relationship between maximum shear stress, cohesion, and soil friction angle as a function of stress. This was expanded to describe failure in three-dimensional stress state as the Mohr-Coulomb criterion. A later combination of the linear elastic Hooke's law with the Mohr-Coulomb criterion, such as that presented by Smith and Griffith (1982), was established as a first order model of soil behavior.

Nonlinear soil behavior has been modeled using concepts such as nonlinear elasticity, hardening plasticity, critical state theory, and hypoplasticity. Due to complexity and computational limitations, finite element modeling had very little practical application through most of the twentieth century. It has only been within the last 20 years that user-friendly finite element software has been made widely available and proven cost-effective for use in consultative practice. (Brinkgreve 2005, 70)

Extensive research has been performed concerning various aspects of constitutive soil models. The geotechnical academic community has embraced the challenges of model development, and as software and computing power improve, more complex and accurate models will continue to evolve. As is often observed at the early stages of innovation, there is a lag between academia and professional practice. The July/August 2006 publication of *Geo-Strata*, the bi-monthly professional trade publication of the American Society of Civil Engineers Geo-Institute, devoted the entire content of the issue to geotechnical modeling. Krahn and Barbour (Geo-Strata, 2006) contribute an article entitled "The Purpose of Numerical Modeling" describing the status and benefits of geotechnical modeling in today's geotechnical practice. They write:

> "Numerical modeling is increasingly taking its rightful role in geotechnical practice due largely to the software tools and computing power that are now so readily available. However, proper use of these powerful numerical tools remains somewhat immature. Too often the expectation of what is to be achieved is unrealistic, and the purpose of the numerical modeling is unclear."

It is apparent that the professional geotechnical community is still evolving in the acceptance and development of broad-based application of finite element constitutive soil modeling.

1.4 Existing Applicable Constitutive Soil Models

While a large number of constitutive soil models have been researched and published in the literature, a relative minimal number are commonly applied in commercial software. In the interest of both examining the evolution of constitutive soil models and providing a comparison of the advantages and limitations of each, this study will briefly examine the following applicable models:

- Hooke's law
- Mohr-Coulomb
- Drucker-Prager
- Duncan-Chang
- Modified Cam Clay

1.4.1 Hooke's law

1.4.1.1 Model Description

Hooke's law was conceived to represent the linear stress-strain response of an isotropic elastic material as shown in Figure 4. When described in terms of general one-dimensional stress, it has two input parameters: Young's modulus, E, and Poisson's ratio, ν. Hooke's law can be manipulated to represent principal

stresses and strains, referring to the orthogonal axes x, y, and z (Wood 2004, 101), or to include anisotropy of stiffness (Brinkgreve, 75-76).

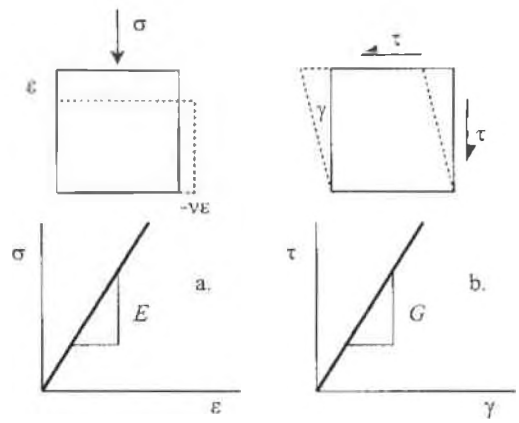

Figure 4 - Hooke's Law Linear Elastic Stress-Strain Response (Source: Wood 2004, 98)

1.4.1.2 Advantages and Limitations

Hooke's law is accurate in modeling the linear elastic response characteristics of a given material. However most soils require very minimal elastic response characteristics, as a majority of the behaviors being modeled are typically in the non-linear plastic range. While Hooke's law is generally considered too rudimentary for practical application, it is often included as the elastic component of other elastic-plastic constitutive soil models (Brinkgreve 2005, 76).

1.4.2 Mohr-Coulomb

1.4.2.1 Model Description

The Mohr-Coulomb model is an elastic-perfectly plastic model that combines Hooke's elastic stress-strain response with the generalized Coulomb failure criterion. Figure 5a and Figure 5b show the stress-strain response and associated effective stress path, respectively. The material response is elastic at stresses up to some critical value, at which point the material instantly translates into a perfectly plastic state, deforming continually without any change in stress. Figure 6 shows the two-dimensional yield surface in the p'-q plane, which is the triaxial stress plane defined by a vertical axis of distortional stress "q" and a horizontal axis of mean effective stress (or volumetric stress) "p'", where

$$q = \sigma_1 - \sigma_3 \qquad \text{(Eq. 3)}$$

$$p' = (\sigma_1 + \sigma_2 + \sigma_3)/3 \qquad \text{(Eq. 4)}$$

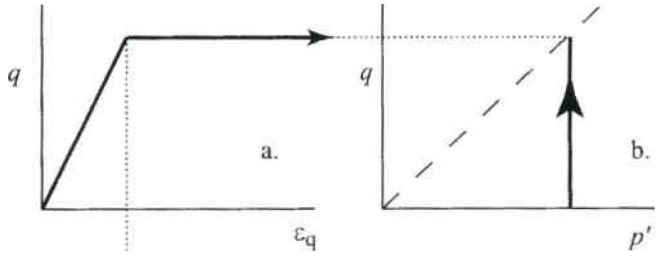

Figure 5 - Mohr-Coulomb a) Stress-Strain Response, b) Effective Stress Path (Source: Wood 2004, 127)

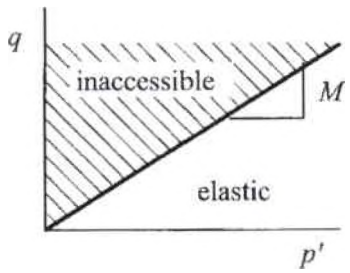

Figure 6 - Mohr-Coulomb Yield Surface (Source: Wood 2004, 124)

The Mohr-Coulomb model is comprised of five input parameters: Young's modulus, E, and Poisson's ratio, ν, for the elastic component; the friction angle, φ, and cohesion, c, for the Coulomb failure criterion; and the dilatency angle, Ψ. The dilatency angle is required because the Mohr-Coulomb model for soils makes use of a non-associated flow rule, as will be defined in Section 1.6.1. The yield surface for the Mohr-Coulomb model in the deviatoric plane is represented by a hexagon as shown in Figure 7. The deviatoric plane is defined as the plane in principal stress space that is orthogonal to the line defined by $\sigma_1 = \sigma_2 = \sigma_3$. (Brinkgreve 2005, 76-77)

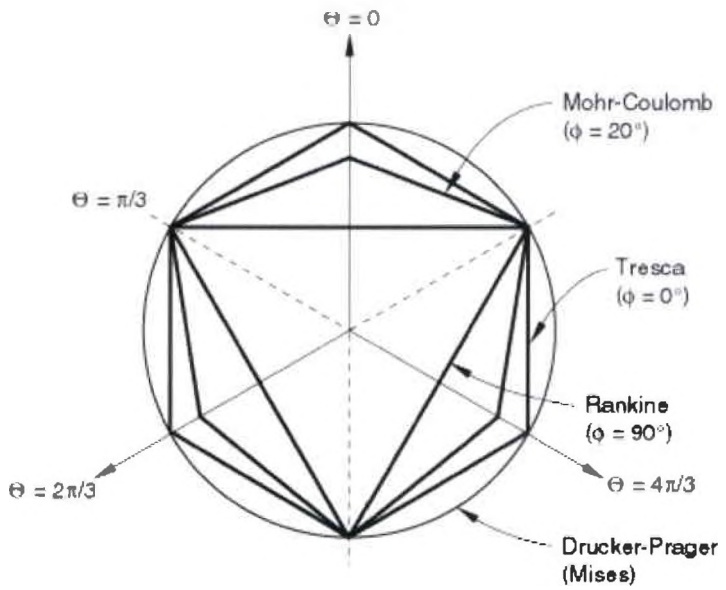

Figure 7 - Various Yield Surfaces in the Deviatoric Plane (Source: ABAQUS "Analysis Users Manual")

1.4.2.2 Advantages and Limitations

The Mohr-Coulomb model, along with other elastic-perfectly plastic models, is typically used to calculate the stress conditions at failure in geotechnical modeling. According to Brinkgreve (2005, 77), the hexagon shape of the yield surface in the deviatoric plane correlates well with the stress results of true-triaxial soils tests. However, given the simplicity of the elastic component as modeled by Hooke's law, there is little reliability in the deformation response prior to failure. Wood (2004, 129-133) notes that the linear stress-strain response in the elastic stress regions provide a poor correlation with the elastic hardening typically observed in laboratory testing. Brinkgreve (2005, 76) recommends that "the Mohr-Coulomb model could be used to get a first estimate of deformations…but an accuracy of more than 50 percent should not be expected."

While the Mohr-Coulomb model is applied quite frequently in practice due to its simplicity, the professional is cautioned to thoroughly understand the implicit shortcomings of the model under pre-failure stress conditions.

1.4.3 Drucker-Prager

1.4.3.1 Model Description

The Drucker-Prager model, published in 1952, was produced as a simplification of the Mohr-Coulomb model. The hexagonal yield surface in the deviatoric plane is replaced by a circle, producing a three-dimensional cone in principal stress space as shown in Figure 8. The same input parameters as the Mohr-Coulomb model are required. (Drucker-Prager, 1952)

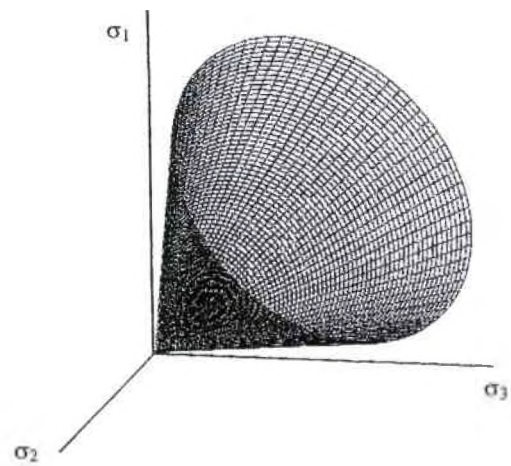

Figure 8 - Drucker-Prager Yield Surface in Principal Stress Space (Source: Brinkgreve 2005, 78)

1.4.3.2 Advantages and Limitations

The Drucker-Prager model is constrained by similar limitations as outlined for the Mohr-Coulomb model. For loading conditions that include only one stress path, the Drucker-Prager model can be well calibrated to the output of the Mohr-Coulomb model. However, if multiple stress paths are modeled it becomes impossible to select one set of input parameters that will produce the same output as the Mohr-Coulomb model (Brinkgreve 2005, 78). Failure behavior is subsequently impossible to reliably produce. While this model may be more simple to construct, it produces outputs with the same limitations as the Mohr-Coulomb model plus the additional limitation that only one stress path may be justifiably represented.

1.4.4 Duncan-Chang

1.4.4.1 Model Description

Duncan and Chang (1970, 1629-1653) published a soil response relationship that made multiple improvements upon the Mohr-Coulomb theory based upon observations of laboratory testing that had not previously been accounted for in constitutive models. The model utilizes a hyperbolic stress-strain response through both the elastic and plastic stress regions, and includes a stress-dependent stiffness parameter to better reflect the difference in a soil's observed

response under varying effective stress conditions. In addition, the model distinguishes between primary loading stiffness and unloading and reloading stiffness as a function of effective stress. The Duncan-Chang model is classified as an elastic model because no explicit differentiation is made between elastic and plastic behavior criterion. Rather, the model is represented by one continuous hyperbola as shown in Figure 9 (Brinkgreve 2005, 78-79).

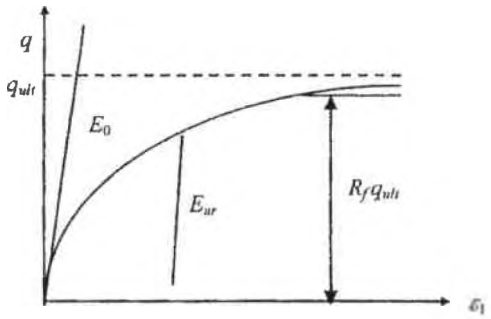

Figure 9 - Duncan-Chang Stress-Strain Response to CD Traxial Test (Source: Brinkgreve 2005, 79)

1.4.4.2 Advantages and Limitations

Because the initial "elastic" regions of the model are curved instead of linear, the Duncan-Chang model provides a better correlation to real drained soil stiffness behavior than the Mohr-Coulomb model, especially in the pre-failure stress-strain regions. The hyperbolic curve approaches an asymptote, which defines the failure criteria for the model, and as such does not include a proper plasticity formulation as in the other models. Accordingly, a disadvantage is that the Duncan-Chang model cannot describe dilatency (Brinkgreve 2005, 79). In addition, the stiffness parameters are defined as applicable for loading, unloading, and reloading, but do not include a solution for a neutral state. As a

result the user must select a stiffness coefficient from the two alternatives, which may lead to significant differences in distortion response. The hyperbolic shape of the curve is applicable only under drained soil conditions, and would provide no advantage (and likely a significant disadvantage) over the Mohr-Coulomb model for undrained conditions. In summary, the Duncan-Chang model is more like a hyperbolic curve-fit to observed drained triaxial tests as opposed to a true adaptable mathematical model formulation. However, the model may be successfully employed within the context of the inherent limitations, and does provide a superior pre-failure distortion response for drained conditions in comparison to the Mohr-Coulomb model.

1.4.5 Modified Cam Clay

1.4.5.1 Model Description

Modified Cam Clay, discussed by Schofield and Roth (1968) of the University of Cambridge, is a work-hardening elastic-plastic model specifically formulated to represent near-normally consolidated cohesive soils. Schofield and Roth based their work upon the original formulations of the Cam Clay model as developed by Roscoe, Schofield, and Wroth (1958), Roscoe, Schofield, and Thurairajah (1963) and Roscoe and Burland (1968). The model assumes a logarithmic relationship between effective stress and void ratio, with a linear stiffness constant applied dependent upon whether the soil state is within primary plastic compression or

an unload/reload cycle. The deformation response of the soil exhibits a plastic hardening characteristic; that is, as deviatoric strains increase from a normally-consolidated state, subsequent volumetric plastic strains occur that reduce to zero as cumulative deviatoric strain increases. The Critical State is reached when zero volumetric strain is accompanied by infinite deviatoric strain. Additional description of the Modified Cam Clay model is provided in Section 1.6.1. (Brinkgreve 2005, 79-81)

1.4.5.2 Advantages and Limitations

The Modified Cam Clay model has been specifically formulated to represent normally-consolidated cohesive soils, and the input parameters have proven quite successful in modeling pre-failure stress-strain response characteristics. While the model has a similar yield surface in the deviatoric plane as the Drucker-Prager model, and accordingly maintains the same limitations at and beyond failure, the Modified Cam Clay model has more options to control the pre-failure non-linear and stress-path dependent behaviors. (Brinkgreve, 79-81)

1.5 Soil model selection criteria

1.5.1 Modeling Objectives

For the purpose of the airfield matting study, the list below outlines criteria that have been established to aid in selection of the appropriate soil model (Johnson and Frank 2006; Frank 2006).

The soil model shall:

- provide an accurate representation of the soft Buckshot clay behavior under undrained, pre-failure conditions;
- "capture both the plastic deformation of the soil in the area near the tire, while capturing the proper stiffness in the large area away from the tire that provides most of the support for the airfield matting" (Frank 2006);
- be capable of appropriately modeling unload-reload action as a result of repeated tire pressure application, specifically at the matting joint locations;
- have input parameters that can easily be determined from common laboratory experiments;
- be capable of being efficiently input in the ABAQUS finite element analysis software currently employed by UDRI for this research.

1.5.2 Selected Model

The Modified Cam Clay model was selected as the most appropriate model for this modeling study. The model was mathematically formulated specifically to represent soft cohesive soils such as Buckshot clay, and provides several parameters that allow accurate calibration to represent pre-failure stress-strain response characteristics. Frank and Whitney (2004) and Johnson and Frank (2006) have found that the soil model representing the interaction with the matting will likely be required to characterize plastic deformation with higher strains immediately below the tire load, but reduced strains and elastic unloading-reloading for the remainder of the model volume. Modified Cam Clay is well-suited to separately accommodate the plastic initial loading and elastic unload-reload scenarios as a logarithmic function of void ratio and effective stress. The input parameters for the model can be derived from simple one-dimensional consolidation and triaxial testing, both tests commonly performed in any comprehensive commercial or academic soil laboratory.

The ABAQUS software package (Version 6.5-3, 2005) used by UDRI for this research includes pre-packaged Mohr-Coulomb, Drucker-Prager, and Modified Cam Clay models with various adaptations. The use of this model will eliminate the need to develop compatible input code to represent the soil constitutive model, enhancing the efficiency and cost-effectiveness of the research.

Additionally, the ABAQUS Extended Modified Cam Clay model provides several additional input variables that improve the performance of the original Modified Cam Clay model. These additions will be discussed in Section 1.6.2.

1.5.3 Scope of work

In order to produce an appropriate soil response characterization utilizing the Modified Cam Clay constitutive model, the following scope of work is required:

- Establish the definition of and derivation methods required for the various input parameters required for the original Modified Cam Clay model and pursuant ABAQUS Extensions;
- Compile existing soils testing data of the Vicksburg clay as developed by others;
- Perform laboratory testing consisting of soil classification, California Bearing Ratio, Proctor analysis, and consolidated-undrained triaxial testing to derive engineering soil material properties of the Vicksburg clay;
- Correlate the results of the Vicksburg clay soils testing from this study with the existing Vicksburg clay soils testing data to produce a combined data set;
- Using the combined data, establish values for each laboratory-determined soil characteristic from which to derive the ABAQUS Extended Modified Cam Clay parameters;

- Calibrate the ABAQUS Extended Modified Cam Clay material representation within a finite element model of the CBR testing apparatus such that the soil stiffness response is equivalent to a CBR 6 soil along the standardized curve;
- Review the output of soil pressure gauges installed at depths of 15 and 30 inches for field testing of the soil-matting response to simulated loading completed at Vicksburg;
- Compare the finite element response of the calibrated soil parameters to field testing results;
- Modify the calibration, as required, to permit the finite element model to represent the field testing results;
- Discuss differences between the soil response as calibrated to CBR 6 and field testing results, and suggest avenues of future research.

1.6 Selected Constitutive Soil Model

1.6.1 Detailed Description of the Selected Constitutive Model

Modified Cam Clay is a critical state model for describing the behavior of near-normally consolidated soft soils such as saturated clays. The proposed Modified Cam Clay model was published and improved upon through a series of articles from the University of Cambridge, beginning with an article entitled "On the yielding of soils" (Roscoe, Schoefield, and Wroth 1958).

Modified Cam Clay is a work-hardening elastic-plastic model. The response of the model to varying stress conditions is formulated as a function of strain, which is decomposed into elastic and plastic components governed by an elasticity theory, a yield surface, a flow rule, and a hardening rule. The elastic component response is produced within and up to the state of pre-consolidation effective stress (known as "unloading and reloading"), while a plastic component response is produced beyond the pre-consolidation stress (known as "primary loading"). In general terms, the soil model responds to loading via a plastic strain hardening response from the point of normal consolidation up to the critical stress state. At the critical stress state the model will exhibit unrestricted deviatoric plastic flow under constant effective stress. Any unloading and reloading will be modeled via a linear elastic response.

The linear elastic stress change response is governed by the average slope of the isotropic consolidation unload-reload line. This slope is identified by a soil constant *k* as graphically demonstrated in Figure 10. Note that this graph is formulated in $e - ln\ p$ space, as opposed to $e - log\ p$ space of a traditional isotropic consolidation curve. *k* is a function of the traditional swelling index C_s. Any stress path within the yield surface is modeled as fully elastic, moving up and down the unload-reload line with zero net plastic strain. No dilatency or pore pressure effects are considered.

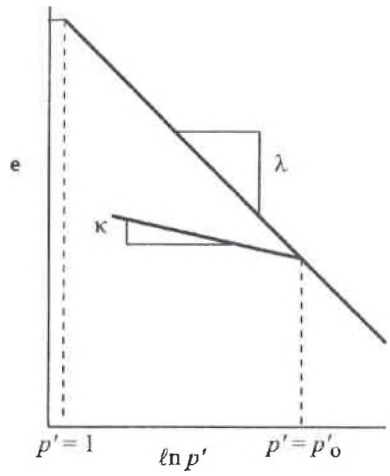

Figure 10 - Isotropic Consolidation Curve (Source: Wood 2004, 155)

Modified Cam Clay assumes that each yield surface is in the shape of an ellipse within the triaxial stress plane defined by a vertical axis of distortional stress q and a horizontal axis of mean effective stress p', as described in Equations 3 and 4. Each yield surface ellipse is thus governed by two controlling variables: the aspect ratio of the ellipse M which controls the shape, and the p-axis maxima p'_0 which controls the size. Each yield surface ellipse size will be governed by an independent p'_0, but all surfaces will be related by a common shape governed by M. Figure 11 shows the geometric configuration of a typical yield surface in $p' - q$ space. In three dimensional stress space the critical state surface takes on the shape of a cone as shown in Figure 12.

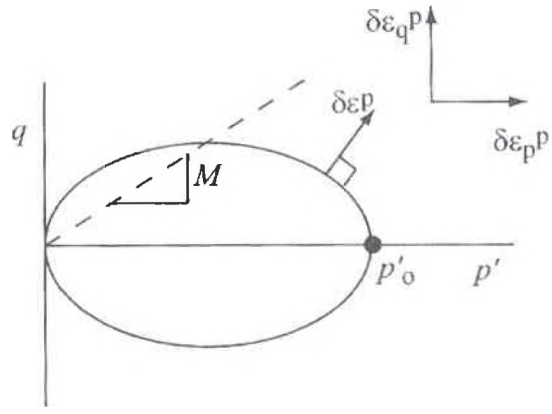

Figure 11 - Typical Yield Surface in the Triaxial Stress Plane
(Source: Wood 2004, 156)

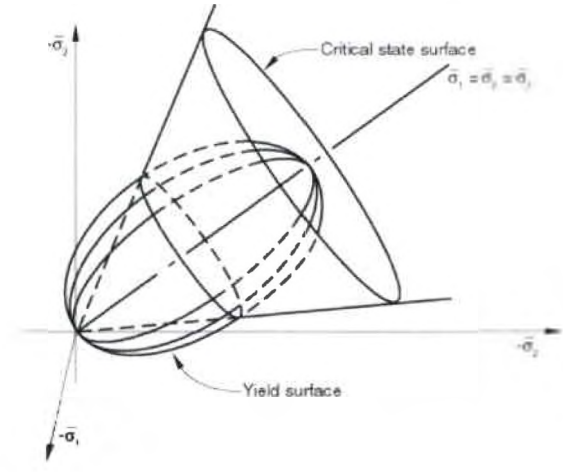

Figure 12 - Critical State and Yield Surfaces in 3-Dimensional Stress Space
(Source: ABAQUS Analysis user's manual)

The non-linear model response during primary loading is a function of a flow rule and a hardening rule. Modified Cam Clay observes an associated flow rule, meaning that the plastic strain increment vector is assumed to be normal to the yield surface at the current stress ratio, *n'*, defined as the distortional stress "*q*" divided by the mean effective stress "*p*'". The hardening/softening response of

the model is determined dependent only upon the stress ratio at which yielding is occurring.

If the stress ratio is less than M, known as the "wet" side, the soil will exhibit a hardening behavior, implying compression plus distortion. The yield surface will grow in size towards the critical state. If the stress state is greater than *M*, known as the "dry" side, the soil will soften and dilate, implying expansion plus distortion. The yield surface will reduce in size towards the critical state. Figure 13 provides a graphical representation of the growth or shrinkage of the yield surface as described above. The stress path upon which the soil will travel to reach the critical state line is a linear function of λ, or the slope of the isotropic compression curve in $e - \ln p$ space. See Figure 10.

As *n* approaches *M* from either side of the critical state line, the plastic volumetric strains reduce toward zero. Dependently, the stress increments reduce toward zero, and thus the change in p'_0 reduces toward zero. The plastic compliance matrix, the derivation of which is beyond the scope of this report, will thus tend towards infinity, indicating that shear stiffness has reduced to zero, or critical state (Wood 2004, 159). Upon reaching this critical state from either side the soil will experience infinite distortion without change in yield locus, effective stress, or volumetric strain. This is the Critical State soil failure condition in the Modified Cam Clay model.

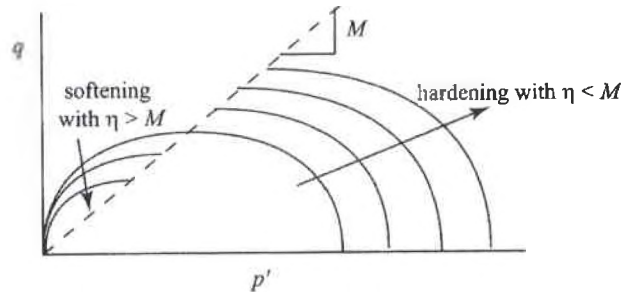

Figure 13 - Hardening and Softening of the Yield Locus in p' – q Space
(Source: Wood 2004, 162)

1.6.2 Extension of Modified Cam Clay Theory in ABAQUS

ABAQUS allows the user to select between two methods of defining elastic behavior: linear elasticity or porous elasticity. The Linear Elastic response is governed by Hooke's law and can be defined using the Modulus of Elasticity and Poisson's Ratio, or by providing engineering constants. As an alternative, the user can specify the Porous Elastic response in which the bulk elastic stiffness of the material is increased as the material undergoes compressive strain and increased shear. The porous elasticity response is a function of the logarithmic bulk modulus, Poisson's ratio, and the elastic tensile limit. The porous elastic response is valid only for strains less than five percent, so care must be taken in the final modeling scenario to ensure that this criterion is met.

The Modified Cam Clay model utilizes a circular section to describe the surface of the principal deviatoric stress plane as shown in Figure 14. ABAQUS provides the option to modify this shape to more closely reflect the Mohr-Coulomb hexagonal shape, which has been widely accepted as accurate in current

literature (Brinkgreve 2005, 76-77). The variable *K* is used to make the aforementioned modification, and is maintained between 0.778 and 1.0 to ensure convexity.

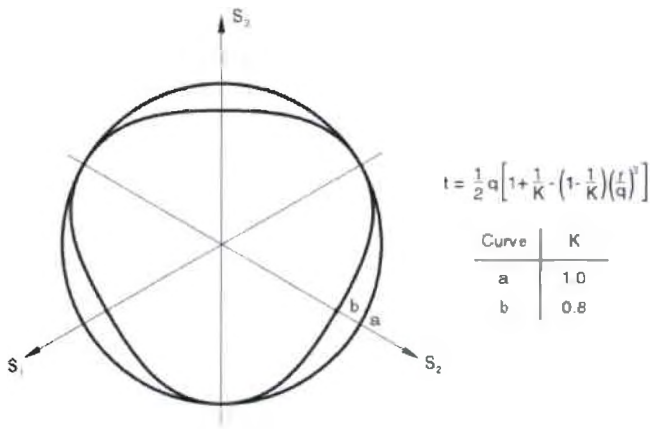

Figure 14 - Effect of K on the Shape of the Principal Deviatoric Stress Plane (Source: ABAQUS Analysis user's manual)

In addition, ABAQUS provides a variable β to modify the shape of the yield surface on the "wet" side of critical as shown in Figure 15. This will allow a unique yield surface to have two different elliptical degrees of curvature, permitting greater flexibility in model calibration. Beta is typically less than one on the "wet" side of critical, and equal to one on the "dry" side.

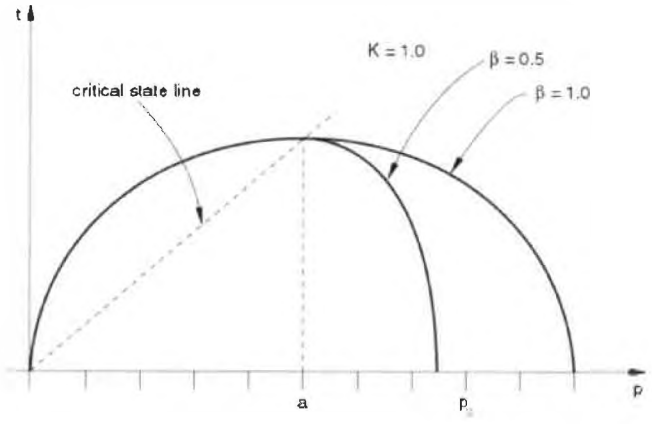

Figure 15 - Effect of on β Yield Surface Curvature
(Source: ABAQUS Analysis user's manual)

CHAPTER 2 – EXPERIMENTAL WORK

2.1 Introduction

The Army Corp of Engineers has identified a "fat" clay soil, commonly referred to as the Buckshot Clay, to maintain consistency between this study and other airfield pavement studies completed to date and in the future. Buckshot clay has a high affinity for water, exhibiting a wide range of material properties at varying moisture contents. This variability of material properties is a valuable characteristic in evaluating the effectiveness of constitutive soil model because a wide range of model responses can be compared to laboratory results for the same soil. However, the soil is more challenging to manipulate in the laboratory due to low permeability and high swell potential, making moisture conditioning difficult.

Laboratory testing was performed for this study for three purposes:

- Establish a correlation between the soil tested in this study to an existing reference laboratory database on Buckshot clay compiled by the Army Corps of Engineers;

- Obtain additional material property data needed for the ABAQUS Extended Modified Cam Clay finite element model that does not currently exist in the literature;
- Calibrate the ABAQUS Extended Modified Cam Clay Model.

2.2 Testing Program

Various laboratory experiments of the Buckshot clay were performed from May through October 2006 as referenced in the matrix of tests in Table 1. A majority of the experiments were conducted at the University of Dayton's Geotechnical Engineering Laboratory. Several laboratory tests were subcontracted to a local independent testing laboratory due to the unavailability of pertinent equipment and facilities due to renovations occurring during this time period.

Table 1 - Summary of Laboratory Testing Performed

Test	Procedure	Quantity
Grain-Size Distribution	ASTM D422	1
Atterberg Limits	ASTM D4318	1
Modified Proctor Analysis	ASTM D1557(B)	1
One-Dimensional Consolidation	ASTM D2435	4
California Bearing Ratio (Saturated)	ASTM D1883	3
California Bearing Ratio (Partially Saturated)	ASTM D1883	3
Consolidated Undrained Triaxial Testing with Pore-Pressure Measurements	ASTM D4767	1

A brief description of each test along with the results is presented herein.

2.3 Grain Size Distribution

One grain-size distribution analysis was performed in accordance with ASTM D422 via combination of sieve and hydrometer tests for the purpose of comparing to existing data on Buckshot clay in the literature. The soil was air dried and broken up into constituent particles using a rubber mallet, taking care not to crush any individual particles. The soil was then passed through a No. 10 sieve. The soil retained on the No. 10 sieve was oven dried and weighed, while the soil passing the No. 10 sieve was subsequently passed through a series of additional sieves of decreasing aperture size to a minimum No. 200 sieve (aperture size of 0.075 mm). Soil passing the No. 200 sieve was mixed into a soil-water slurry for hydrometer analysis. Over a period of 24 hours, hydrometer readings of the slurry settlement were obtained, providing a grain size analysis of the finest particles.

2.4 Atterberg Limits

One set of Atterberg limits tests was performed in accordance with ASTM D4318 to establish the liquid and plastic limits of the soil with respect to values for Buckshot clay in the literature. The liquid limit defines the moisture content at which the soil transitions from plastic to liquid behavior characteristics. A representative sample of soil passing the No. 40 sieve (aperture size 0.425 mm)

was mixed with an appropriate amount of distilled or demineralized water as determined by experience. The mixture was allowed to sit for a period of at least 16 hours to achieve moisture equilibrium. Then the soil sample was placed in a liquid limit device and grooved with a standard tool. At a constant rate the soil sample was dropped from a constant height and the number of blows required to close the groove were counted. The liquid limit is defined as the soil moisture content at which 25 blows are required to close the groove. Typically a soil with a liquid limit greater than 40 is considered highly plastic and potentially expansive.

The plastic limit defines the moisture content at which the soil transitions from plastic to semi-solid behavior characteristics. A representative sample of soil passing the No. 40 sieve was prepared in the same manner as for the liquid limit test, but at a lower moisture content. The soil was then rolled on a glass plate into threads. The plastic limit is defined as the moisture content at which 1/8-inch soil threads lose their cohesiveness and begin to crumble. The plasticity index is determined by subtracting the plastic limit from the liquid limit.

2.5 Modified Proctor Analysis

Five compaction tests were performed at varying moisture contents employing consistent compaction energy to establish a Proctor curve. For the purpose of this analysis ASTM D1557 Method B analysis was performed, implying that soil

passing a 3/8-inch sieve was compacted in a 4-inch diameter cylindrical mold in five layers using 25 blows per layer. Each blow is defined as the energy applied by dropping a 10 lb_f rammer a distance of 18 inches, which imparts 56,000 lb_f.

Berney (2004) and Freeman (2004), engineers from the Army Corp of Engineers who have previously studied of Buckshot clay, performed similar compaction tests but at varying compaction energies. Berney (2004) employed ASTM D1557 Method A which uses the same compaction energy, but performed on soil that has passed a No. 4 sieve (aperture size 4.75 mm). Freeman (2004) employed ASTM D1557 Method C which uses a six-inch diameter mold and 55 blows with the rammer per lift.

2.6 One-Dimensional Consolidation Tests

Four sets of one-dimensional consolidation tests were performed on remolded samples of Buckshot clay using a unidirectional loading apparatus in accordance with ASTM D2435 Method A. The clay was air-dried to a moisture content between 40 and 50 percent before sample preparation. To promote consistency of soil density and moisture content, all four samples were extracted from one large remolded soil mass. Compaction of the remolded mass was performed using a modified Proctor effort on soil placed in a six-inch diameter modified Proctor mold. The soil was placed in five lifts to a height of approximately six inches. After extrusion from the mold, the soil mass was cut horizontally with a

wire saw into four separate 1.5 inch soil disks. A 2.5-inch diameter consolidation specimen ring with cutting edge was passed through each soil disk to create the perimeter shape of the consolidation samples, and a wire saw and soil knife were used to trim the ends flush. The samples were arranged in a double-draining consolidometer between two porous stones with filter paper and mounted to the loading apparatus.

After filling the consolidometers with water, testing was initiated by placing a 0.45 lb/in^2 load on the specimen. Deformation versus time readings were taken automatically by computer software through primary consolidation. Upon reaching primary consolidation, an additional load was applied and again deformation versus time readings were obtained for the sample. From this data a specific void ratio corresponding to 100 percent of primary consolidation was obtained. Upon completion of testing a plot of void ratio of 100 percent primary consolidation versus load was produced in semi-log space. The slope of the virgin compression curve, i.e. the slope of the steepest part of the void ratio versus applied pressure plot, is identified as the variable C_c as defined in Equation 5:

$$C_c = \frac{e_2 - e_1}{\log p_2 - \log p_1} \qquad \text{(Eq. 5)}$$

where e_i and p_i represent the void ratio and pressure, respectively, at the two points which define the slope of the virgin compression curve.

After determining the slope of virgin compression curve the soil sample was unloaded to determine the elastic rebound curve. Several unloading steps were performed, measuring the soil expansion in response to incremental reduction in load. From this the slope of the rebound curve was established, identified as the variable C_s calculated in the same manner as Equation 5.

Berney (2004) performed nine additional consolidation tests by an alternative consolidation method. The remolded samples were placed in a triaxial apparatus and varying back and chamber pressure increments were imposed. The difference between back and chamber pressure is the effective stress acting on the specimen. Measurement of the axial deflection of the sample during loading and unloading was obtained, and a plot of effective stress versus void ratio was determined in accordance with ASTM D2435.

2.7 California Bearing Ratio

The California Bearing Ratio (CBR) test was originally developed by the California State Highways Department as a means of determining relative roadway subgrade stiffness for pavement design and construction inspection. Today the CBR test has been standardized in accordance with ASTM D1883 and

is used nationwide as a measurement of soil stiffness. Numerous studies have correlated the CBR to a number of soil properties, notably the subgrade soil modulus. To perform the test, a piston with a cross-sectionaly area of three square inches is pushed into the soil at a rate of 0.05 inches per minute and measurement of penetration resistance versus depth of penetration is obtained. The pressure required to penetrate 0.10 inch into the soil is divided by a standard penetration stress of 1,000 pounds per square inch. This standard penetration stress represents the average stress required to penetrate 0.10 inch into crushed aggregate. The test is continued through at least 0.20 inches of penetration. If the CBR determined at 0.02 inch penetration is greater than the CBR at 0.01 inch penetration, the test must be rerun. If the CBR value at 0.02 inch penetration is yet again greater, the CBR for the soil is determined to then be the value at this deeper penetration.

The CBR test can be performed at any soil moisture and density condition as deemed appropriate by the design engineer. For the purpose of this study, the goal was to determine what moisture and density condition of Buckshot clay would produces a CBR of 6 percent. The goal of the testing was to produce a remolded sample that achieved a CBR of 6 percent. However, given the moisture sensitivity of Buckshot clay, it was known that this would be difficult to achieve. Accordingly, sufficient test data was both gathered from the literature and performed for this study to provide an acceptable data curve from which to interpolate the required soil characteristics at CBR 6.

Six sets of CBR tests were performed in accordance with ASTM D1883 at varying moisture and density conditions. Three of the tests were performed under saturated conditions and at dry densities varying from 95.3 to 97.3 pcf. Saturation was obtained by soaking the samples for 96 hours. Per the ASTM Standard a surcharge of 10 pounds was applied during the soaking, and measurement of the soil swell at the end of the 96 hour period was obtained. The remaining three tests were performed in a partially saturated condition and at dry densities varying from 98.2 to 98.8 pcf. No saturation or swelling measurements were performed.

Additional laboratory CBR tests were performed by the Army Corp of Engineers and are discussed in a subsequent section of this document.

CBR testing may also be performed in the field in accordance with ASTM D4429. This test involves jacking a similar piston into the subgrade soils and measuring the penetration resistance as a function of depth of penetration. Surcharge weights are placed surrounding the piston to eliminate upward soil displacement around the testing location. Field CBR tests are performed solely to determine the in-situ CBR value for the subgrade moisture and density condition at the time of testing. Test results are invalidated by any soil disturbance or moisture content change. For the purpose of this study laboratory CBR tests in

accordance with ASTM D1883 were performed to maintain stricter controls on the moisture and density of the soils.

2.8 Consolidated Undrained Triaxial Tests

Triaxial testing of a soil specimen is accomplished by applying external pressure to the specimen in each of the three principal stress planes, σ_1, σ_2, and σ_3 under controlled drainage and loading conditions. Soil specimens are typically formed in a cylindrical shape, although cubic triaxial tests are possible. The prepared soil specimens are wrapped in an impermeable membrane to control pore fluid transfer and immersed in a water bath confined within a thick-walled glass or plastic vessel. The triaxial testing apparatus has the ability to control the pressure of the fluid both within the specimen (pore fluid pressure) and surrounding the specimen (confining or radial pressure, $\sigma_2 = \sigma_3$), and permits an axial stress (σ_1) to be applied to the specimen via a piston. Three types of loading scenarios are typically employed: isotropic compression ($\sigma_1 = \sigma_2 = \sigma_3$), triaxial compression ($\sigma_1 > \sigma_2 = \sigma_3$), and triaxial extension ($\sigma_1 < \sigma_2 = \sigma_3$). Load paths can be applied under various configurations of fluid pressure control, wherein the degree of saturation and consolidation are designed to meet the needs of the tests. Additionally, the drainage configuration of the soil specimen can be controlled to permit or prohibit pore fluid flow within the sample.

For the purpose of this study, a consolidated undrained (CU) triaxial compression test was performed on a cylindrical remolded soil specimen in accordance with ASTM D4767. This method was selected because it permits correlation with equivalent testing previously performed by Berney (2004) and Peters (1982) and would allow back calculation of the soil friction angle at the remolded unit weight and moisture content.

Prior to remolding the sample, the soil was moisture cured to bring the soil moisture content to approximately 34 percent, which is the moisture content required to achieve CBR 6 as detailed in Section 3.6.2. Moisture curing consisted of measuring the pre-cure soil moisture content and adding an appropriate amount of water to the soil in a sealed container. The soil was left to cure for a period of ten days, agitating daily. Upon completion of the moisture curing the soil moisture content was again measured to ensure that the required 34 percent had been achieved. The soil was then compacted in a 2.5 inch diameter mold in a series of five lifts using an aggregate tamper. Between subsequent lifts the surface of the compacted soil was roughened to eliminate potential horizontal slip surface discontinuities and promote consistency throughout the sample. The soil was compacted to a height of six inches in the mold and then trimmed using a miter box to a height of 5.25 inches as measured using calipers. The unit weight of the soil was calculated using the measured soil volume and weight. The desired unit weight of Buckshot clay to produce a CBR 6, as outlined in Section 3.6.2, was 85.0 pcf. The first remolded soil sample was

measured at a unit weight of 83.9 pcf, which was determined to be acceptable for this study.

The soil specimen was encased in a filter paper cage to improve the rate of drainage of the specimen by providing alternative routes for fluid transfer to the top and bottom platens of the triaxial apparatus during testing. Filter paper and porous stones were placed at the top and bottom of the specimen, and the specimen was then wrapped in a 3.5 mil impermeable membrane. The specimen was mounted onto the triaxial testing chamber bottom platen and O-rings were installed to make the connection to the platens impenetrable by the chamber pressure fluid. The plastic confining chamber was installed around the specimen, the axial load piston was lowered to contact the top porous stone, and the chamber was filled with water to an effective seating pressure of five psi. Figures 16 and 17 show the triaxial testing chamber and overall apparatus configuration, respectively.

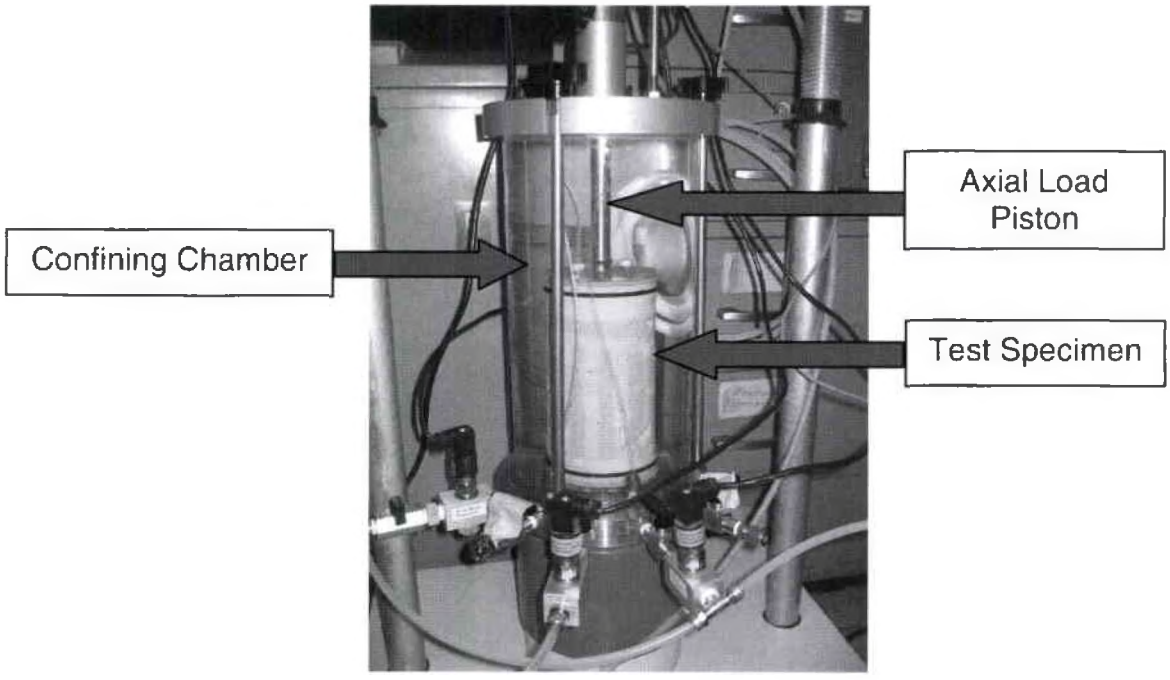

Figure 16 - Triaxial Testing Chamber

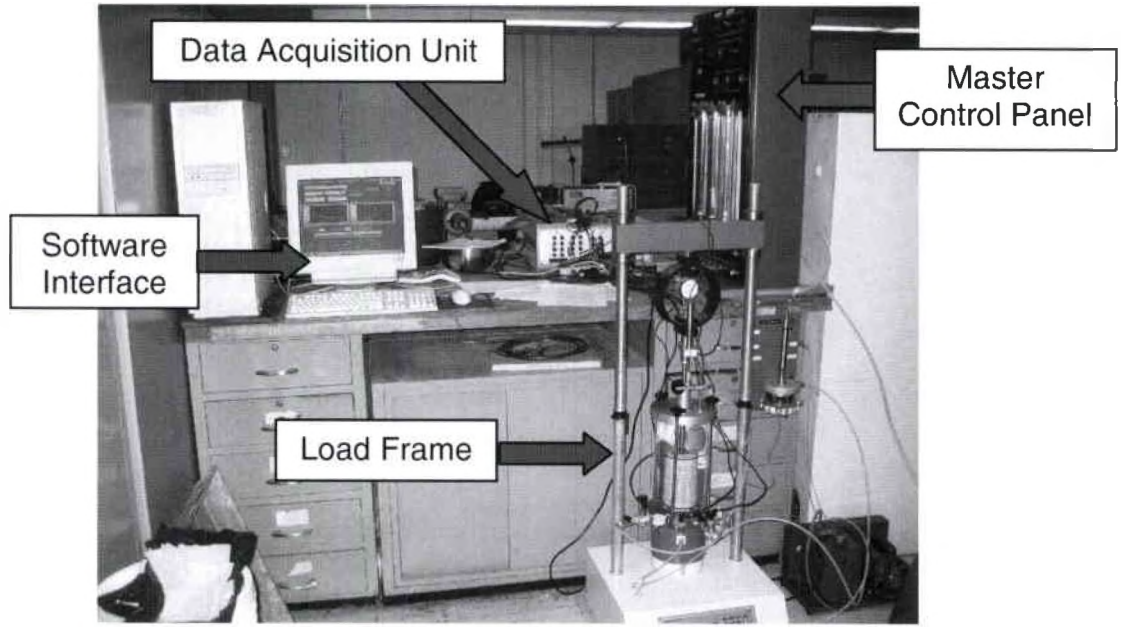

Figure 17 – Triaxial Testing Apparatus

Once the sample had been successfully seated and no leaks were observed, the saturation stage was initiated. This stage consisted of alternating cell pressure and back pressure increments designed to fill all voids in the specimen with water while not inducing unnecessary stress on the sample. The cell pressure is the radial pressure imposed on the circumference of the sample by the chamber fluid, while the back pressure is the pore pressure imposed throughout the sample as applied through the porous stones. The effective pressure on the soil sample, or the cell pressure less the pore pressure, never exceeded three psi during the saturation phase. The Skempton B values, which represent the ratio of pore water pressure increase to cell pressure increase for a given effective stress increment, were calculated at each increasing 10 psi increment. Upon reaching a B value of about 0.95 the saturation stage was considered complete. For this soil a back pressure of 69.83 psi was required to achieve a B value of 0.94. This was achieved over seven cycles of cell and back pressure increments, averaging approximately 48 hours per cycle for a total of approximately 28 days to achieve sample saturation. This time period to saturation is quite long in comparison to other soils, and can be attributed to the high impermeability of the Buckshot clay and to the size of the specimen tested. Berney (2004, 126) compacted smaller samples with a diameter of only 1.5 inches and a height of 3 inches. This is one-fifth the volume of the samples testing in this study, which increased the rate of sample saturation.

Consolidation of the specimen was performed after complete saturation of the sample had been obtained. An effective stress of 20 psi was imposed by increasing the cell pressure to 76.84 psi while maintaining the back pressure at 56.79 psi. The consolidation stage was completed when the plot of cumulative volume change versus time stabilized to a constant value. For this study a consolidation period of nearly 100 hours was required to achieve completion of consolidation, which is a relatively long time period compared to other soil types. Berney (2004, 131) experienced similar time to consolidation in his testing, ranging from 24 to 96 hours for the smaller specimen size.

Triaxial shearing of the specimen was performed in a Digital TriTest Load frame with a load proving ring with a capacity of 2250 psf capacity and an accuracy of +/-0.1 lb. Axial deflection was measured using a digital dial gauge. Both the load ring and dial gauge were automated via an autonomous data acquisition unit. The desired rate of strain was calculated using ASTM D4767 Equation 3 (2005, 922)

$$'\varepsilon = \frac{4\%}{10 * t_{(50)}} \qquad \text{(Eq. 6)}$$

Per the ASTM Standard, this equation assumes that failure will occur at four percent strain. t_{50} is derived from the findings of the consolidation tests performed previously. In this study, t_{50} ranged from 38 to 68 minutes. As such $'\varepsilon$ was calculated to range from 0.01 to 0.006 percent per minute. For this study, a

strain rate of 0.01 percent per minute was selected and triaxial shearing occurring over a period of approximately 36 hours. At this time the triaxial specimen had demonstrated shear banding as discussed in Section 3.7.1 and no additional meaningful data could be derived by continuing the test.

The sample was unloaded and the cell and back pressures reduced, never permitting the back pressure to exceed the cell pressure. The testing chamber was drained and the specimen removed for weighing and moisture content determinations.

2.9 Additional Data – Army Corp of Engineers

Additional laboratory testing of Buckshot clay has been performed by the Army Corps of Engineers, which has been reproduced for comparison in this study (Tingle 2006). This data, provided by the Army Corps of Engineers Engineering Research and Development Center – Waterways Experiment Station in Vicksburg, Mississippi, is for the internal use of the Army Corps and has not been published publicly in the literature. As a result, no literary references are available and little written documentation exists regarding the specifics of the testing procedures. However, the data is considered to have been accurately determined from applicable standard methods, and will be considered reliable for this study. For clarity of source and acquisition method, this data has been kept separate from the data provided in previous sections.

Table 2 provides the data compiled by the Army Corps of Engineers. Note that the samples have been compacted at low, standard, and modified energies. The standard and modified compaction energies are equivalent to the standard ASTM D698 and ASTM D1557 procedures, respectively. The "low" compaction energy was achieved by utilizing the same equipment and methods outlined in ASTM D698 with the modification that each layer was compacted with 15 blows in lieu of 25 as the ASTM Standard prescribes.

A discussion of the relevance of this data is included in Chapter 3.

Table 2 - Army Corps of Engineers Buckshot Clay Data (Source: Tingle, 2006)

Test Type	Moisture Content (%)	Dry Density (pcf)	CBR
modified	12.8	101.8	96.5
modified	14.8	101.7	92.8
modified	17.2	102.6	70.6
modified	19.0	103.9	76.5
modified	21.0	103.6	57.0
modified	23.2	101.5	34.4
modified	24.4	99.7	26.2
standard	26.1	95.7	23.7
low	31.1	87.8	10.1
low	34.0	85.1	8.3
low	34.6	83.4	4.3
low	38.0	79.9	3.9
low	38.9	78.6	3.2
low	41.5		3.0
low	43.0		2.6
low	44.5		1.3
low	45.0		1.8
low	46.0		1.3

CHAPTER 3 – DISCUSSION AND CORRELATION OF LABORATORY TEST RESULTS

3.1 Introduction

This chapter will present the laboratory test results, discuss the findings and sources of error for the laboratory tests, and correlate the findings to existing data by others. A discussion of the application of these findings to the derivation of Modified Cam Clay model input parameters is provided in Chapter 4.

3.2 Grain Size Distribution

3.2.1 Laboratory Test Results

In order to complete the grain size distribution testing, the soil was required to be dried, the individual soil particles separated (but not crushed or broken), and then subjected to sieve and hydrometer analyses. The adjective "Buckshot" in Buckshot clay was given because, when dried, the clay soil develops high strength inter-particle bonds (Berney 2004, 119). It tends to form hard soil masses that resemble buckshot ammunition. This clumping tendency makes drying and separating the soil particles difficult. The soil must be repeatedly

worked and broken down as drying progresses to separate the particles. Analysis of the repeatability of grain size distribution testing of Buckshot clay should consider this fact, especially when correlating the results of testing from multiple laboratories. Figures 18 and 19 provide the results of the grain-size distribution analyses for this study and for Berney (2004).

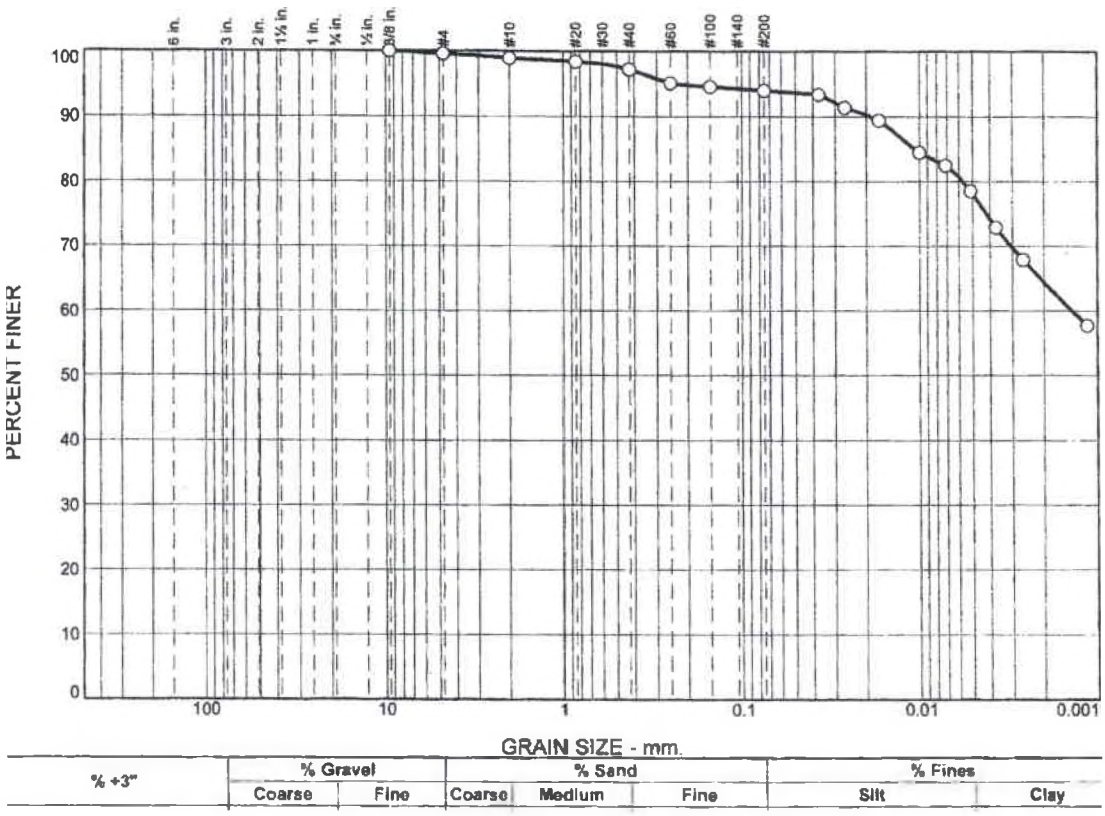

Figure 18 - Grain Size Distribution for Buckshot Clay

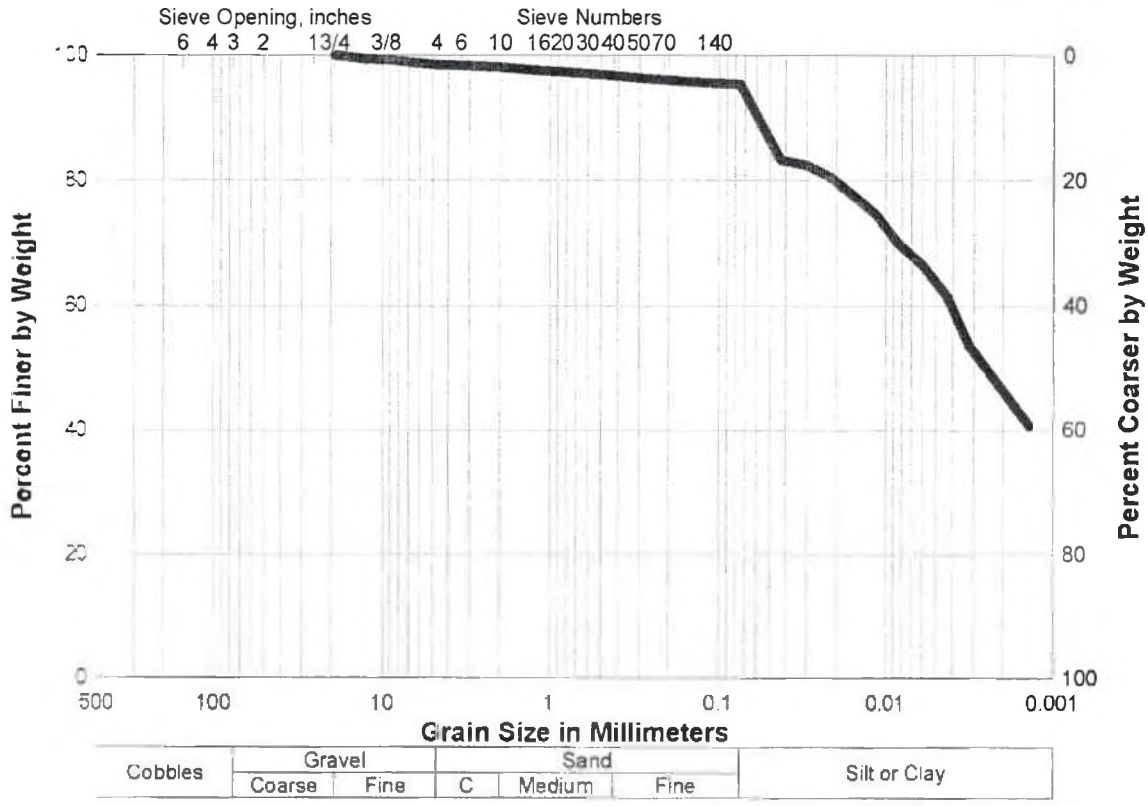

Figure 19 - Grain Size Distribution for Buckshot Clay by Berney (2004)

The grain size distribution of the soil matrix as determined in this study was composed of 6 percent sand and gravel, 15.9 percent silt, and 78.1 percent clay. Clay particles tend to have a high affinity for water and are relatively impermeable. In general, the higher the clay fraction, the greater the likelihood of swelling potential and impermeability of a soil. Clay mineralogy will affect the tendency for absorbing water. The results of grain size distribution testing of Buckshot clay has shown a relatively high clay fraction at 78.1 percent. It was observed in this study that CBR testing, which includes a measurement of the swelling potential of the soil, found that Buckshot clay swelled upwards of 20 percent during saturation. Additionally, the one-dimensional consolidation and

consolidated-undrained triaxial testing both required significantly longer time durations to achieve completion of the primary saturation and consolidation stages of testing than is typically observed for most lean clay or cohesionless soils. This is because the Buckshot clay soil has a very low permeability, and pore pressures require greater time to dissipate.

3.2.2 Correlation to Existing Data

Figure 20 provides a comparison of the findings of this study and Berney (2004). As can be seen from the plot, both curves follow the same trends over time. The value of "percent finer" by Berney appears to drop sharply between 0.007 and 0.004 millimeters. Sharp changes in curvature are uncommon in consistent cohesive soil deposits such as Buckshot clay. A potential laboratory procedural error or inconsistency in the soil sample may have caused the drop. If this drop had not been recorded, both plots would have fallen on nearly exact paths. The slopes of the plots throughout the ranges of grain sizes are nearly identical. Because the plots follow near-identical trends, and barring one inconsistency, it can be reasoned that the two sets of laboratory data correlate well.

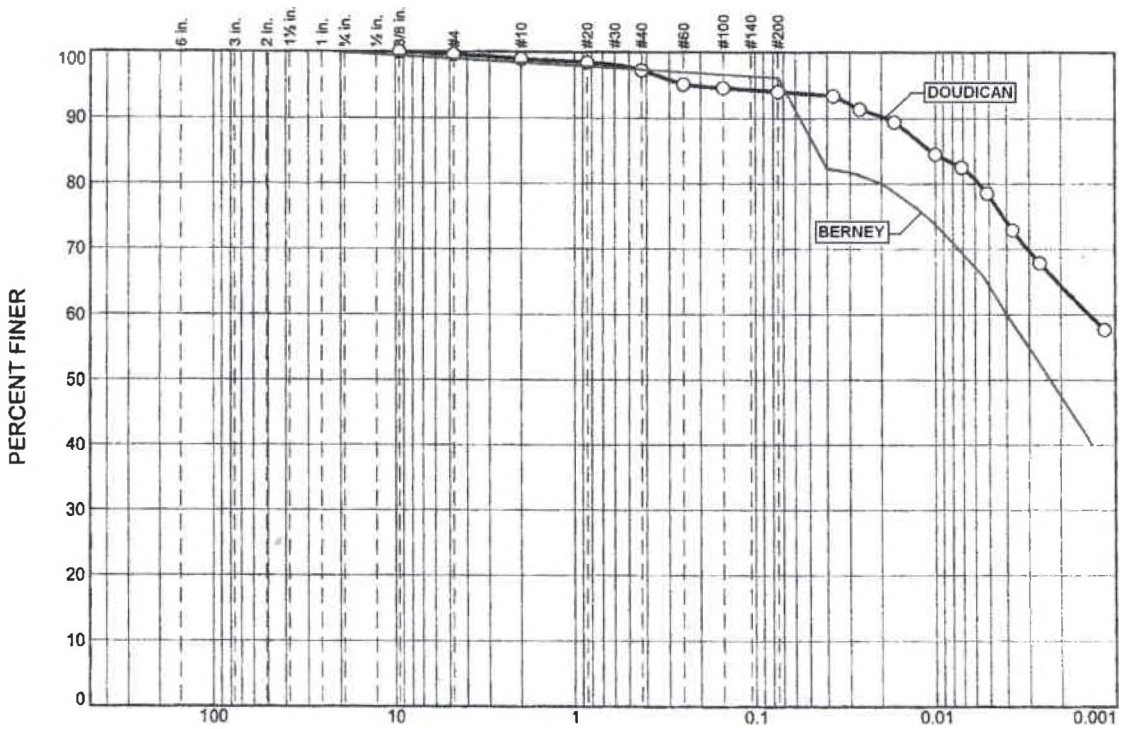

Figure 20 - Grain Size Distribution for Buckshot Clay by Berney and This Study

3.3 Atterberg Limit Tests

3.3.1 Laboratory Test Results

Atterberg limit test results established the liquid limit to be 78 percent, the plastic limit to be 27 percent, and the plasticity index to be 51 percent, as shown in Table 3. These results are consistent with a highly plastic clay. In physical terms, the soil begins to behave like a liquid at 78 percent moisture and begins to behave like a semi-solid at 27 percent moisture. The fact that the clay does not begin to act like a liquid until 78 percent of the soil matrix consists of water shows the high moisture-affinity of the clay. Each individual clay particle is able to

attract many times its own mass in water due to the strong negative charge of the clay particles, causing double layer attraction in addition to absorption. Additionally, there is a 51 percent moisture range between the solid and liquid phases as represented by the plasticity index. This implies that a majority of the soil behavior under varying moisture conditions will be plastic in nature. However, given the clay fraction of the soil, it can be expected that soil stiffness will be high at moisture contents less than 27 percent, then rapidly drop as moisture content increases.

3.3.2 Correlation to Existing Data

The findings for Atterberg limits testing are presented in Table 3 below. Also presented in the table are the experimental data of Buckshot clay by Berney (2004), Peterson (1987), Peters et. al (1982), and Freeman (2004).

Table 3 - Summary of Classification Test Results

Property	Doudican 2006	Berney 2001	Peterson 1981	Peters 1991	Freeman 1988	Ave.
Liquid Limit	78	75	56	54	83	69.20
Plastic Limit	27	24	21	17	27	23.20
Plastic Index	51	51	35	37	56	46.00
Clay Fraction	78.1	46	43	40	39	49.22

Overall, it can be seen that the values for liquid and plastic limits and plasticity index obtained in the present study correlate well to Berney and Freeman, with the Peterson and Peters values typically somewhat lower. This overall trend may

be a function of variations as the Buckshot clay source has been excavated over time, variations in laboratory procedures, or discrepancies due to the inherent non-homogeneity of soil materials. The clay fraction obtained in the present study averages about 30 percent higher than the other comparable experiments. This could be a result of soil crushing during the drying phase of preparation, resulting in finer (albeit broken) particles, or an improvement in preparation methods that permits the soil to be more efficiently separated. Regardless of the reasons for difference in clay fraction, the soil Atterberg indices for this study and historical studies are similar. While the clay fraction percentages have been found to vary significantly, the Atterberg limit data, which represents the soil response characteristics to variations in moisture content, were found to correlate within an acceptable degree of variation. Specifically, the most recent testing performed in this study and by Berney (2004) were nearly identical except for the clay fraction, which has been discussed previously. Given the known source of the material for all tests coupled with the expectation of some numerical differences due to non-homogeneity, the data has been assumed to establish a reasonable correlation to permit use in final model parameter determination.

3.4 Modified Proctor Analysis

3.4.1 Laboratory Test Results

Five tests were performed for this study at moisture contents varying from 10 to 26 percent. The curve developed is shown in Figure 21.

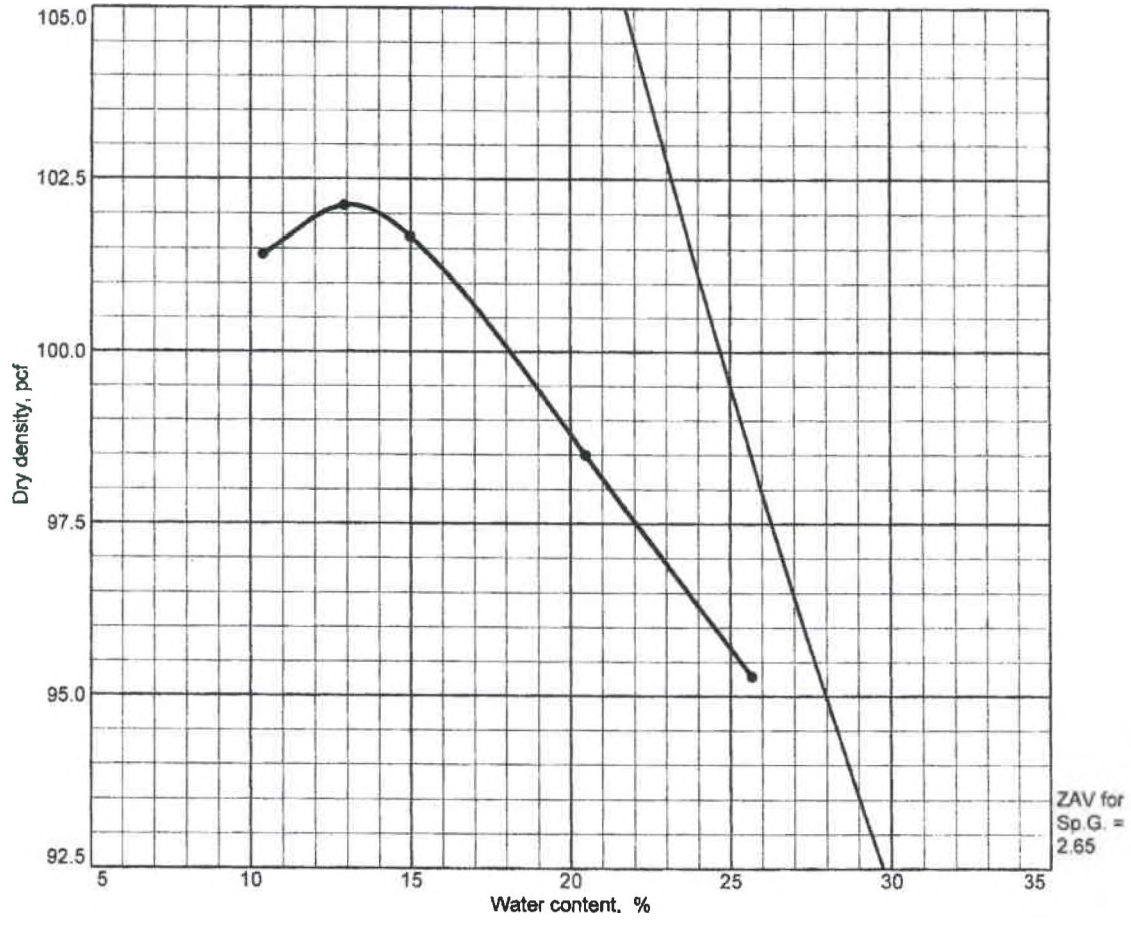

Figure 21 - Modified Proctor Compaction Testing Results

Figure 22 shows the results of compaction tests performed by Berney (2004) and Freeman (2004).

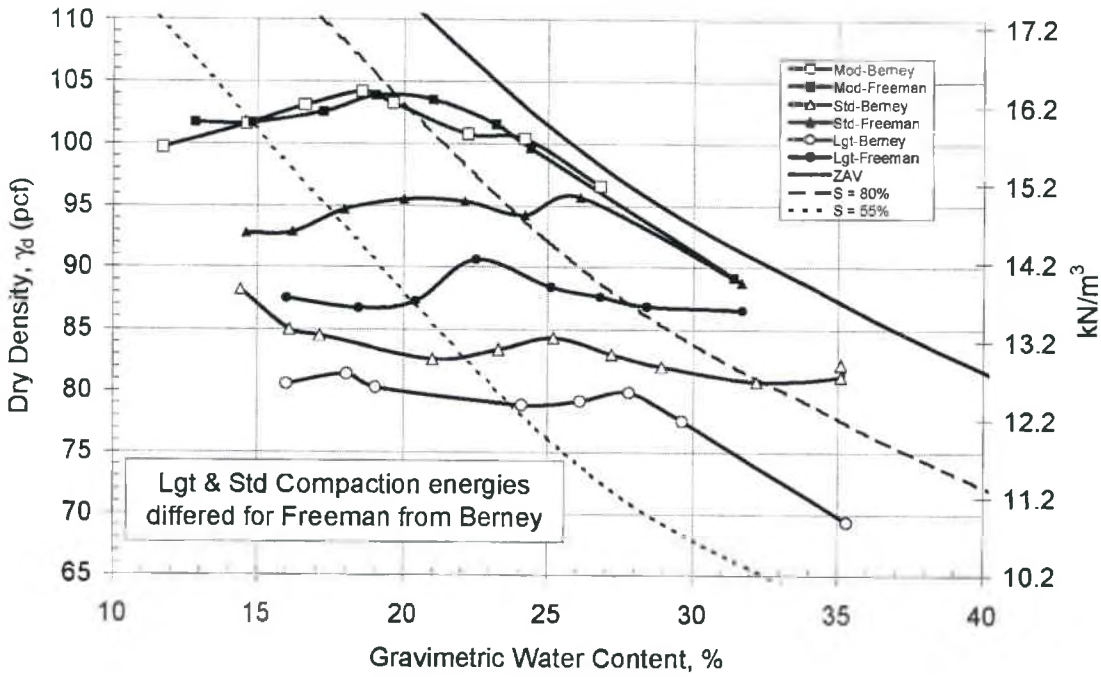

Figure 22 - Modified Proctor Compaction Testing Results by Berney (2004) and Freeman (2004) (Source: Berney 2004, 125)

Modified Proctor compaction tests at various moisture contents yielded a consistent unit weight versus moisture content curve. The resulting maximum dry unit weight and optimum moisture content were 102.1 pounds per cubic foot and 13.1 percent, respectively. The optimum moisture falls below the plastic limit, as would be expected, and the maximum dry unit weight was within a typical range for highly-plastic clays. At moisture contents below 13.1 percent the density was observed to decrease. This is a result of inter-particle friction in the soil matrix whereby the soil particles resist sliding past one another to form a denser configuration, introducing a greater void ratio and subsequent lower unit

weight. At moisture contents higher than 13.1 percent the soil particles have sufficient lubrication to slide past one another, but the water begins to take up greater volume in the soil matrix. This increases the void ratio and lowers the dry unit weight.

The relative steepness of the graph can be used to interpret the moisture sensitivity of a given soil. As steepness increases, the rate of change of unit weight increases as a function of moisture content. In the range of moisture contents tested for this study, the graph forms a relatively flat curve. This implies that as moisture fluctuates within the 10 to 25 percent moisture content range, the relative dry unit weight will only fluctuate by approximately seven pounds.

The results of relative compaction unit weight relations will be employed to identify the unit weight corresponding to a CBR of 6. This will be discussed further in section 3.6.

3.4.2 Correlation to Existing Data

Figure 23 provides a comparison of all moisture-unit weight relations as produced herein and by Bernie (2004) and Freeman (2004). It can be observed that the general graph slopes are consistent. The maximum dry unit weight achieved in this study is within two pcf of the maximum achieved by Berney (2004) and Freeman (2004); however, the optimum moisture content is over five

percent lower. This may be attributed to the differences in compaction energy and sample preparation methods as discussed in Section 2.6. Beyond the discrepancy in optimum moisture, the range of test results tend to correlate well.

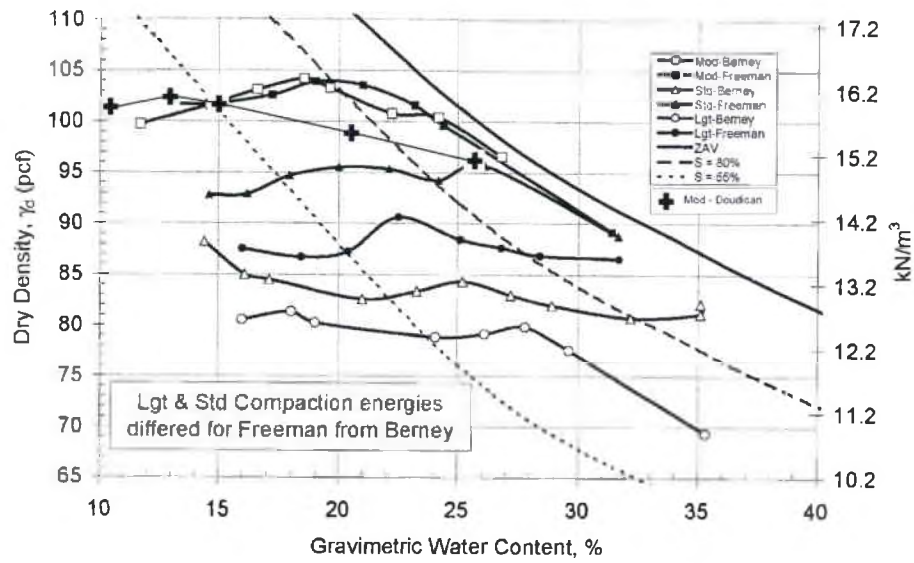

Figure 23 - Combined Compaction Test Results (Modified from Berney)

3.5 One-Dimensional Consolidation Tests

3.5.1 Laboratory Testing Results

Four sets of one-dimensional consolidation tests were performed for this study on remolded normally-consolidated samples of Buckshot clay. The results are provided in Figure 24.

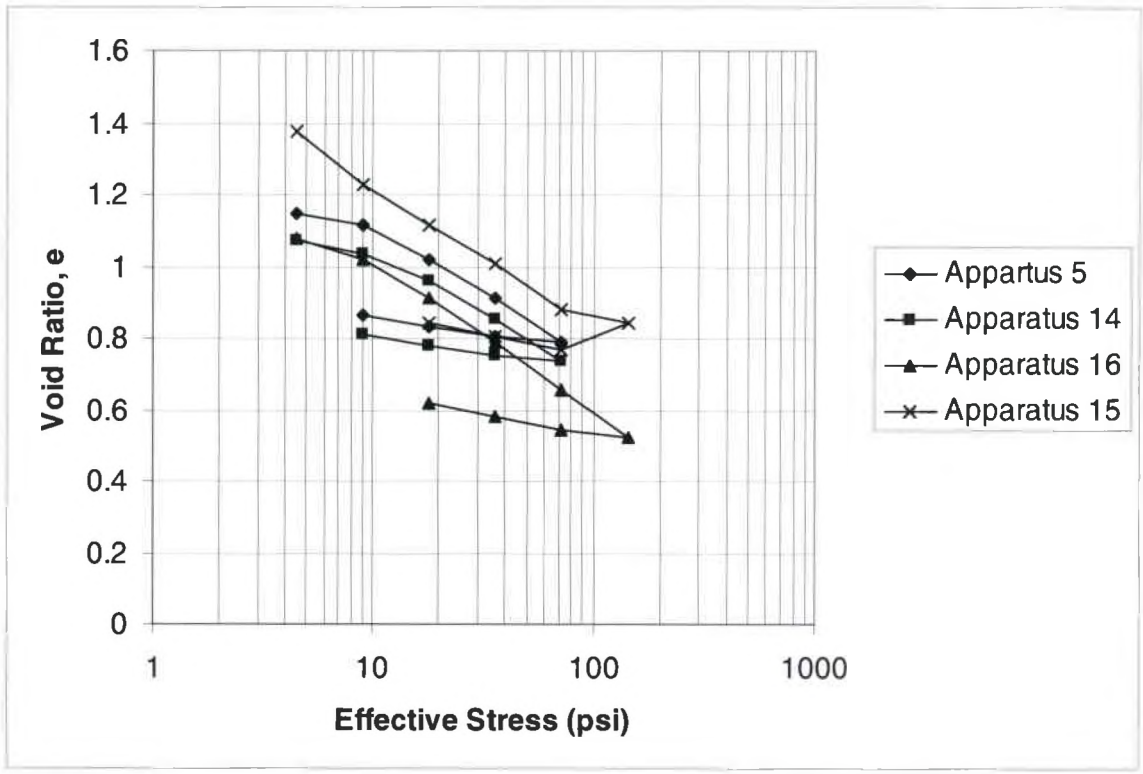

Figure 24 - Consolidation Test Results

The resulting consolidation curves showed strong consistency in both the primary consolidation and unload-reload phases of testing. For each iteration of increasing or decreasing load it was observed that up to 96 hours was required for the samples to complete primary consolidation. This incremental load duration was ancitipated due to the highly plastic and relatively impermeable characteristics of Buckshot clay. As discussed in prior sections, the pore water pressures that build upon load application dissipate over time as a function of soil permeability. The time required for each load increment in this study is significantly longer than is typical for other soil types, but within a typical range for highly plastic relatively impermeable clays.

The consolidation curves for all four tests show a linear relationship for all primary consolidation load increments applied except the first data point. This indicates that a slight overconsolidation of the molded samples existed prior to testing initiation. This is likely due to the compaction energy applied to produce the samples being greater than the initial pressure increment in the consolidometer. After exceeding the stress of compaction, the soils exhibited linear compression and unload-reload responses.

One likely erroneous data point was encountered during the maximum load increment for one of the tests. This data point was not included in the calculation of C_c or C_s for this curve. All other data points appear accurate.

For comparison, the results of the nine consolidation tests as performed by Berney (2004) are provided in Figures 25 through 27 organized by final triaxial chamber confining pressure. A discussion of the different consolidation testing methodologies has been provided in Section 2.6.

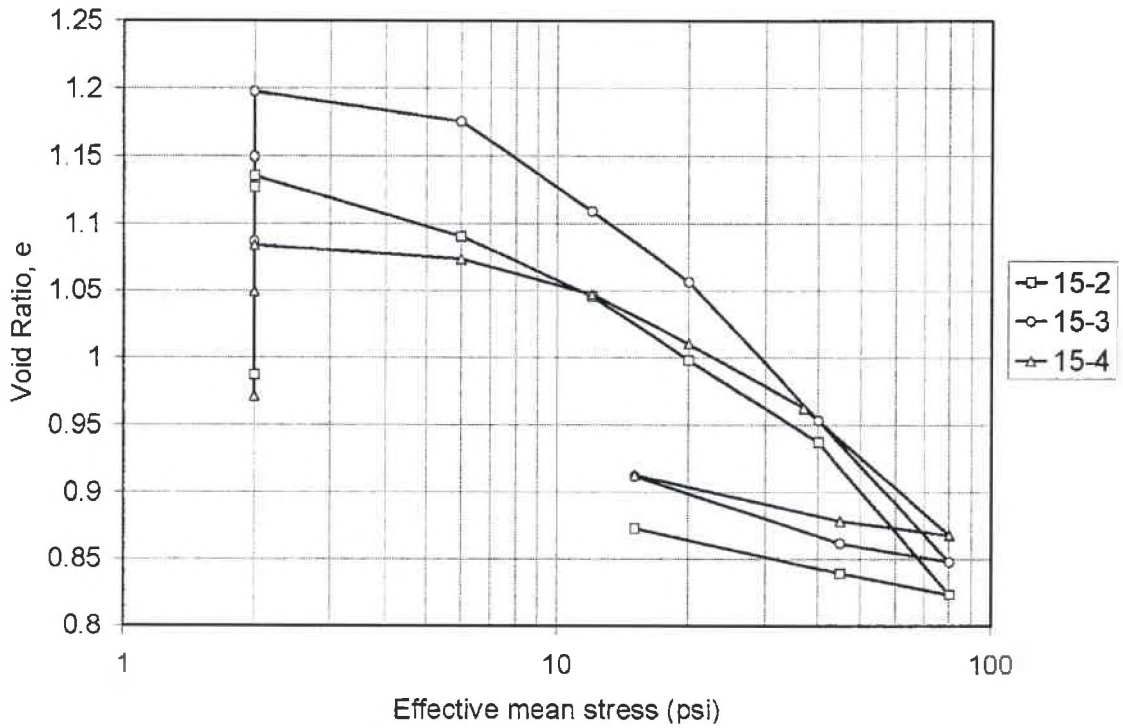

Figure 25 - Consolidation Test at 15 psi Confining Pressure
(Source: Berney 2004, 133)

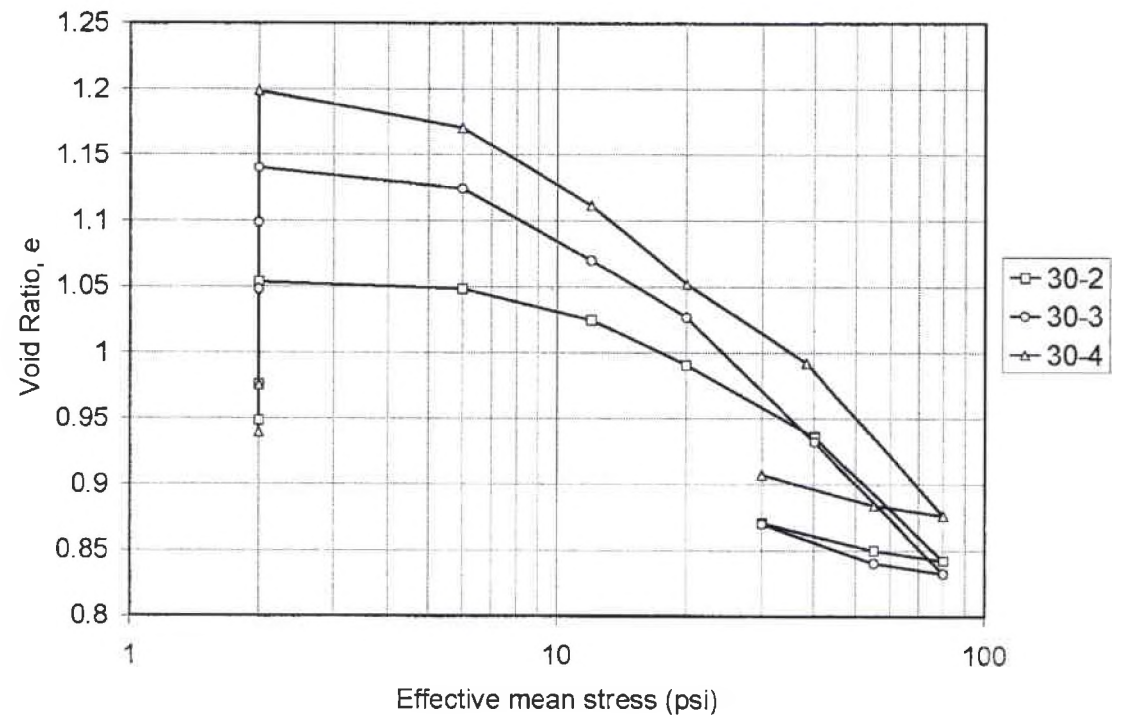

Figure 26 - Consolidation Test at 30 psi Confining Pressure
(Source: Berney 2004, 133)

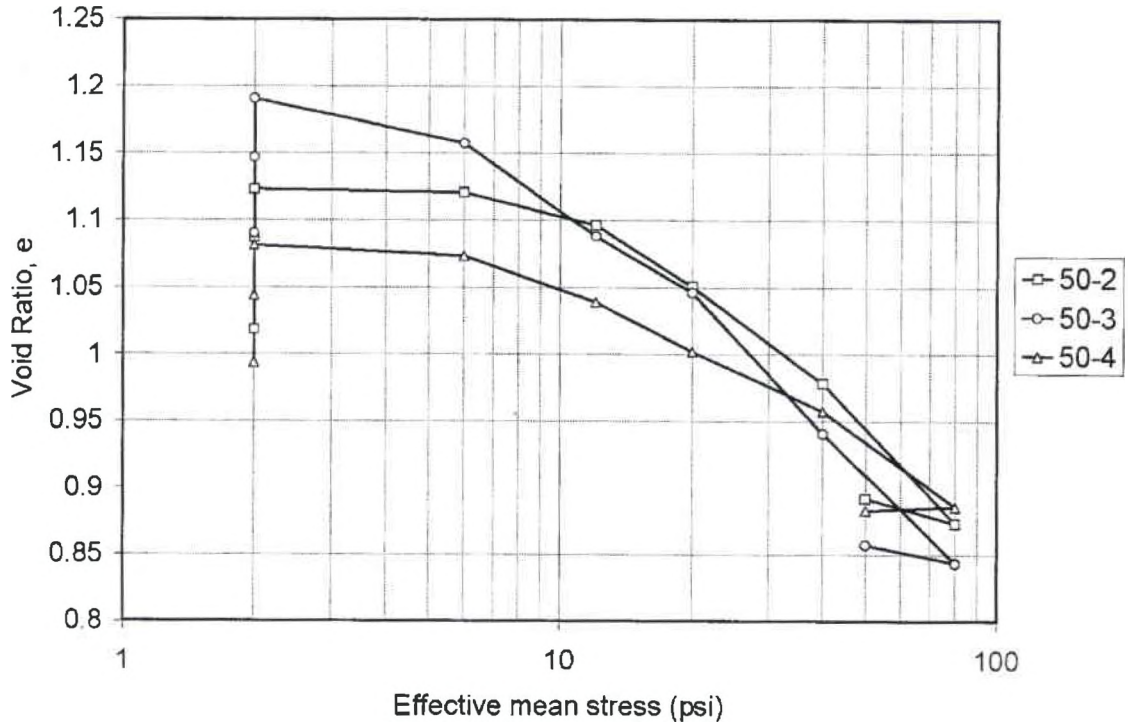

Figure 27- Consolidation Test at 50 psi Confining Pressure
(Source: Berney 2004, 134)

3.5.2 Correlation to Existing Data

Table 4 provides list of the compression and swelling indices for the one-dimensional consolidation tests performed for this study as well as those by Berney (2004).

Table 4 - Compression and Swelling Indices

Source (Testing ID)	C_c (1/psi)	C_s (1/psi)
Present Study (1)	0.442	0.126
Present Study (2)	0.429	0.126
Present Study (3)	0.415	0.100
Present Study (4)	0.392	0.103
Present Study Average	**0.420**	**0.114**
Berney (15-2)	0.378	0.063
Berney (15-3)	0.351	--
Berney (15-4)	0.283	0.126
Berney (30-2)	0.312	--
Berney (30-3)	0.332	0.084
Berney (30-4)	0.363	0.076
Berney (50-2)	0.348	0.114
Berney (50-3)	0.323	0.114
Berney (50-4)	0.237	--
Berney Average	**0.325**	**0.096**
Delta (Δ)	**0.095**	**0.018**

The average laboratory-determined values for the compression and swelling indices vary by 29 and 19 percent, respectively. In the context of soil consistency and the typical laboratory values derived form the literature as described in Section 4.2.1 and 4.2.6, the correlation can be reasoned acceptable.

3.6 California Bearing Ratio (CBR)

3.6.1 Laboratory Testing Results

The directive of the AFRL/MLBC was to model the airfield mats interacting with the soil subgrade with a CBR of 6. Buckshot clay was selected as the soil for

testing because this was the soil used in field tests at a CBR 6 condition. Cohesive soil strength and stiffness characteristics are governed in part by the density and void ratio of the sample at the time of testing. In order to properly represent a soil with a CBR of 6 in the finite element model, a relationship between initial conditions and CBR was required to be established. From this relationship the required density and moisture content to produce a CBR 6 soil could be derived. This unit weight and moisture content would become the required initial condition for the remolded sample to be used in triaxial testing. The triaxial test results are used to establish the slope of the critical state line, and are therefore critical to the derivation of the appropriate model input parameters.

Six sets of CBR tests were performed in two rounds of testing at a range of unit weight and moisture contents varying from 95.3 to 98.8 pcf and 8.8 to 17.9 percent, respectively, as shown in Figures 28 and 29 below. The first round of CBR tests was performed in accordance with the standard sample preparation process, which included saturation of the sample for 10 days prior to testing. The intent of this saturation is to represent the worst potential soil strength conditions expected to be encountered in the field; i.e. completely saturated. After the 10 day soak, the prepared samples had swelled and were measured at unit weights of 77.0, 79.4, and 82.9 pcf and moisture contents of 39.0, 34.5, and 31.0 percent, respectively. The significant lessening of the unit weights was a result of expanded volume due to swelling up to 23.8%. The results from this first round

of testing produced CBR values of 1.2, 1.3, and 1.5 percent, respectively. These first tests failed to provide independent conclusive evidence as to the required unit weight and moisture content to achieve a CBR of 6. It was apparent that it would be impossible to achieve a CBR of 6 for completely saturated Buckshot clay.

After a discussion of these primary test results with UDRI and AFRL/MLBC, it was determined that it would be unnecessary to simulate saturated conditions and that a partially saturated sample preparation would be acceptable. Given the moisture sensitivity of Buckshot clay, it was anticipated that by testing at a lower moisture content and not saturating the samples prior to testing, a significant increase of the CBR would be observed. A second round of testing was initiated. Three additional samples were prepared and the soaking stage was omitted. The tests produced CBRs of 49.1, 45.7, and 49.6 percent. This was far in excess of the required CBR 6 and confirmed the assumption that a change in moisture content would have dramatic impact on the soil stiffness.

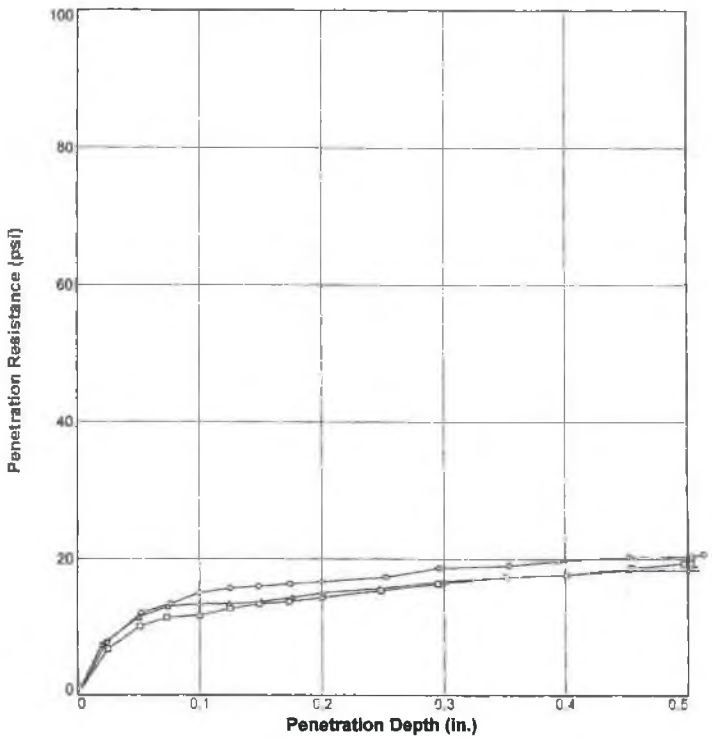

Figure 28 - Soaked CBR Test Results

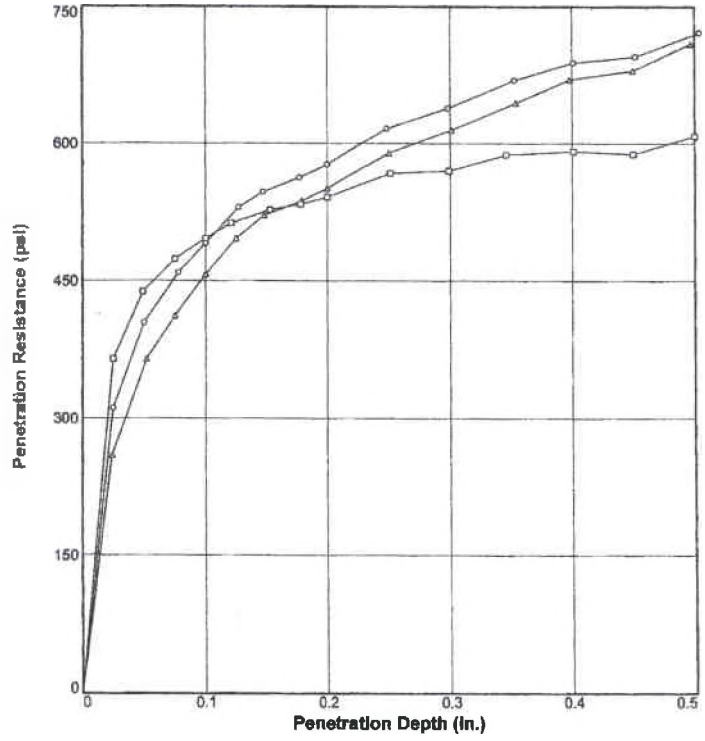

Figure 29 - Partially Saturated CBR Test Results

3.6.2 Correlation to Existing Data

The laboratory experimental data was plotted along with existing data as provided by the ACOE to produce a curve comparing the unit weight to CBR value for Buckshot clay. Figure 30 shows the CBR versus unit weight for each individual laboratory set of test results. It can be seen that both sets of data follow a similar trend of initial gradual increases in CBR as unit weight increased from 75 to 90 pcf, followed by a marked exponential increase over the remaining unit weight range from 90 to 105 pcf.

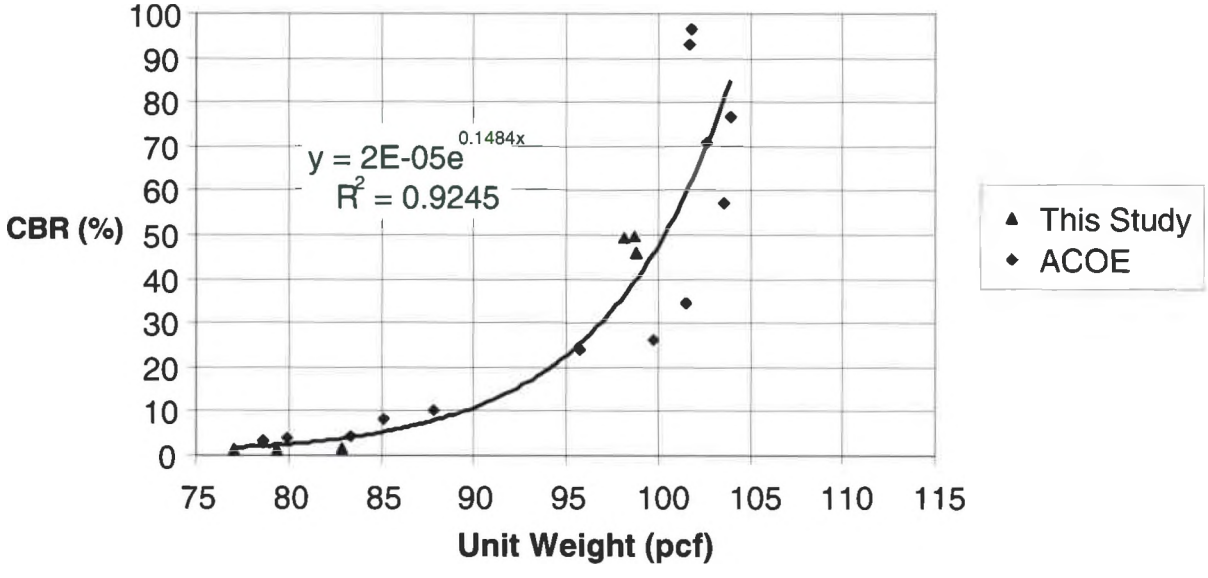

Figure 30 - Data and Trendline for Unit Weight vs. CBR

An equation describing the relationship between CBR and unit weight was prescribed by combining the two sets of data together and applying an

exponential trendline as shown in the insert in Figure 30. The R^2 value was calculated as 0.9245 and is considered acceptable given the relatively scattered nature of the data.

Using the exponential equation trendline the unit weight required to produce a CBR of 6 for the Buckshot soil was calculated at 84.98 pcf. The moisture content required for a CBR of 6 was determined to be approximately 34 percent as interpolated from the Army Corps data shown in Figure 31.

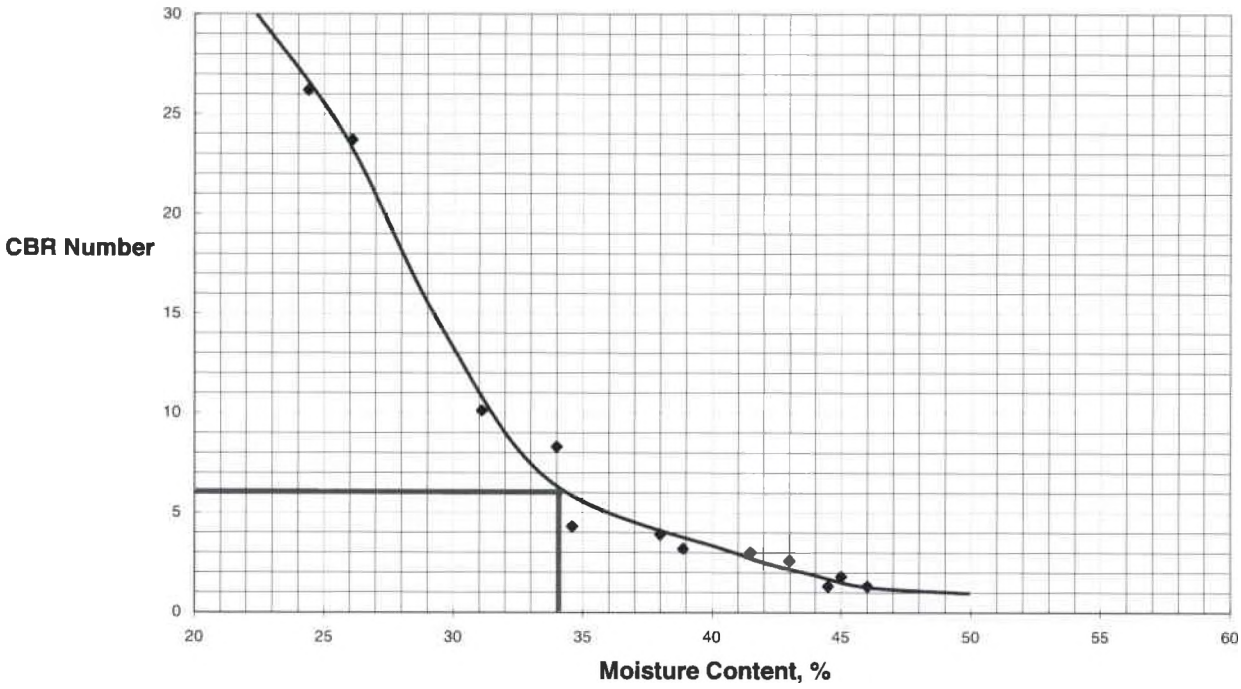

Figure 31 - CBR vs. Moisture Content (Source: Tingle 2006)

3.7 Triaxial Tests

3.7.1 Laboratory Test Results

One consolidated-undrained (CU) triaxial shear test was completed for this study. Figures 32, 33, and 34 provide plots of deviator stress versus axial strain, pore pressure versus axial strain, and the *p' – q'* diagram, respectively for the testing in this study. Figure 35 provides the *p' – q'* diagram for the CU triaxial tests by Berney (2004). Deviator stress is defined as the axial stress (P) acting on the sample as a result of the piston pressure, and is calculated as P divided by the area (A) of the specimen cap, which in this case is the surface area of the porous stone. The p' – q' diagram is a modified Mohr-Coulomb diagram wherein p' is defined as $(\sigma_1 + \sigma_3)/2$ and q' is defined as $(\sigma_1 - \sigma_3)/2$. Note that in the case of this testing σ_2 equals $\sigma_{3,}$, and therefore p' in this case is equivalent to Equation 4 described previously. However, q' is defined differently in this application than the definition provided in Equation 3. By plotting the effective values of p' and q' at specimen peak strength of a series of CU triaxial tests the Mohr-Coulomb failure envelope for effective stresses can be determined.

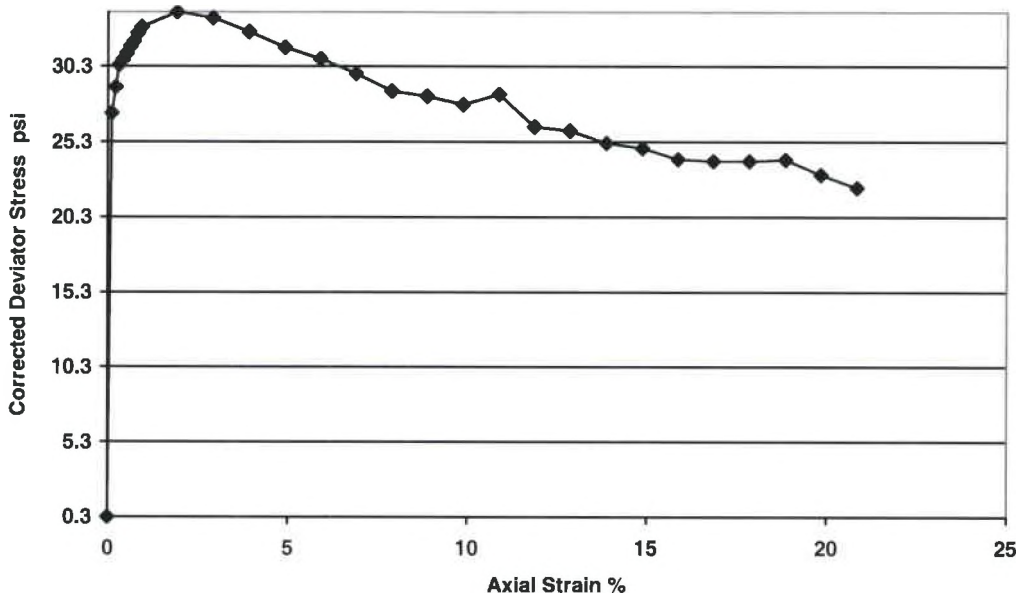

Figure 32 - Deviator Stress vs. Axial Strain

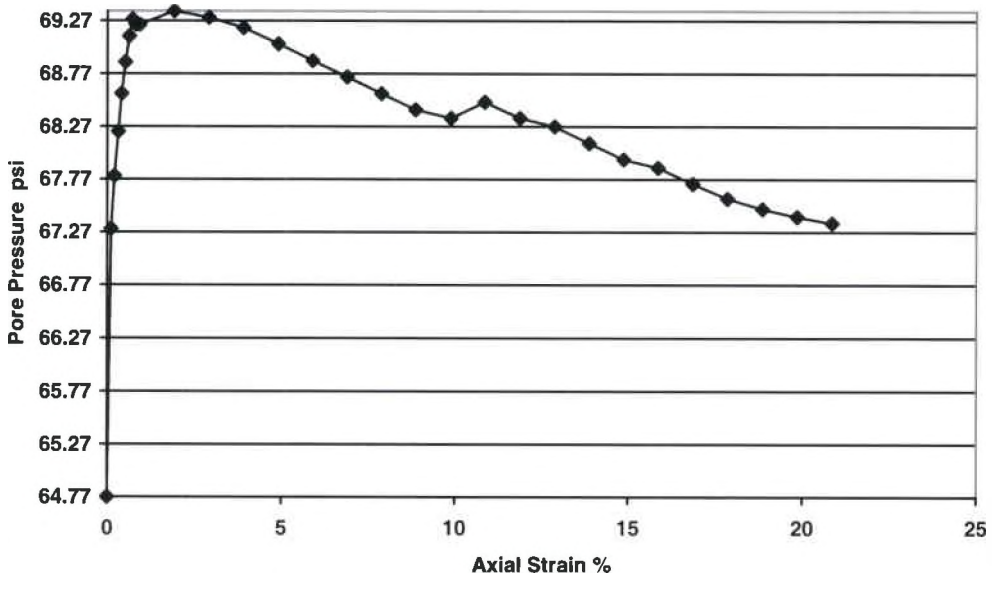

Figure 33 - Pore Pressure vs. Axial Strain for CU Triaxial Test

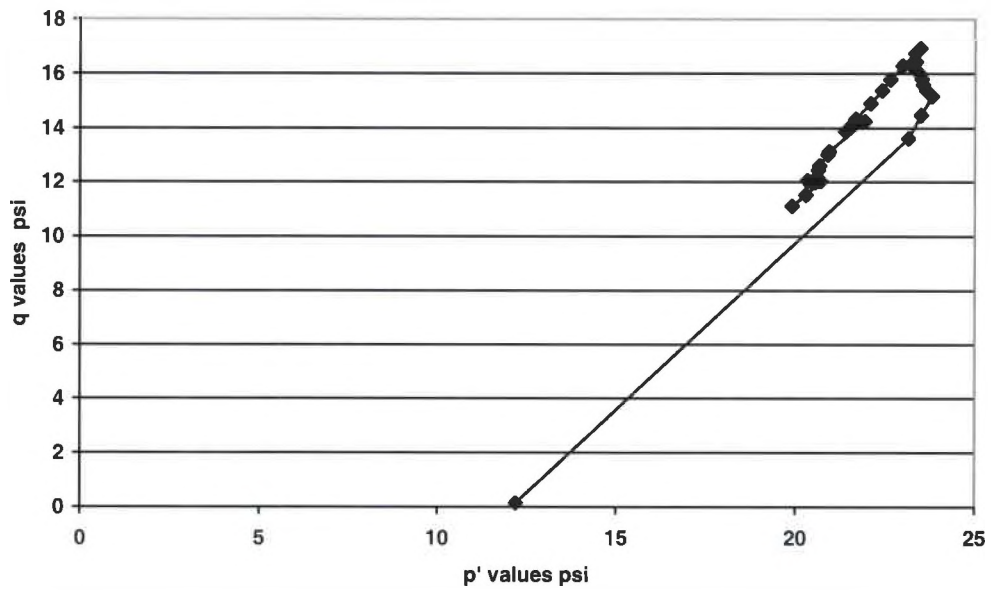

Figure 34 - p' – q' Diagram for CU Triaxial Test

Figure 36 represents the Mohr-Coulomb failure surface for the CU triaxial testing by Berney (2004) and Peters (1982) as plotted on a p' – q' diagram. Note that Peter's data shows a higher friction angle, and thus a greater strength, than Berney's data. This is due to the sample preparation methods for each. Peters prepared his samples by a slurry method while Berney employed a compaction method. The slurry method produces a sample that is more consistent throughout and has a higher density than if prepared by a compaction method, which leads to the observed greater strength. The specimens prepared for this study employed the compaction method of sample preparation and are subsequently expected to fall closer to Berney's curve.

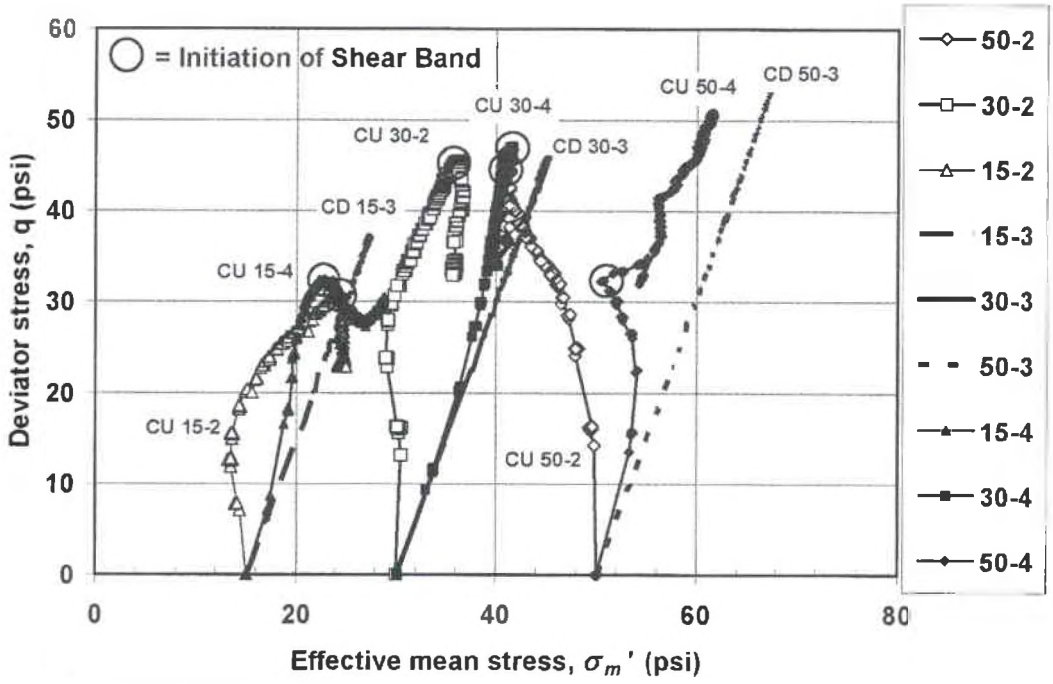

Figure 35 - p' – q' Diagram by Berney (2004, 164)

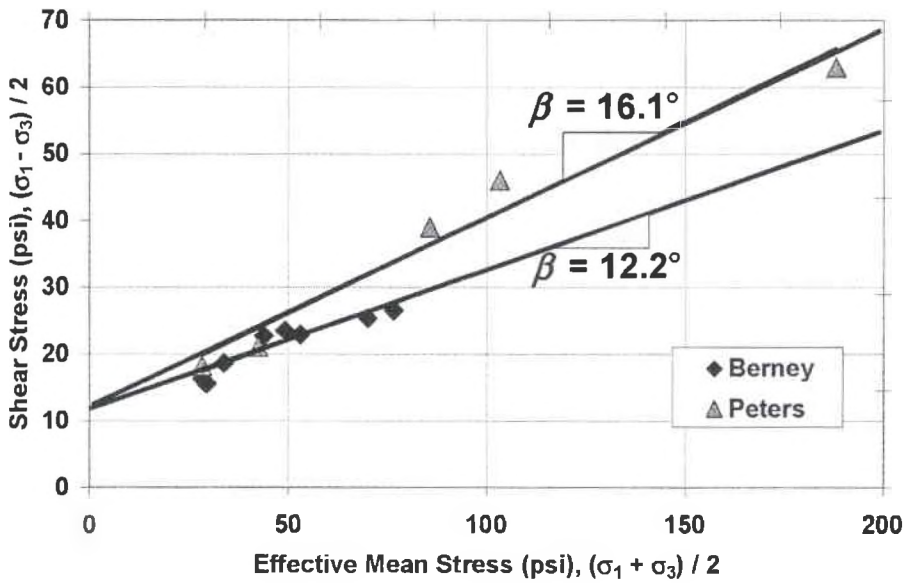

Figure 36 - Modified Mohr-Coulomb Failure Surface for Buckshot Clay by Berney and Peters (Berney 2004, 167)

The determination of true peak and ultimate strength of Buckshot clay is difficult to obtain in laboratory testing due to a phenomenon called shear banding. According to Berney (2004),

> "Shear-banding is the result of a premature failure occurring within the sample during triaxial shear in which a localized plane of weakness or slip plane is generated... A slip plane is a saturated surface passing diagonally through the triaxial specimen that separates it into two angular halves that continue to slide relative to one another without any further change in material behavior with increased loading." (162)

The significance of this is that the test specimens, after shear banding, do not reach their ultimate strength states. Additionally, the peak strength is associated with the strength at which shear banding has occurred which may not represent that soil's true peak strength. The CU triaxial test performed in this study exhibited shear banding similar to that observed in Berney's testing as demonstrated in Figure 37.

A picture of the shear band failure surface within the triaxial sample is provided in Figure 38. The picture shows the shiny slickenside surface, which is characteristic of the slip plane of a failed cohesive soil. Additionally, a piece of gravel observed within the sample along the failure plane is likely to have caused a stress concentration within the sample wherein the slip surface formed.

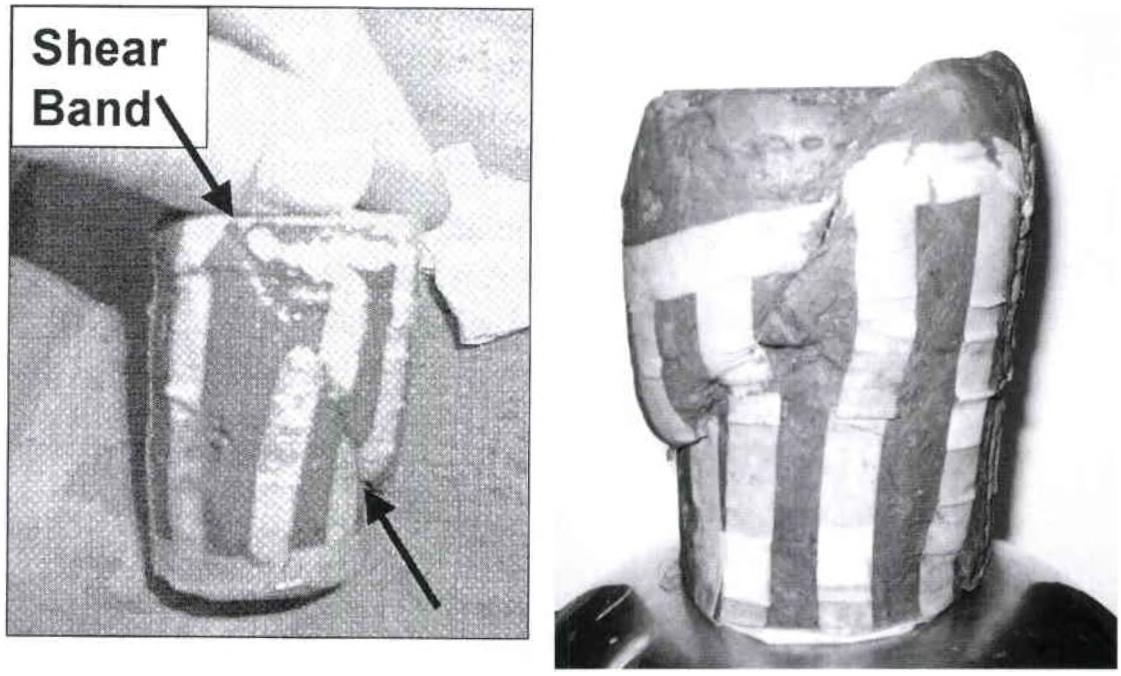

(a) (b)

Figure 37 - Shear Band Surfaces by (a) Berney (2004, 162) and (b) This Study

Figure 38 - Failure Surface within Shear-Banded Triaxial Specimen

3.7.2 Correlation to Existing Data

As stated previously, the Mohr-Coulomb failure surface can be determined by evaluating the peak stress states for a series of CU triaxial tests. The curve that is fit to represent the trend of these tests defines the shear strength characteristics of the given soil. Figure 39 is a modification of Figure 36 to include the peak stress state as evaluated in this study. As was predicted, the peak stress state for this study fell on the trendline for the samples by Berney prepared by the compaction method.

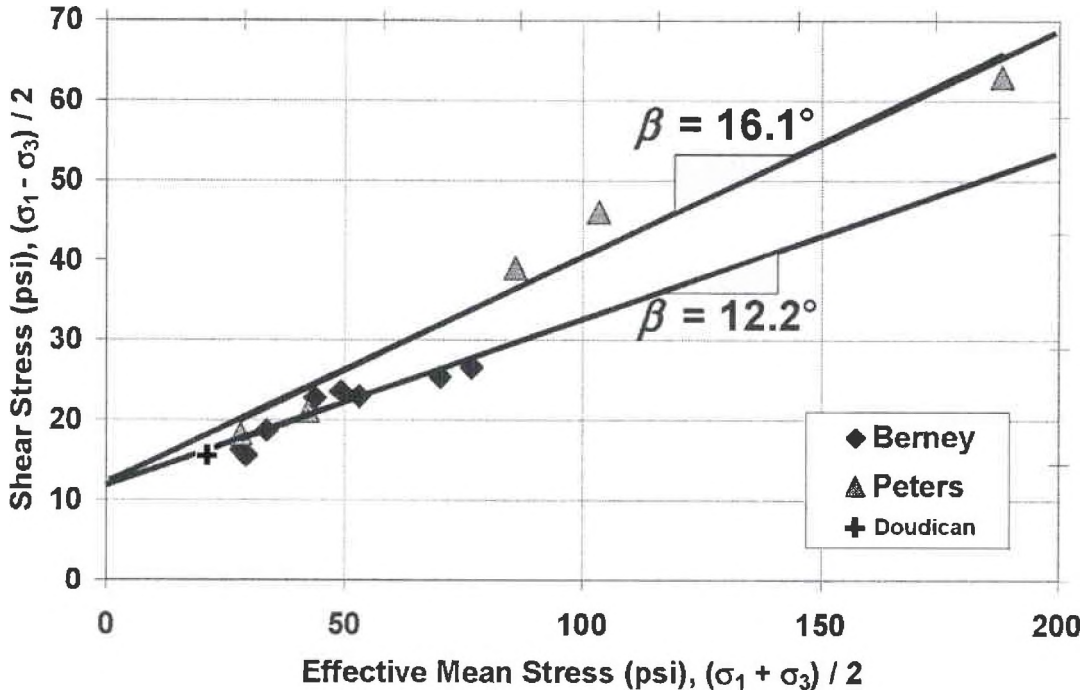

Figure 39 - Modified Mohr-Coulomb Failure Surface for Berney, Peters, and This Study (Modified from Berney 2004, 167)

CHAPTER 4 – SOIL MODELING

4.1 Introduction

A successful correlation has been established between the Buckshot clay tested in this study and the reference database. Additionally, gaps in the available soil data have been filled by the laboratory testing. To complete the establishment of input parameters for the soil model, this chapter will:

- Derive values of ABAQUS Extended Modified Cam Clay model parameters employing the correlated laboratory data;
- Calibrate the soil model to produce a CBR 6 soil response in a finite element model of the CBR testing apparatus;
- Review the findings of an instrumented field test of the composite airfield matting and CBR 6 subgrade as performed by the Army Corps of Engineers;
- Evaluate the calibrated soil model response with respect to the findings of the field testing;
- Recalibrate the soil model as required to achieve optimum correlation to the field testing.

4.2 Derivation of Input Parameters from Lab Testing and Correlations for Use in the ABAQUS Extended Modified Cam Clay Model

4.2.1 Logarithmic Bulk Modulus

The logarithmic bulk modulus, kappa (κ), is a soil constant defined by the average slope of the unload-reload line on a one-dimensional consolidation graph. As described in Section 1.6.1, κ is used to provide a linear elastic volumetric response. As κ is defined in the $e - \ln p$ space, its value can be derived from the soil swelling constant C_s as:

$$\kappa = \frac{C_s}{\ln 10} \qquad \text{(Eq. 7)}$$

For the purpose of this study, four one-dimensional consolidation tests were performed on samples of Buckshot clay. In addition, six additional one-dimensional consolidation tests with unloading stages were performed on the same material by Berney (2004) on the same soil. Table 5 summarizes the results of each study.

Table 5 - Summary of Lab-Derived Kappa Values

Source (Testing ID)	Cs (1/psi)	κ (1/psi)
Present Study (1)	0.126	0.0548
Present Study (2)	0.126	0.0548
Present Study (3)	0.100	0.0433
Present Study (4)	0.103	0.0448
Present Study Average	**0.114**	**0.0498**
Berney (15-2)	0.063	0.0273
Berney (15-4)	0.126	0.0546
Berney (30-3)	0.084	0.0364
Berney (30-4)	0.076	0.0330
Berney (50-2)	0.114	0.0495
Berney (50-3)	0.114	0.0495
Berney Average	**0.096**	**0.0417**
Delta (Δ)	**0.018**	**0.0077**

There are numerous references in the literature that provide tables of typical C_s values. Table 6 outlines some typical values of C_s as provided by Das, and the corresponding calculated value of κ.

Table 6 - Summary of Literature-Derived Kappa Values (Das 2000, 167)

Description	Cs	κ
Boston blue clay	0.07	0.03
Chicago clay	0.07	0.03
New Orleans clay	0.05	0.02
Montana clay	0.05	0.02
Average	0.06	0.025
Delta (Δ)	0.02	0.01

It can be seen that the laboratory-determined values for C_s and κ are within the same scale of magnitude and difference in value (delta) as other cohesive soils in the United States. It is reasonable that the C_s values for Buckshot clay are on

the higher end of most others in the literature because of its observed affinity for water and subsequent tendency to swell. As the pressure is released during unloading, Buckshot clay tends to expand at a greater magnitude than other less water-affinitive soils and the void ratio increases at a greater rate. For the purpose of model calibration the values of κ should be calibrated from an initial value of 0.045, the combined data average.

4.2.2 Poisson's Ratio

Poisson's ratio (ν) is the ratio of the contraction strain normal to the applied load divided by the extension strain parallel to the applied load. Most mechanical materials have a Poisson's ratio that falls within the range of 0.0 to 0.5. Measurement of Poisson's ratio for a given soil is challenging in that the soil is likely to be highly heterogeneous within any given sample and is difficult, if not impossible, to measure in the laboratory. Thus, an average Poisson's ratio based on established literature is typically used.

The U.S. Army Corps of Engineers has produced several comments on the Poisson's ratio for various soil types. The following table was compiled from the U.S. Army Corps of Engineers (1990), Joint Departments of the Army and Air Force (1983), and Das (2000):

Table 7 - Typical Values of ν from the Literature

	Poisson's Ratio
Saturated Clays [1]	0.5
Partly Saturated Clays [1]	0.3
All Soils, Range, with Saturated Soils Approaching 0.49[2]	0.25 – 0.49
Reasonable Value[2]	0.4
Medium Clay[3]	0.20 – 0.50
Sand and Gravel[3]	0.15 – 0.35

[1] TM 5-818-1, pg 5-4; [2] EM 1110-1-1904, pg. D-12; [3]Das, pg. 125

For the purpose of model calibration, Poisson's ratio should be calibrated from an initial value of 0.03, the average of the cohesive soils values.

4.2.3 Elastic Tensile Limit

The elastic tensile limit, $P_t(el)$, is the maximum allowable tensile stress, for the constitutive model. This parameter is used by the ABAQUS "Porous Elasticity" material model to describe the elastic tensile behavior. For Buckshot clay, and most soils, the tensile strength is assumed to be zero.

4.2.4 Initial Void Ratio

The initial void ratio, e_0, is calculated by dividing the volume of voids by the volume of solids in a soil specimen. "Void" is defined as the volume within the sample filled by either water or gas. The void ratio is affected by the unit weight of a sample, and thus for the purpose of this model the void ratio is required to be

known at 85 pcf, the unit weight that produces a CBR equal to 6. Void ratio can be determined from a one-dimensional consolidation test; however, no one-dimensional consolidation tests were performed with samples at a unit weight of 85.0 pcf. In order to determine the initial void ratio for this constitutive model, linear extrapolation is required. Figure 40 compares the initial void ratio versus unit weight for the four consolidation tests performed in this study as well as the resultant linear trendline established.

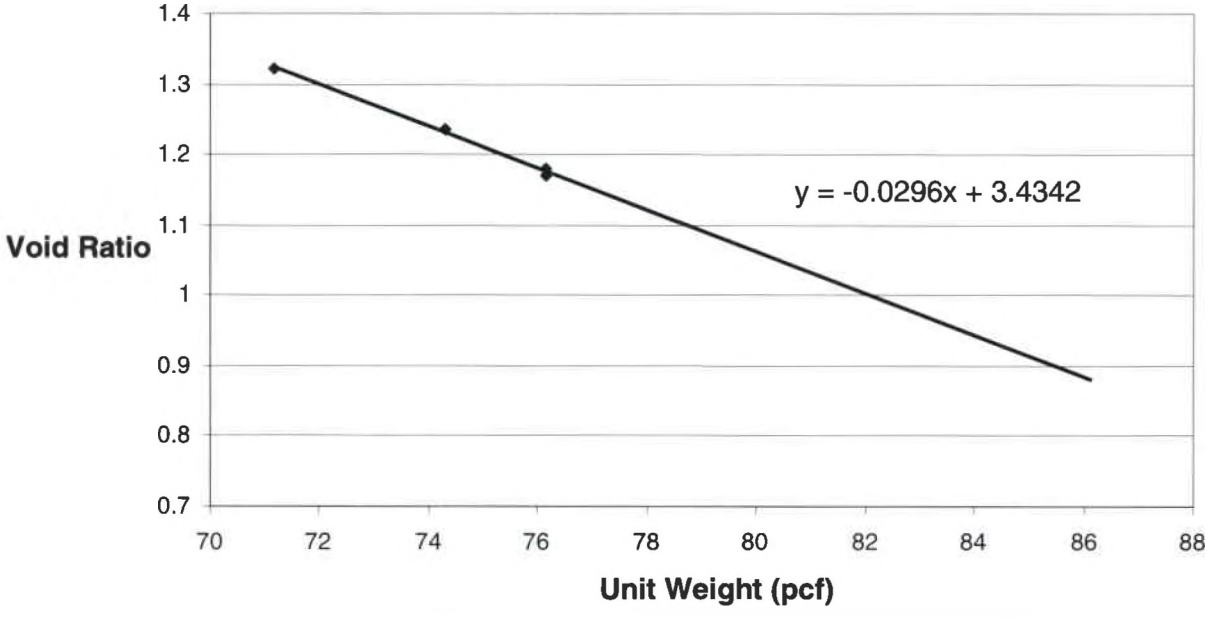

Figure 40 - Void Ratio vs. Unit Weight Including Trendline

Based on the linear extrapolation shown above, the initial void ratio should be approximately 0.92 at a unit weight of 85 pcf for this constitutive model. ABAQUS provides the option to vary the void ratio as a linear function of depth. Given that the subgrade depth influenced in this analysis is relatively shallow,

such that the overburden soil pressures are unlikely to have caused a significant change in soil void ratio, it is recommended that a constant void ratio be maintained throughout all depths.

4.2.5 Initial Pressure Stress

The user-input initial pressure stress, P_0, is used by ABAQUS to establish equilibrium in the first iterative steps of the numerical analysis and to establish the size of the initial yield surface. The user has the choice to enter two separate initial pressure intensities, one for each usage by ABAQUS, or to allow one input to represent both cases. For this discussion, we shall define the two cases as "Equilibrium" and "Yield Surface."

4.1.5.1 Initial Pressure Stress – "Equilibrium"

For the "Equilibrium" case, ABAQUS uses the input initial pressure stress to reconcile any numerical differences between the user-input initial horizontal and vertical pressure stresses, boundary conditions, and pore fluid pressures to the numerically-calculated values in the first iterations of the analysis. Depending on the type of finite element model being evaluated, the user may determine to use this method if the initial pressure on the system is known and no densities have been input for the various materials in the model. The ABAQUS software will skip all gravity loading and induce the input initial pressure at time zero. From

this initial pressure state ABAQUS will iteratively attempt to achieve equilibrium prior to proceeding to the next step. For the case of the finite element CBR model used for calibration in this study, the equilibrium initial pressure method was employed using an initial pressure of -1.0 psi, the seating pressure of the piston and confining ring.

4.1.5.2 Initial Pressure Stress – "Yield Surface"

For the "Yield Surface" case, the initial pressure stress is defined as the initial value of the equivalent total pressure stress acting on the soil as a function of pore pressures, vertical (typically gravitational) loading, horizontal (typically earthquake) loading, and boundary conditions. This initial stress state should take into account both the stress history of the soil (the overconsolidation state) as well as the current imposed pressure stresses. For the purpose of this study, the soil is assumed to be in a "normally consolidated" stress state. "Normally consolidated" means that the existing in-situ soil stress state is the maximum ever experienced by the soil. The only in-situ stresses acting on the soil are due to gravity effects on the overlying soil stratum and pore pressures due to 100 percent saturation of the soil sample. No horizontal loading should be included. As provided by ABAQUS (2005) the equation for determination of the existing pressure stress is:

$$\sigma_{zz} = \gamma_{(dry)} * (z - z_0) - \gamma_{(water)} * (1 - n_0) * (z - z_{w0}) \qquad \text{(Eq. 8)}$$

where $\gamma(dry)$ is the dry unit weight of the soil, z is the elevation for which the pressure is being determined, z_0 is the elevation of the surface of the porous media, $\gamma(water)$ is the unit weight of water, n^0 is the ratio of the initial void ratio to the initial specific volume, and z_w^0 is the elevation of the phreatic surface. For this model, the dry unit weight is equal to 85 pcf, $z_0=z_w^0=0$, the unit weight of water is 62.4 pcf, and $n^0=(0.92)/(1.92)=0.479$, as derived from the laboratory testing. The value of z is dependent on the depth of soil intended to be modeled.

If we assume, for the purpose of calibration with existing load cell data, that the soil is at a depth of 15 inches below grade and that the soil density is 85 pcf, the resulting stress acting on an infinitely small representative soil sample is 65.61 psf or 0.456 psi.

In theory, the initial stress state of a soil sample and the stress induced upon it should cancel one another in equilibrium, producing zero net initial displacement of the sample. ABAQUS performs an initial geostatic load step to ensure that this is true, and will make moderate adjustments to a_0 to ensure compliance if there are small discrepancies, or abort the iteration process altogether in the event of large discrepancies.

4.2.6 Logarithmic Hardening Modulus

Lambda (λ) is a soil constant defined by the average slope of the virgin consolidation line on a one-dimensional consolidation graph. As described above, λ is the logarithmic hardening constant that defines the plastic compressibility characteristics of the clay. Because λ is defined in the *e – ln p* space, its value can be derived from the soil swelling constant C_c as:

$$\lambda = \frac{C_c}{\ln 10} \qquad \text{(Eq. 9)}$$

where:

$$C_c = \frac{e_{(n+1)} - e_{(n)}}{\log p_{(n+1)} - \log p_{(n)}} \qquad \text{(Eq. 10)}$$

and *n* and *n+1* are the data points that characterize the slope of the virgin consolidation line.

For the purpose of this study, four one-dimensional consolidation tests were run on samples of Buckshot clay. In addition, nine one-dimensional consolidation tests were performed on the same soil by Berney (2004). Table 8 outlines the findings of each study.

Table 8 - Summary of Lab-Derived Lambda Values

Source (Testing ID)	C_c (1/psi)	λ (1/psi)
Present Study (1)	0.442	0.192
Present Study (2)	0.429	0.186
Present Study (3)	0.415	0.180
Present Study (4)	0.392	0.170
Present Study Average	**0.420**	**0.182**
Berney (15-2)	0.378	0.164
Berney (15-3)	0.351	0.152
Berney (15-4)	0.283	0.123
Berney (30-2)	0.312	0.135
Berney (30-3)	0.332	0.144
Berney (30-4)	0.363	0.158
Berney (50-2)	0.348	0.151
Berney (50-3)	0.323	0.140
Berney (50-4)	0.237	0.103
Berney Average	**0.325**	**0.141**
Delta (Δ)	**0.095**	**0.041**

An extensive amount of research has been compiled in the literature regarding typical values for C_c. Table 9 outlines the findings of Holtz and Kovacs (1981), and the calculated corresponding values of λ.

Table 9 – Summary of Literature-Derived Lambda Values
by Holtz and Kovacs (1981)

Description (USCS Classification)	C_c (1/psi)	λ (1/psi)
Normally consolidated medium sensitive clays	0.2 to 0.5	0.086 to 0.217
Chicago silty clay (CL)	0.15 to 0.30	0.065 to 0.130
Boston blue clay (CL)	0.3 to 0.5	0.130 to 0.217
Vicksburg Buckshot clay (CH)	0.5 to 0.6	0.217 to 0.261
San Francisco Bay Mud (CL)	0.4 to 1.2	0.174 to 0.521
San Francisco Old Bay clays (CH)	0.7 to 0.9	0.304 to 0.391

It can be seen that the laboratory-determined values for λ fall within the range of values observed in other cohesive soils as described in the literature. For the purpose of model calibration the values of κ should be calibrated from an initial value of 0.154, the combined data average.

4.2.7 Critical State Ratio

The Critical State Ratio, *M*, is the slope of the critical state line, as defined previously. As the plastic volumetric strains of a stressed sample approach the critical state, the sample tends towards constant strain without change in stress or volume. Subsequently, a relationship has been established relating the ultimate value of the angle of shearing resistance to *M*, as follows:

$$M = \frac{6\sin\phi}{3-\sin\phi} \qquad \text{(Eq. 11)}$$

As discussed previously, the determination of ultimate shear strength for a sample of Buckshot clay is difficult due to shear banding. To overcome the inherent limitations imposed on the ability to determine peak strength parameters, a series of p' – q' diagrams have been plotted together and evaluated for trends. A plot of the p' – q' diagrams for tests by Berney (2004) and Peters (1982) up to and including the point of shear banding is shown in Figure 41. This data is for both saturated and unsaturated soil specimens, and as such the values of mean (p') and shear (q') stress have been normalized by

an appropriate reference pressure (Berney 2004, 70). A discussion of unsaturated soil mechanics and reference pressures is beyond the scope of this study.

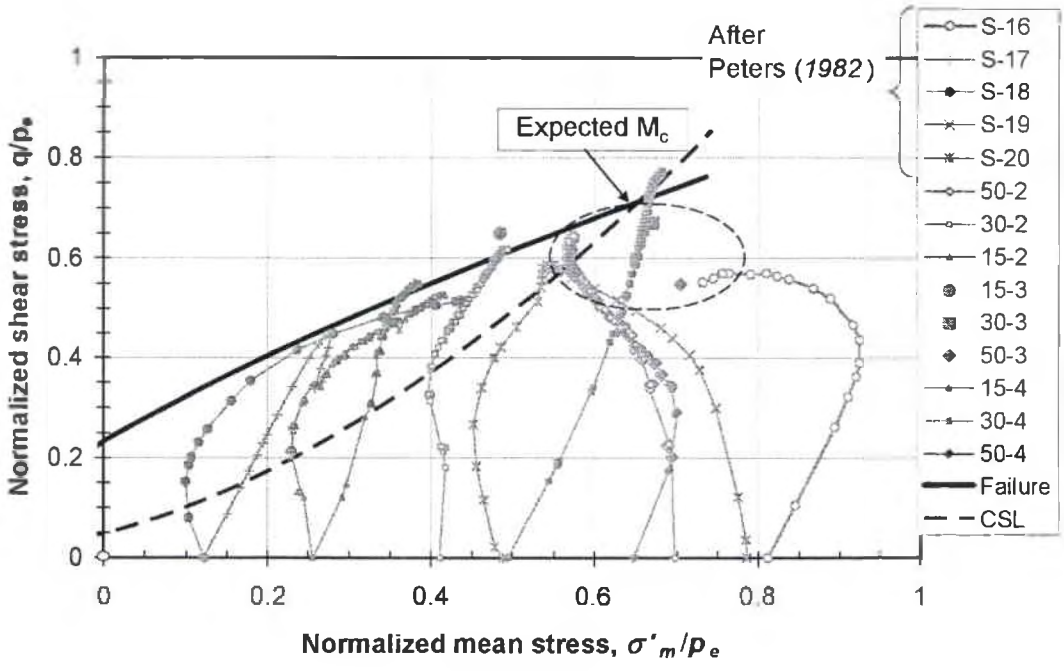

Figure 41 – Stress Paths with Failure Surface and Critical State Line (Source: Berney 2004, 167)

The solid line in the figure represents the Mohr-Coulomb failure surface, which was evaluated based upon the trend of shear banding failure for the tests. The dashed line represents the trend of the critical state line, which is the visually-interpreted line that follows a path tangent to the tail ends of the stress paths. In soils that do not exhibit shear banding, the critical state line is equivalent to the failure surface. The discrepancy in this diagram is due to the shear banding effect, which does not permit a true, non-shear banded failure stress path to be established. However, the trends of the critical state lines and the failure surface

lines progress towards one another. This intersection point represents the anticipated point of maximum yield stress the soil can be expected to resist prior to initiation of plastic failure, or critical state. The slope of the critical state line can be evaluated using this point, plus or minus a tolerance inherent in the curve fitting. From this evaluation, Berney predicted that the value of *M* for Buckshot clay is represented by an average value of 1.02.

4.2.8 Initial Overconsolidation Parameter

The parameter "*a*" is used to define the size of the yield surface within the Modified Cam Clay model. The initial overconsolidation parameter, a_0, is the size of the yield surface at initiation of loading and is given by the equation

$$a_0 = \frac{1}{2}\exp\left(\frac{e_1 - e_0 - \kappa \ln p_0}{\lambda - \kappa}\right) \text{ (psi)} \qquad \text{(Eq. 12)}$$

where p_0 is the value of the initial equivalent pressure stress and e_1 is the intercept of the virgin consolidation line with the void ratio axis in $e - \ln p$ space as shown in Figure 42.

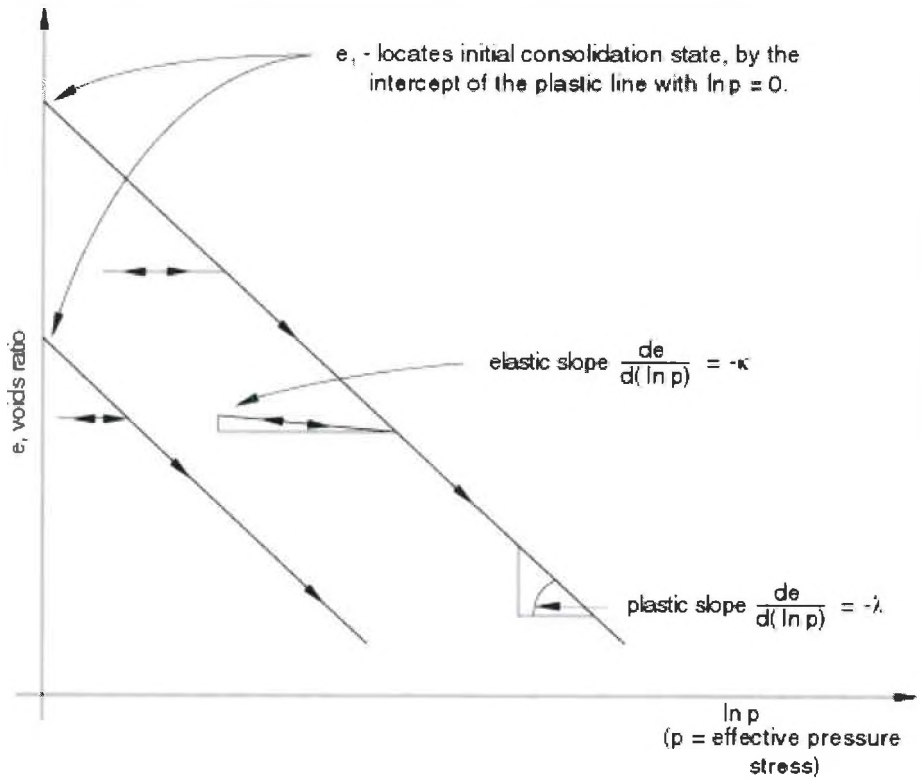

Figure 42 - Graphical Representation of e_1 (ABAQUS Theory Manual 4.4.3)

To define a_0 in ABAQUS, the user must define e_0, e_1, λ, κ, *and* p_0. These parameters, with the exception of e_1, were defined in previous sections of this report. The value of e_1 as determined through testing by Berney and this study was calculated as show in Table 10.

For the purpose of model calibration, e_1 should initially be input as 1.61, the average of the combined data.

Table 10 - Summary of Laboratory-Derived e_1

Source (Testing ID)	e_1
Present Study (1)	1.84
Present Study (2)	2.04
Present Study (3)	1.91
Present Study (4)	1.79
Present Study Average	**1.90**
Berney (15-2)	1.53
Berney (15-3)	1.48
Berney (15-4)	1.40
Berney (30-2)	1.47
Berney (30-3)	1.53
Berney (30-4)	1.58
Berney (50-2)	1.50
Berney (50-3)	1.42
Berney (50-4)	1.39
Berney Average	**1.48**
Delta (Δ)	**0.42**

4.2.9 Wet Yield Surface Size

The wet yield surface size, beta (β), is a user-specified constant used to control the shape of the yield surface on the wet side of the critical state. It allows the user to create a two-piece yield surface with two different degrees of curvature for the yield surface ellipses; one for each side of the critical state. β is typically taken as 1.0 on the dry side of critical and varied from 0.5 to 1.0 on the wet side of critical, with 1.0 representing the original formulation of the Modified Cam Clay model. According to the ABAQUS Analysis User's Manual, β is calibrated from a series of triaxial tests performed at high confining pressures. The completion of these high confining pressure triaxial tests exceeds the limitations of the lab

equipment and was beyond the scope of this study. For the purpose of model calibration β should be assumed to be equal to 1.0, and can be varied between 0.5 and 1.0 as a supplemental calibration parameter, as required.

4.2.10 Flow Stress Ratio

The flow stress ratio, *K*, is defined as the ratio of the flow stress in triaxial tension to the flow stress in triaxial compression, and, as described above, determines the shape of the yield surface in the principal deviatoric stress plane. *K* controls the yield dependence on the third stress invariant, and calibration is obtained by performing a series of true cubical triaxial tests. These tests are beyond the capabilities of most laboratories, and ABAQUS recommends the use of a user-defined value for *K* or ignore this effect altogether which will default to $K = 1.0$. The original Modified Cam Clay model is represented by $K = 1.0$, and this value should be used in the modeling for this project.

4.3 Summary of Modified Cam Clay Model Parameters

Table 11 provides a summary of the Modified Cam Clay Model parameters as derived from the laboratory testing results and other data from the literature.

Table 11 - Summary of the Modified Cam Clay Model Initial Values

Variable	Initial Value
Kappa (κ) (1/psi)	0.045
Nu (v)	0.3
$P_{t(el)}$ (psi)	0
e_0	0.92
P_0 (Equilibrium) (psi)	-1.0
Lambda (λ) (1/psi)	0.154
M	1.02
e_1	1.61
β	1.0
K	1.0

4.4 Model Calibration

4.4.1 Introduction

The purpose of this study is to produce a constitutive soil model to represent a CBR 6 Buckshot clay soil subgrade for the finite element analysis of the fiber reinforced polymer composite airfield matting panels. The requisite laboratory testing has been performed and adequate correlations have been established to produce a compiled reference database of soil parameters. These parameters have been evaluated in the context of the ABAQUS Extended Modified Cam Clay constitutive soil model and the value of anticipated initial input variables has been produced. Calibration is the final stage required to meet the scope of this study.

Two stages of calibration have been undertaken to produce a set of constitutive soil model input parameters. The first stage calibrated the Buckshot clay model

input parameters for a finite element model of the CBR testing apparatus to produce the CBR 6 curve. The second stage evaluated the calibrated soil material input parameters in a finite element model of the field testing configuration at Tyndall Air Force Base as compared to the pressure cell data acquired from the field testing. As required, additional soil model calibration was performed to improve correlation of the finite element model soil response characteristics to those measured in the field.

While the finite element analysis and calibration of the CBR model was performed by the author of this study, the ABAQUS finite element base model input file upon which the calibration model was built was created by Dr. Geoff Frank of UDRI. Additionally, given the CPU capacity required and proprietary nature of the finite element model input files, Dr. Frank performed all finite element analyses of the airfield matting system field tests on the Air Force ASC/HPC computer network, and produced the post-process analyses of the performance of various soil models provided by the author.

4.4.2 Calibration to Standard CBR 6 Curve

In the first stage of calibration, the finite element model input parameters were iterated to produce a stress-displacement diagram that mirrors the standard CBR curve using the initial parameter values derived from the laboratory testing along with the correlated reference database. The standardized stress-strain curve

representing a CBR of 100 was produced in accordance with ASTM D1883 and scaled by a factor of 0.06 to produce the standard CBR 6 curve shown in Figure 43. The goal of model calibration, then, was to reproduce the CBR 6 curve using the ABAQUS Extended Modified Cam Clay (MCC) constitutive soil model.

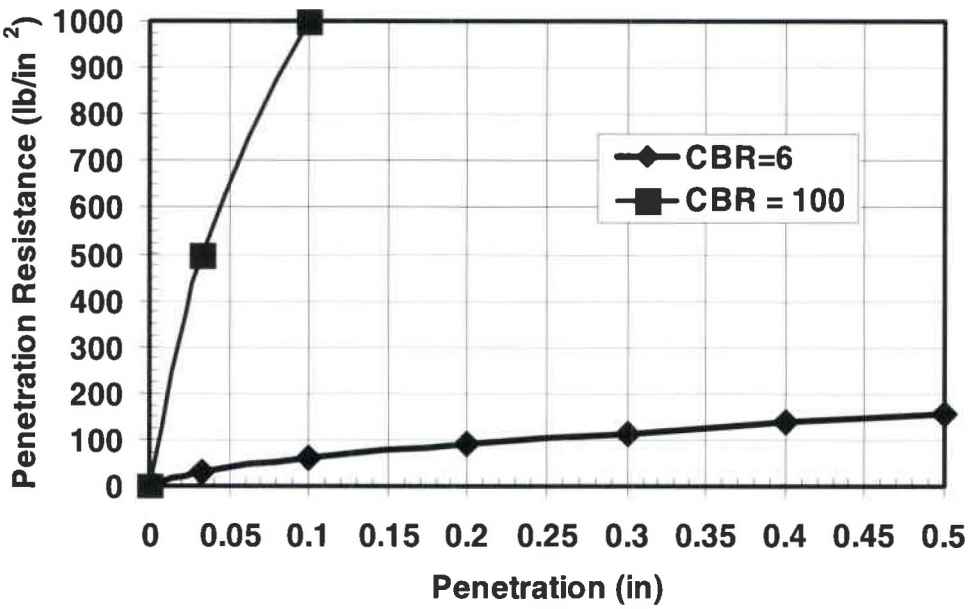

Figure 43 - Standardized CBR Curves (Source: Frank 2006)

Frank and Whitney (2005, 5) concluded that the approximate range of soil moduli for the Buckshot clay at CBR of 6 would fall between 1,500 and 4,500 psi. To be conservative, they employed a linear elastic modulus of 1,500 psi to describe the soil response characteristics in the initial airfield matting finite element analyses. In addition, Frank and Whitney concluded that the subgrade soils would be subject to strains of up to eight percent. An eight percent strain for the CBR curve, which represents a soil column five inches in height, is equal to 0.4 inches. Accordingly, it is the soil model response from 0.0 to 0.4 inches which is most

important in the airfield matting finite element analysis. Figure 44 shows the stress-strain response of these two linear elastic moduli in comparison to the CBR 6 curve. The 4,500 psi line more accurately reflects the initial trends of the CBR 6 curve, but over-predicts the actual plastic stiffness at penetration greater than 0.05 inches. The 1,500 psi line more accurately reflects the long-term trends, but under-predicts the initial elastic soil stiffness. As discussed previously, both the elastic and plastic stiffness response is critical to the accurate modeling of the airfield matting. Under F-15 tire loads the majority of the soil model will experience elastic unloading and reloading, while the area very near to the tire footprint will experience plastic strains. A more accurate non-linear elastic-plastic model will significantly improve upon these deficiencies.

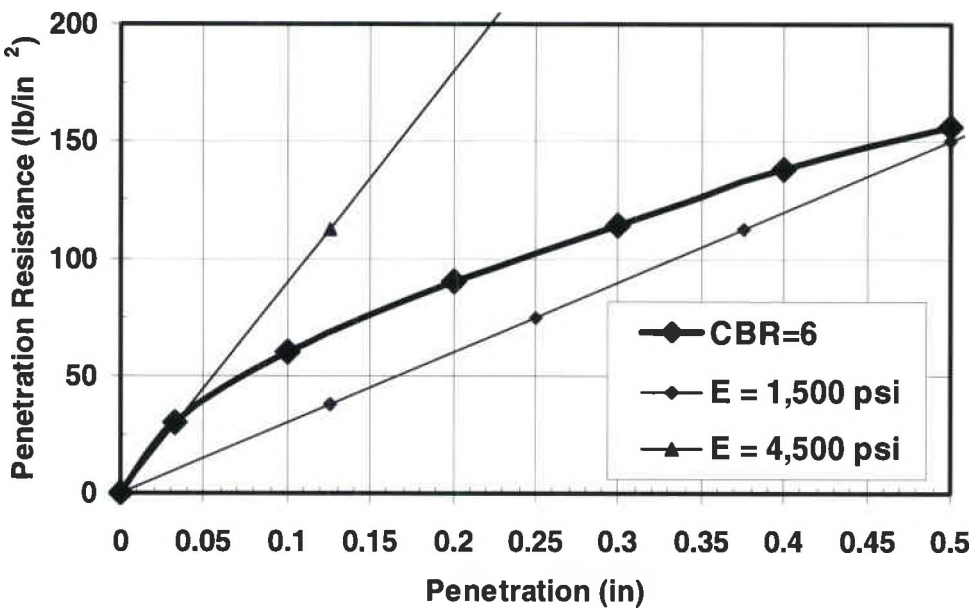

Figure 44 - Stress-Strain Response of Initial Moduli and Standard CBR 6

Frank (2006) created a finite element model using ABAQUS to represent the ASTM D1883 California Bearing Ratio laboratory testing configuration. The finite element model included the geometry of a confining mold, surcharge weight, piston, and the soil being dimensionally consistent with the standard test. Two types of materials were created in the finite element model named Metal and Soil. The Metal material model consisted of an isotropic linear elastic function where the variables were input as Young's Modulus of 29,000,000 psi and Poisson's ratio of 0.3. The Soil material model was defined via the elastic and plastic components of the ABAQUS Extended Modified Cam Clay (MCC) Model discussed previously. This finite element model was able to simulate the piston penetration as prescribed by the ASTM Standard and produce tabular incremental records of the penetration resistance and penetration depth.

Using this model, various configurations of the input parameters were iterated to produce individual CBR plots for each increment. By systematically iterating and observing the resulting graphical trends the model was able to be calibrated to mirror the Standard CBR 6 response curve. A total of 26 calibration iterations were required to produce the calibrated parameters and the resulting finite element stress-strain plots are reproduced in Table 12 and Figure 45, respectively.

Table 12 - Calibrated Parameters for Modified Cam Clay CBR 6 Soil Model

Variable	Initial Value	Calibrated Value
Kappa (κ) (1/psi)	0.045	0.03
Nu (v)	0.3	0.27
P_t(el) (psi)	0	0
e_0	0.92	0.92
P_0 (psi)	-1.0	-3.0
Lambda (λ) (1/psi)	0.154	0.19
M	1.02	0.9
e_1	1.61	1.61
β	1.0	1.0
Kf	1.0	1.0

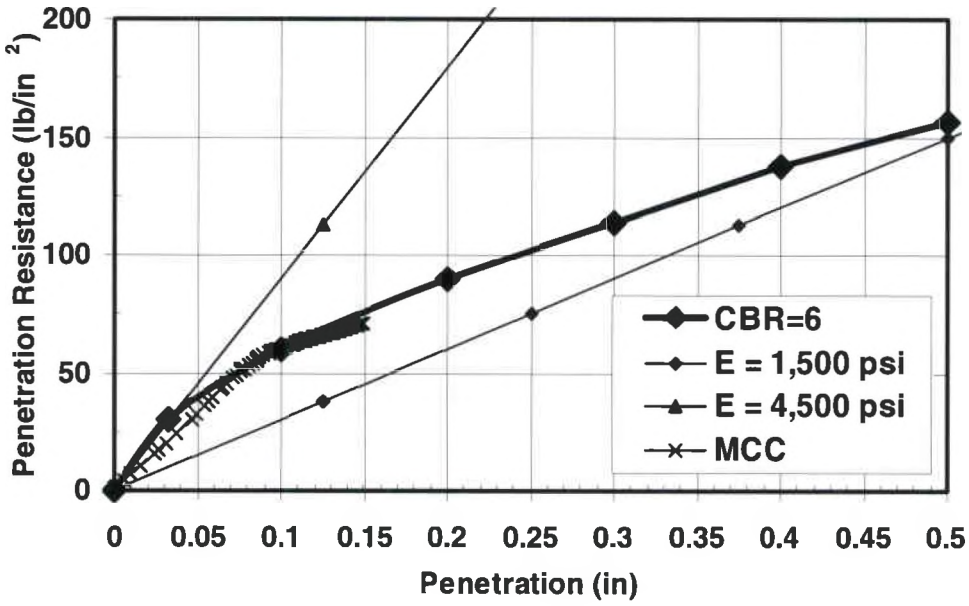

Figure 45 - Finite Element Stress-Strain Response Including Modified Cam Clay (Modified from Frank 2006)

The calibrated MCC model provides a nonlinear stress-strain response that more accurately represents the Standardized CBR 6 curve. It should be noted that the MCC finite element model has not been extrapolated to a full penetration of 0.5 inches. This is due to numerical limitations in the ABAQUS CBR finite

element model file. Additional finite element modeling may be warranted to confirm that the MCC model will indeed accurately represent these further strains. However, given the general linear trend of the CBR 6 curve beyond 0.15 inches of penetration and observing the correlating linear trend in the finite element model, it can be reasoned that the Modified Cam Clay model will continue along a similar trend.

4.4.3 Field Testing of Prototype Composite Airfield Matting Panel

In May 2006, field testing was performed to evaluate the performance of the airfield matting system under true aircraft traffic loading conditions. Prototype fabricated composite airfield mats were assembled over subgrade soils that had been compacted to a CBR of 6. Earth pressure cells were placed within the compacted subgrade at depths of 15 and 30 inches below top-of-subgrade elevation. Sufficient panels were placed so that the panel being tested could be placed at an "interior" location, thus negating the effects of any perimeter panel eccentric loading. Figure 46 shows the panel arrangement and finite element mesh used in the analysis. A uniaxial cart was attached to the front of a four-wheeled construction vehicle. The cart was loaded with 35,235 pounds to simulate the weight on a F-15 jet main gear wheel. A single F-15 jet wheel was used to support the cart, and was pressurized to 350 psi . The construction vehicle pushed the loaded cart back and forth over the instrumented composite airfield mat, passing directly over the centerline, 12 inches left of the centerline,

and 24 inches left of the centerline. The results of the soil pressure cell readings as a function of time are presented in Figure 47.

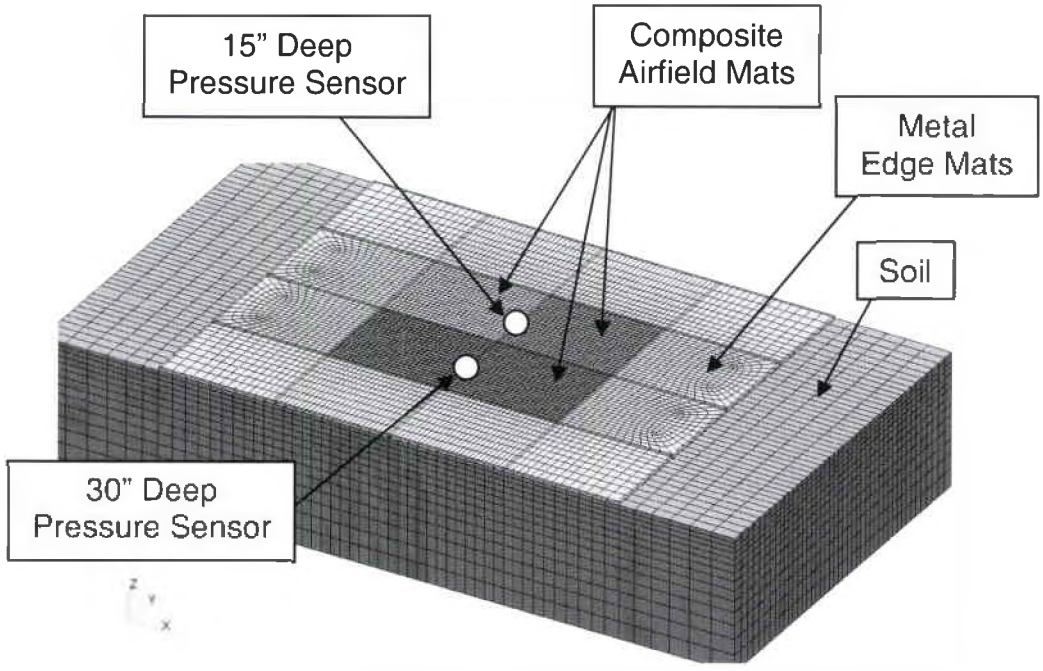

Figure 46 – Panel Arrangement and Finite Element Mesh (Source: Frank 2006)

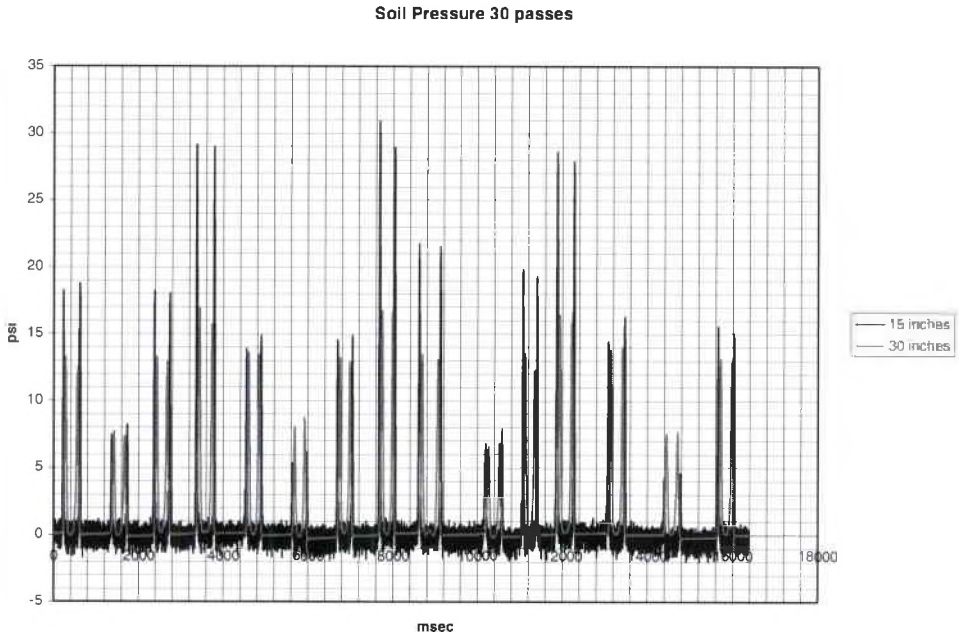

Figure 47 - Load Cell Output (Source: Frank 2006)

4.4.4 Evaluation of Model Parameter Performance in Comparison to Field Test Results

From the load cell data produced in the field tests, the maximum soil stress increase at depths of 15 and 30 inches was evaluated for the loading conditions of 0, 12, and 24 inches measured from the centerline as approximately 29, 17, and 6 psi for the 15 inch deep sensor and 11, 9, and 6 psi for the 30 inch deep sensor (Frank 2006). These values were used as benchmarks to evaluate the performance of the various input soil models, and specifically the calibrated ABAQUS Extended Modified Cam Clay finite element model. The finite element model of the field testing configuration was processed for each of the finite element soil models.

Three types of soil models were tested to evaluate their respective performance: linear elastic, elastic-plastic, and ABAQUS Extended Modified Cam Clay. The linear elastic model is the simplest and represents Hooke's law. In this model the elastic modulus of 1,500 psi and Poisson's ratio of 0.3 were derived by Frank and Whitney (2005) from the literature as described previously. The elastic-plastic model is similar to the Mohr-Coulomb model and incorporates a yield stress and subsequent plastic deformation. Arbitrary values for the input parameters were back calculated by Frank and Whitney from the field testing data. An initial elastic modulus of 8,000 psi was selected based on Equation 2, Poisson's ratio

was maintained at 0.3, and the yield stress of 7.5 psi was calibrated by iterating finite element model solutions to match the field test results. The ABAQUS Extended Modified Cam Clay model is by far the most complex, with parameters derived as discussed in this study. Figures 49 to 54 provided at the end of this section were developed by Frank (2006) to evaluate the input finite element soil models. Table 13 as adopted from Frank (2006) summarizes the findings.

Table 13 - Comparative Soil Model Accuracy – First Iteration

	Percent Error for Each Load Case (%)		
Load Cell Depth - Location	**Linear Elastic E=1,500 psi, v=0.3**	**Elastic-Plastic E=8,000 psi, v=0.3, Yield Stress=7.5 psi**	**Modified Cam Clay per Section 4.4.2**
15" – Centerline (CL)	-14%	-14%	-34%
15" – 12" off CL	-15%	1%	-33%
15" – 24" off CL	-5%	22%	-15%
30" – CL	-34%	-23%	-48%
30" – 12" off CL	-31%	-18%	-44%
30" – 24" off CL	-24%	-17%	-33%
Average Error[1]	**23%**	**17%**	**36%**

[1] Calculated by quadratic mean method.

A review of the table shows that the best correlation was obtained by the elastic-plastic soil model utilizing a relatively high initial elastic modulus of 8,000 psi and a relatively low yield stress of 7.5 psi. By comparison, the Modified Cam Clay model established in Section 4.4.2 of this report shows nearly double the percent error as compared to the elastic-plastic model. Figure 48 compares the curves of the elastic-plastic soil material model and Modified Cam Clay soil material model within the CBR finite element model.

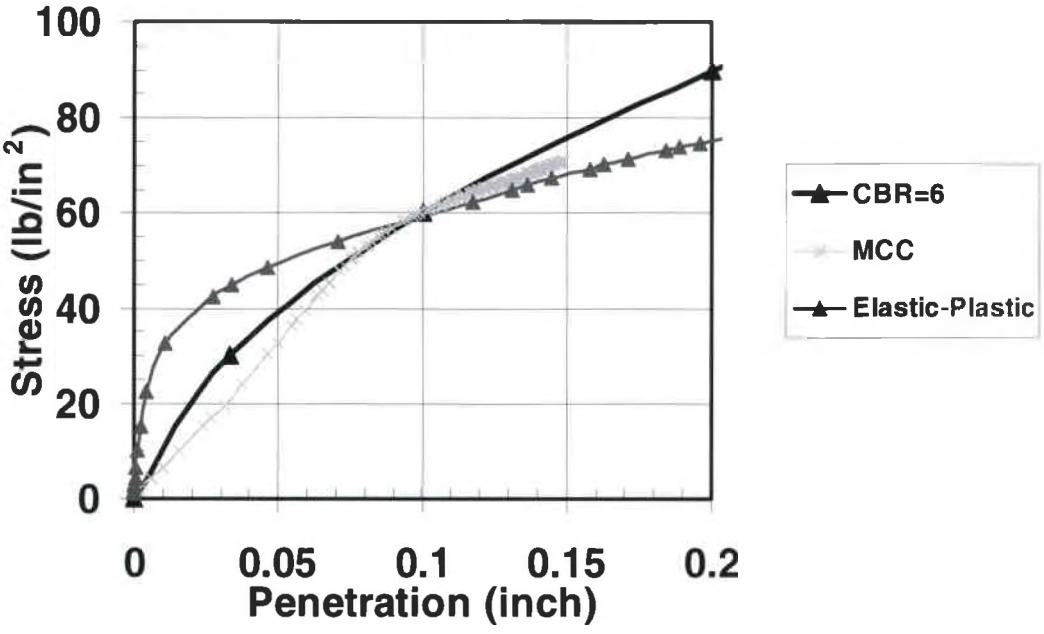

Figure 48 - Comparison of CBR Curves for Two Soil Material Models

A review of the finite element output reveals that the initial elastic modulus of the Modified Cam Clay model calibrated to CBR 6 is approximately 600 psi. As mentioned previously, it was anticipated by Whitney and Frank (2005) that much of the finite element model response would be in the elastic range, with a plastic response found only very near to the applied load. This statement, if assumed true, would account for the impact of the significant difference in the initial moduli between the elastic-plastic and Modified Cam Clay models. Also, a review of the CBR testing performed in this study, while completed at different moisture contents, shows a relatively high initial moduli response in both curves. This provides insight into the probable curve shape in Figure 48.

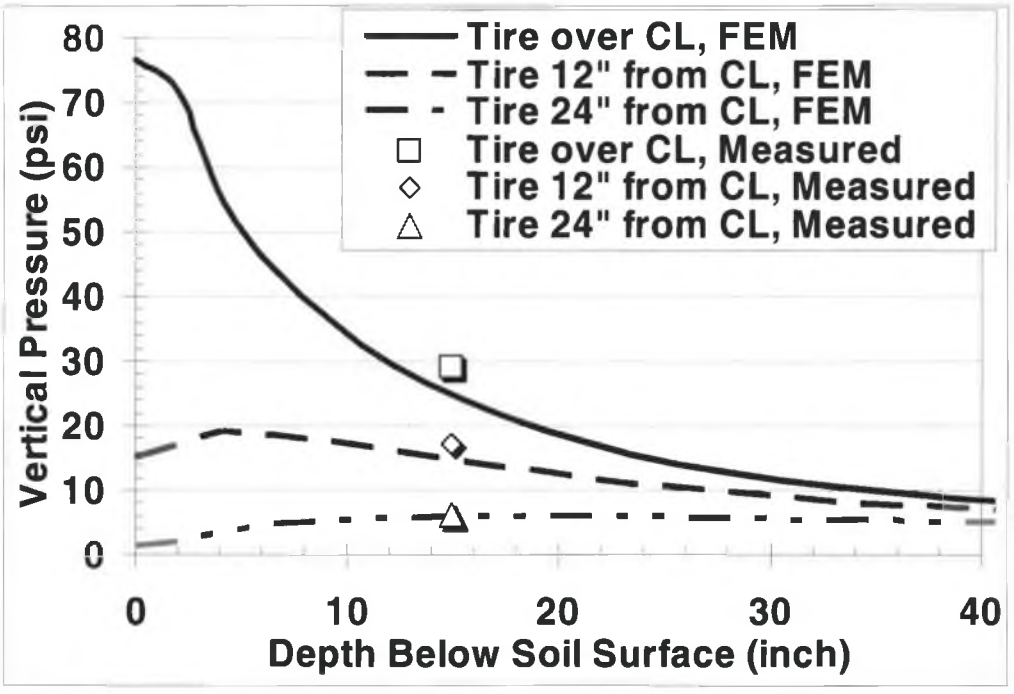

Figure 49 - Linear Elastic Soil Model for Load Cell at 15 Inch Depth, E=1,500 psi, v=0.3 (Source: Frank 2006)

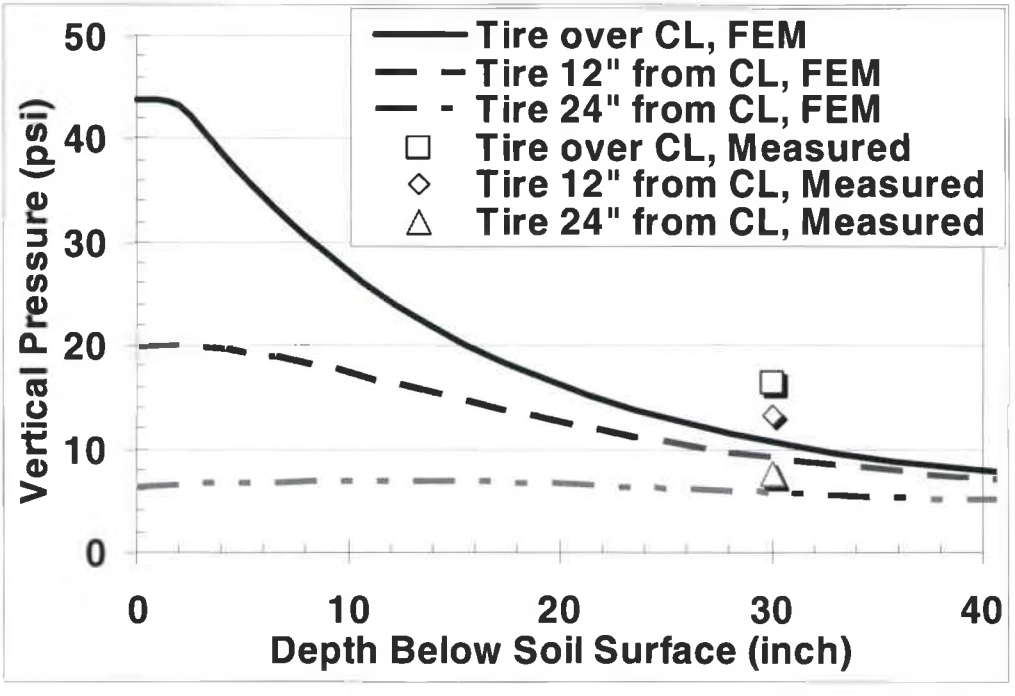

Figure 50 - Linear Elastic Soil Model for Load Cell at 30 Inch Depth, E=1,500 psi, v=0.3 (Source: Frank 2006)

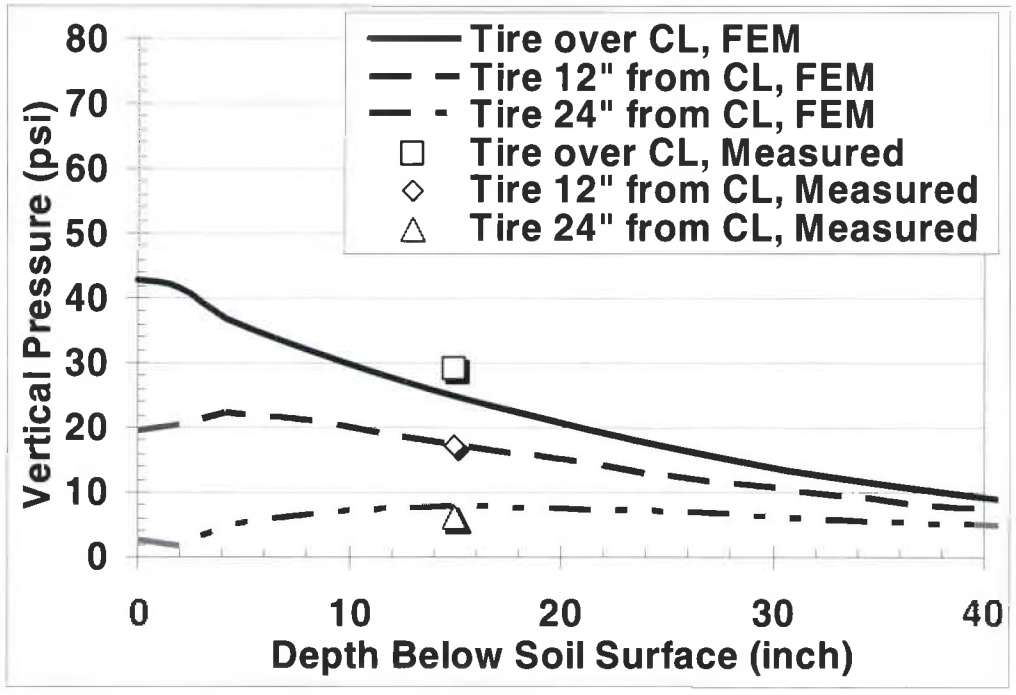

Figure 51 - Elastic-Plastic Soil Model for Load Cell at 15 Inch Depth, E=8,000 psi, v=0.3, Yield Stress = 7.5 psi (Source: Frank 2006)

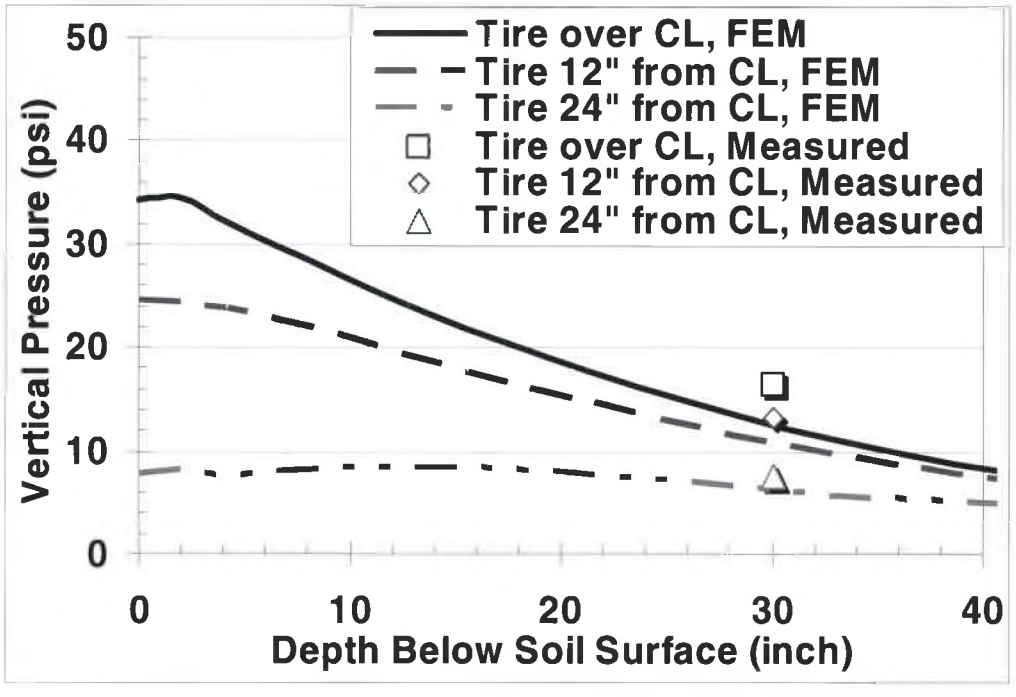

Figure 52 - Elastic-Plastic Soil Model for Load Cell at 30 Inch Depth, E=8,000 psi, v=0.3, Yield Stress = 7.5 psi (Source: Frank 2006)

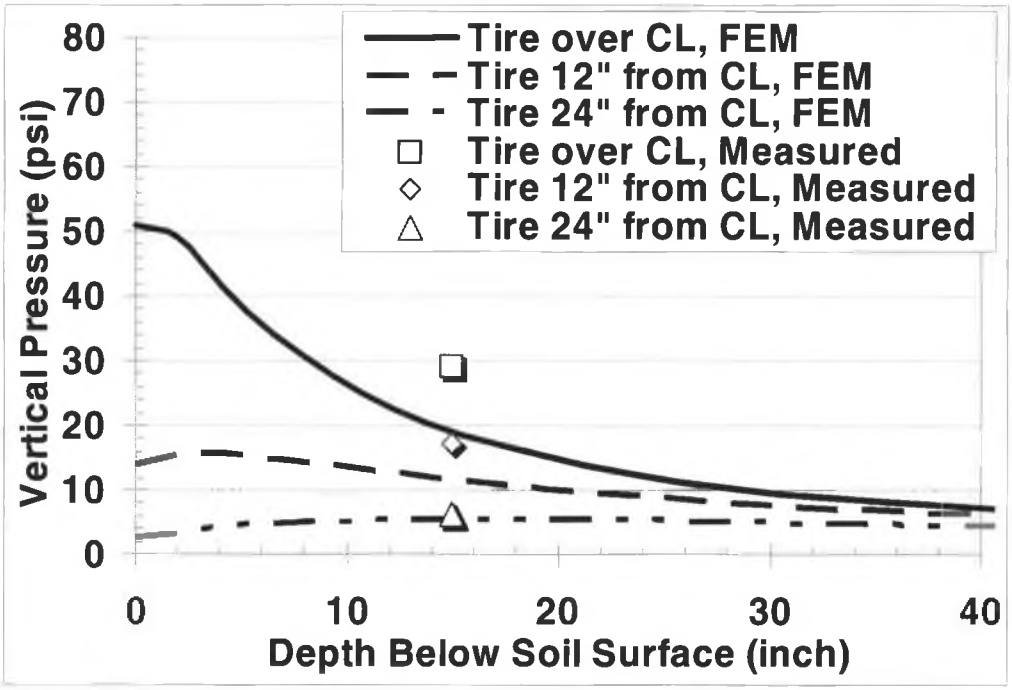

Figure 53 - Modified Cam Clay Soil Model for Load Cell at 15 Inch Depth with Parameters Provided in Section 4.4.2 (Source: Frank 2006)

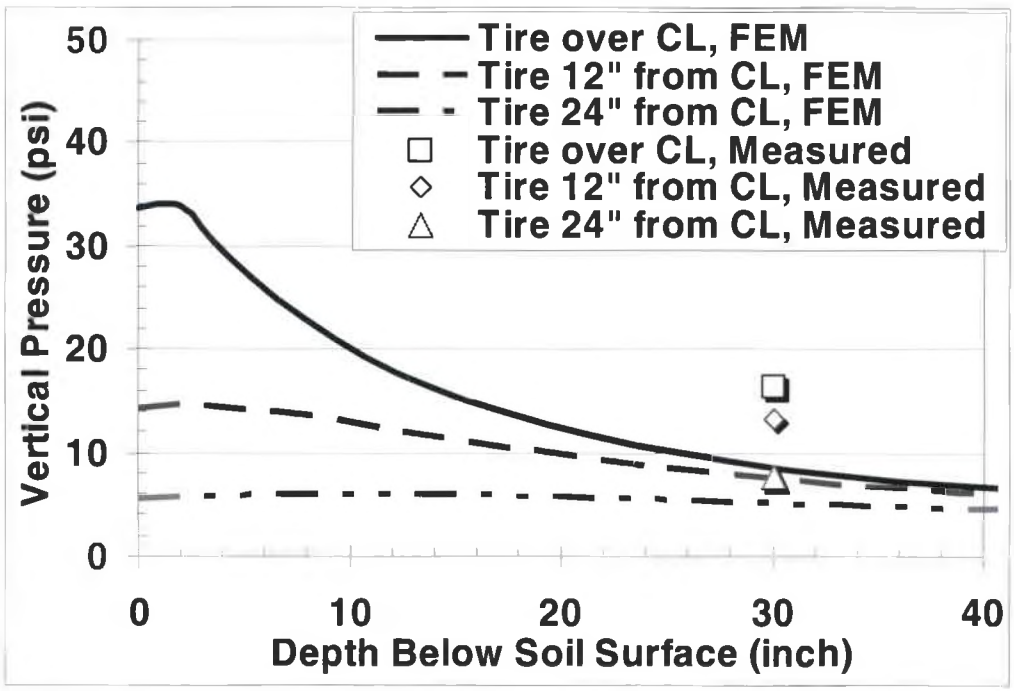

Figure 54 - Modified Cam Clay Soil Model for Load Cell at 30 Inch Depth with Parameters Provided in Section 4.4.2 (Source: Frank 2006)

The following are a list of considerations for evaluation of the first round of calibration of the ABAQUS Extended Modified Cam Clay soil model performance:

- The Modified Cam Clay soil model was calibrated in this iteration using the laboratory-derived soil parameters to produce a CBR 6 stress-strain curve from a finite element analysis of the CBR testing apparatus. While a standard CBR 100 curve is provided in ASTM D1883, this curve does not define the required shape of the CBR curve in testing soils. The definition of a CBR 6 soil is one that produces a stress resistance of 60 psi at 0.1 inch penetration within a standardized apparatus. The shape of the curve at strains less and/or greater than those that produce the 0.1 inch penetration are irrelevant to the soil testing, so long as a consistent soil response is obtained over a series of tests. As such, the field testing in this study has proven false the assumption that the Vicksburg clay soil at CBR 6 will mirror a scaled ASTM Standard CBR 100 curve. The CBR testing performed in this study, while completed at different moisture contents, shows a relatively high initial moduli response in both curves. As described earlier, this provides insight into the probable curve shape.
- A majority of the finite element soil nodal responses for the airfield matting simulation were in the elastic region, and thereby governed by the input elastic soil modulus within each model. As shown in Figure 48, the initial elastic modulus of the elastic-plastic model was over 13 times greater than that of the Modified Cam Clay model.

- Equation 2 calculates an initial elastic modulus of approximately 8,000psi, as employed by Frank (2006). This is much greater than the value derived by the Modified Cam Clay model, and can likely be attributed to pore water pressure effects. Given the highly-impermeable nature of the Buckshot clay, as evidenced repeatedly in the laboratory testing performed for this study, near-instant loading and unloading as is the characteristic of a moving wheel load will be transferred proportionally more by the pore fluid than the soil particle matrix.
- The moisture content of the soil subgrade compacted for the field study is unknown, but likely to be on the order of 35 to 40 percent to produce a CBR of 6. This pore fluid is incompressible, and upon rapid loading is unable to move freely within the soil matrix. Strain compatibility will also play a role, in that the incompressible water will take a greater proportion of the induced stress in comparison to the highly-compressible clay particles. As a result of the confinement and strain compatibility considerations for the 35 to 40 percent moisture in the matrix, the pore fluid pressures will build quickly when loaded and provide an immediate apparent higher soil elastic response than expected. If the load duration were longer the soil would experience a reduction in elastic response as the pore fluid pressures were slowly dissipated.
- All laboratory triaxial shear tests were performed at a shear rate of 0.0004 to 0.0005 inches per minute, as is required for the determination of the

shear strength parameters. This strain rate, however, is many orders of magnitude less than that imposed during tire loading.

- The soil pressure cells in the field tests were placed at depths of 15 and 30 inches below grade in the middle of the mat. Conventional geotechnical knowledge will intuit that at these depths mainly elastic stress states will be induced. The majority of the soil plastic deformation responses, namely rutting, will occur away from the locations of surface rutting and likely immediately below the matting at the joint locations. The Modified Cam Clay model derived in this study is better formulated than the others to handle the response characteristics in regions such as these where elastic and plastic stress states are occurring close together. Should the field testing have been fitted with gauges at more shallow depths near the joint locations the stress-strain response of the Modified Cam Clay model may have outperformed the others.

4.4.5 Second Calibration to Field Test Results

In light of the considerations presented previously, a second round of calibration was undertaken to attempt to more closely align the Modified Cam Clay model to the stress-strain responses measured in the field testing. The calibration procedure was the same as that outlined in Section 4.4.2. The intent of this round of calibration was to more closely align the initial elastic moduli with those of the elastic-plastic model that was found to have the least magnitude of error.

The model was calibrated to the parameters shown in Table 14. Only two variables were changed during calibration, kappa (κ) and lambda (λ).

Table 14 - Calibrated Parameters for Modified Cam Clay CBR 6 Soil Model

Variable	Initial Value	Calibrated Value
Kappa (κ) (1/psi)	0.045	0.005
Nu (ν)	0.3	0.27
P_t(el) (psi)	0	0
e_0	0.92	0.92
P_0 (psi)	-1.0	-3.0
Lambda (λ) (1/psi)	0.154	0.21
M	1.02	0.9
e_1	1.61	1.61
β	1.0	1.0
K	1.0	1.0

Lambda was modified very minimally from 0.19 to 0.21. Kappa, however, was modified from 0.03 to 0.005, an order of magnitude variation. Kappa is the logarithmic bulk modulus, which defines the slope of the elastic unload-reload line and governs the elastic response behavior in the Modified Cam Clay model. If Equation 7 is reevaluated by multiplying by the natural log of 10, and it is assumed that the void ratios will not be affected by the rate of loading, we find that the values of the kappa and subsequently C_s are governed by the order of magnitude of the pressure difference acting on the specimen for a given slope evaluation, i.e. $p_2 - p_1$. Thus to produce kappa equals 0.005, which represents the second round of calibration, the denominator of Equation 7 will be required to be 5.75 times greater than the denominator that produced kappa equals 0.03 in the originally-calibrated set of Modified Cam Clay parameters. In terms of true

physical response, this implies that a greater change in stress is required to cause the same change in void ratio. Since a change in soil void ratio can be related to a net volume change, the relationship between void ratio and stress can be described in terms of stiffness. As discussed earlier, the increased stiffness observed in the field testing is likely due to pore water pressure effects whereby the increased stiffness under rapid loading is a function of incompressible pore fluids being confined by the impermeability of the soil.

A second set of finite element analyses of the airfield matting field tests were performed by Frank (2006) to evaluate the response of the revised Modified Cam Clay model parameters. The revised parameters produced the most accurate soil response of any soil model produced to date for the project with an averaged discrepancy to the field tests results of 15 percent. Table 15 adapted from Frank (2006) provides a comparison of the soil model accuracy of the elastic-plastic, preliminary Modified Cam Clay, and revised Modified Cam Clay in comparison to the field test results. Figure 55 compares the curves of the elastic-plastic soil material model and the second iteration Modified Cam Clay soil material model within the CBR finite element model. Figures 56 and 57 display the measured load cell responses with respect to the finite element model responses for the revised Modified Cam Clay parameters.

Table 15 - Comparative Soil Model Accuracy – Second Iteration

	Percent Error for Each Load Case (%)		
Load Cell Depth - Location	**Elastic-Plastic E=8,000 psi, v=0.3, Yield Stress=7.5 psi**	**Modified Cam Clay per Section 4.4.2**	**Revised Modified Cam Clay per Section 4.4.6**
15" – Centerline (CL)	-14%	-34%	-10%
15" – 12" off CL	1%	-33%	7%
15" – 24" off CL	22%	-15%	-16%
30" – CL	-23%	-48%	-18%
30" – 12" off CL	-18%	-44%	-17%
30" – 24" off CL	-17%	-33%	-19%
Average Error[1]	**17%**	**36%**	**15%**

[1] Calculated by quadratic mean method.

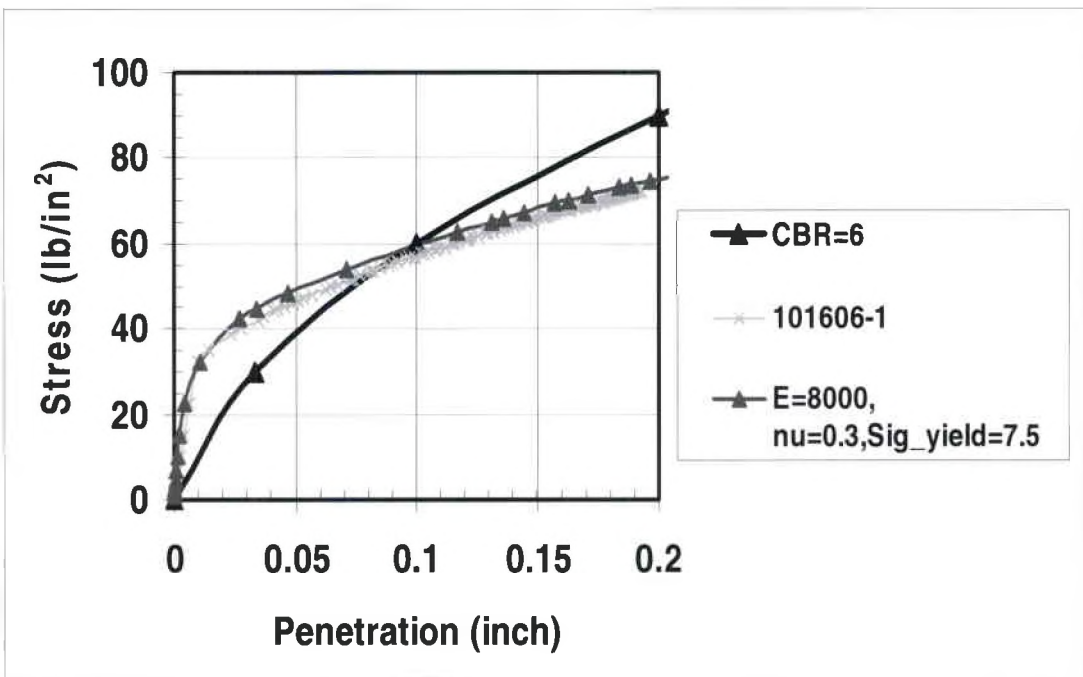

Figure 55 - Comparison of CBR Curves for Second Iteration Soil Material Models

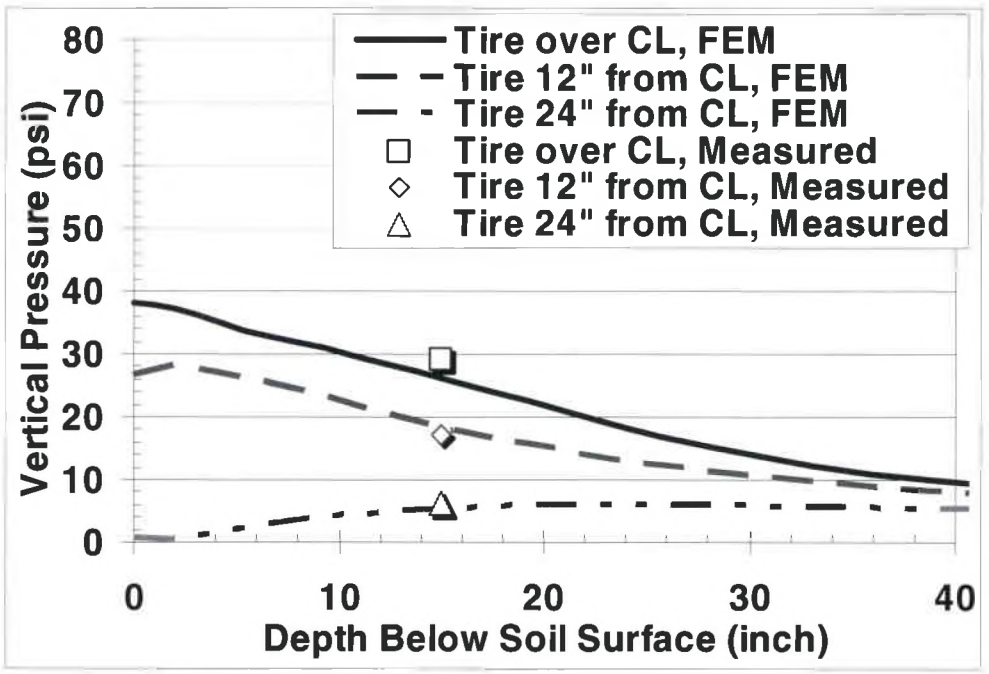

Figure 56 - Modified Cam Clay Soil Model for Load Cell at 15 Inch Depth with Parameters Provided in Section 4.4.5 (Source: Frank 2006)

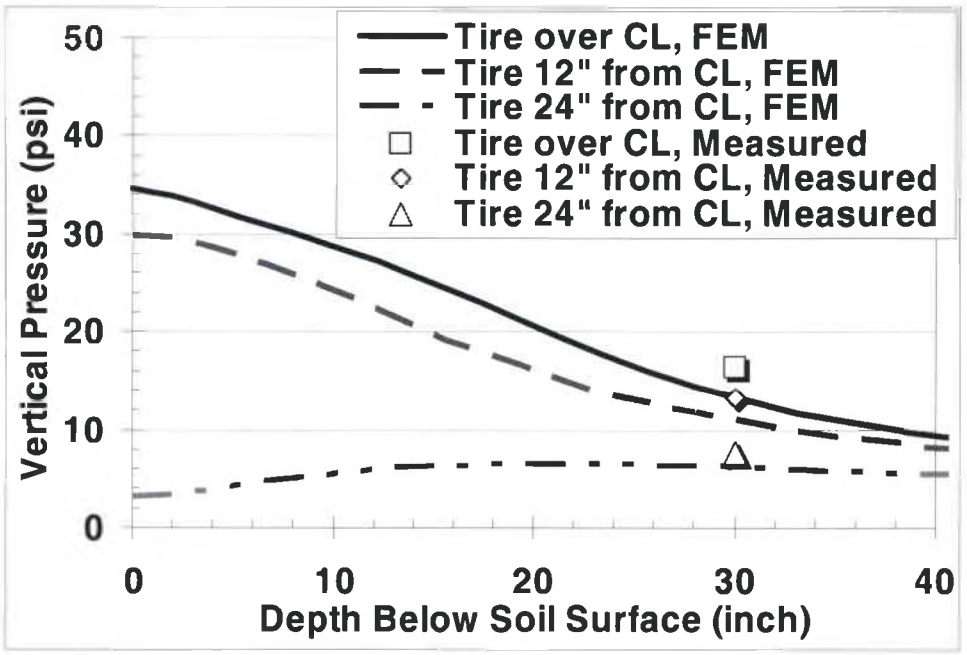

Figure 57 - Modified Cam Clay Soil Model for Load Cell at 30 Inch Depth with Parameters Provided in Section 4.4.5 (Source: Frank 2006)

CHAPTER 5 – CONCLUSIONS AND RECOMMENDATIONS

5.1 Summary of Findings

The University of Dayton Research Institute (UDRI) has been retained by the Structural Materials Branch of the Air Force Research Laboratory's Materials and Manufacturing Directorate (AFRL/MLBC) to employ finite element analysis methods to study concept alternatives and systems designs to replace the current AM-2 Matting System. This study was performed to establish an effective and economical constitutive soil model for use in the matting finite element analyses.

The directive of the Air Force was to provide a constitutive model that represented clay soil with a California Bearing Ratio of 6. To facilitate correlation to field testing results, Vicksburg Buckshot clay was selected as the soil to be modeled. A literature review of constitutive soil mechanics was performed to establish appropriate modeling criteria and to evaluate several alternative constitutive soil models. The Modified Cam Clay constitutive soil model, based upon the work of researchers at Cambridge University in the 1960s and extended by the ABAQUS finite element analysis software, was selected as the most appropriate soil model for this application. The Modified Cam Clay model is a

work-hardening elastic-plastic model appropriate for applications of near-normally consolidated cohesive soils similar to the Buckshot clay soil designated for this study.

A series of laboratory tests were performed for the dual purpose of correlating the Buckshot clay provided in this study to historical Army Corp of Engineers Buckshot clay data and to fill gaps in the existing Buckshot clay material property database. Soil classification, consolidation, California Bearing Ratio, and consolidated-undrained triaxial testing was performed and the results successfully correlated to the existing Buckshot clay data in the literature. The findings of the laboratory testing were used to derive initial values of expected Modified Cam Clay model input parameters. Using the ABAQUS finite element analysis software and the expected initial input parameters as evaluated from the laboratory testing, a finite element model of the California Bearing Ratio testing apparatus was employed to calibrate the Modified Cam Clay constitutive soil model to represent the ASTM Standard CBR 6 curve. The resulting calibrated parameters were evaluated by comparing soil load cell response characteristics of field testing of prototype airfield matting with CBR 6 Buckshot clay subgrade to the numerical results of a finite element model of the field testing setup. It was determined that while the calibrated parameters successfully modeled the ASTM Standard CBR 6 curve, they did not successfully incorporate the increased initial soil stiffness that was a result of the pore pressure response of high-moisture and relatively-impermeable cohesive soils like Buckshot clay. To improve model

accuracy, a second calibration was undertaken to increase the initial elastic moduli. It was required to significantly stiffen the elastic response characteristics of the model, which resulted in one input parameter being modified by an order of magnitude. The remaining model parameters, however, were not required to be modified. The findings of this calibration were again evaluated in comparison to the airfield matting field testing and were found to most successfully represent the CBR 6 Buckshot clay soil response in comparison to all other available models.

5.2 Avenues of Further Research

This study has successfully defined the parameters for an appropriate finite element Modified Cam Clay soil constitutive soil model. In order to complement the findings of this study, several proposed avenues of further research are presented:

- The pore fluid response was determined to be a key governing factor in the performance of the calibrated Modified Cam Clay model. Additional triaxial testing at a high rate of strain similar to that imposed by the tire loading of the airfield matting system would aid in the evaluation of appropriate parameters and calibration of the model, most specifically the pore pressure response.

- This study was evaluated based upon a comparison of the load cell data from field testing to a finite element model of the testing arrangement. The load cells were placed at depths of 15 and 30 inches below grade along the centerline of the matting and were monitored as the loaded tire passed at varying distances from the centerline. It was found that a majority of the soil behavior was elastic in nature given the decreasing stress and strain as the distance from the soil surface increased. Additional field and laboratory testing of the soil-structure interaction near the interface of the soil and mat would show higher stresses and strains, likely including rutting behavior at the joints. This study and the airfield matting studies to date have provided a global evaluation of the matting performance. Upon selection of an appropriate prototype, additional study, field testing, and finite element modeling of the soil-structure interface and the rutting behavior at the joints would serve to add to the depth of analysis of this study.

WORKS CITED

AASHTO. (1993). "Guide for design of pavement structures." American Association of State Highway and Transportation Officials, Washington, D.C.

ABAQUS/CAE Version 6.5-3. 2005. "Analysis user's manual." Documentation packaged with software. ABAQUS, Inc.

ABAQUS/CAE Version 6.5-3. 2005. "Analysis theory manual." Documentation packaged with software. ABAQUS, Inc.

ABAQUS/CAE Version 6.5-3. 2005. Analysis benchmarks manual." Documentation packaged with software. ABAQUS, Inc.

Arduino, P., and Emir Jose Macari. 1995. "Overview of state-of-the-practice modeling of overconsolidated soils." *Transportation Research Record*, no. 1479:51-60.

American Society for Testing and Materials. 2005. Annual Book of ASTM Standards 2005: Section Four – Construction. Vol. 04.08, *Soil and Rock (I): D420 – D5611.* West Conshoshocken: ASTM International.

Berney, Ernest S. 2004. "A partially saturated constitutive theory for compacted fills." Vicksburg: United States Army Engineering Research and Development Center Geotechnical and Structures Laboratory. ERDC/GSL TR-04-4.

Brinkgreve, R. 2005. "Selection of soil models and parameters for geotechnical engineering application." In *Soil Constitutive Models: Evaluation, Selection, and Calibration: Proceedings of Geo-Frontier Conference held in Austin Austin, Texas 24-26 January, 2005*, edited by J. Yamamuro and V. Kaliakin. Reston: ASCE Geo Institute.

Coulomb, C. 1776. "Essai sur une application des regles de maximis et minimis a quelques problemes de statique relatifs a l'archetecture." In *Selection of soil models and parameters for geotechnical engineering application* by R. Brinkgreve, 69-70. Reston: ASCE Geo Institute.

Das, Braja M. 2000. Fundamentals of Geotechnical Engineering. Massachusetts: Brooks/Cole Thompson Learning.

Drucker, D.C. and W. Prager. 1952. "Soil mechanics and plastic analysis or limit design." *Quarterly of Applied Mathematics*, vol. 10, no. 2:157-165.

Duncan, J. and C.Y. Chang. 1970. "Nonlinear Analysis of Stress and Strain in Soils." *Journal of the Soil Mechanics and Foundations Division*, ASCE:1629-1653.

Fisher, J., R. Hartzer, and J. Pratt. 2005. "Ramping up for AM-2's replacement." *Air Force Civil Engineer* magazine, vol. 13, no. 3:10-11.

Frank, G. 2006. Electronic correspondence and collaborative meetings, April through November.

Freeman, R.B., E. Velez, L. Mason, and H. Carr. 2004. "Airfield pavement test section with high repetition traffic," *draft technical report*. Vicksburg: United States Army Engineering Research and Development Center Geotechnical and Structures Laboratory.

Foster, D. and Anderson, M. 2003. "Rapid forward deployment made easier with composite airfield matting." *Advanced Materials and Process Technology Information Analysis Center (AMPTIAC) Quartlery* magazine, vol. 7, no. 1:17-22.

Krahn, J. and P. Barbour. 2006. "The purpose of numerical modeling." *Geo-Strata magazine*, July/August, 12-14.

Heukelom, W. and C. Foster. 1960. "Dynamic Testing of Pavements," *Journal of Soil Mechanics and Foundation Engineering*, vol. 86, no. 1:1-28.

Holtz, R.D. and W.D. Kovacs. 1981. An Introduction to Geotechnical Engineering. New Jersey: Prentice-Hall.

Johnson, D. and G. Frank. 2006. "Analysis of Airfield Matting Systems Designs." *Draft technical report*. Dayton: University of Dayton Research Institute, UDR-TR-2006-00106.

Joint Departments of the Army and Air Force, USA. 1983. Technical Manual TM 5-818-1 / AFM 88-3, Chapter 7, *Soils and Geology Procedures for Foundation Design of Buildings and Other Structures (Except Hydraulic Structures)*.

Lade, Poul V. 2005. "Overview of constitutive models for soils." In *Soil Constitutive Models: Evaluation, Selection, and Calibration: Proceedings*

of Geo-Frontiers Conference held in Austin Austin, Texas 24-26 January, 2005, edited by J. Yamamuro and V. Kaliakin. Reston: ASCE Geo Institute.

Liu, C. and J. Evett. 2003. Soil Properties: Testing, Measurement, and Evaluation 5th Edition. Columbus: Prentice-Hall.

Naval Air Engineering. 2003 "AM2 Airfield Mat and Accessories: Installation, Maintenance, Repackaging, And Illustrated Parts Breakdown." NAVAIR 51-60A-1.

Naval Air Engineering Station – Lakehurst. *Expeditionary Airfield (EAF) History*. 2006. Available at http://www.lakehurst.navy.mil/nlweb/EAF/ dynamic-template01.asp?URLToGet=history-include.htm (Accessed 10/20/06).

Peters, J., and D. Leavell. 1982. "Analysis of strain softening behavior of soil." Vicksburg: United States Army Engineering Research and Development Center Geotechnical and Structures Laboratory.

Peterson, R. 1990. "The influence of soil structure on the shear strength of unsaturated soil," *Miscellaneous Paper GL-90-17*. Vicksburg: United States Army Engineering Research and Development Center Geotechnical and Structures Laboratory.

Potts, D. and Z. Lidija. 2000. "Some pitfalls when using modified cam clay." In *Avdelas, A.,* edited by Soil-Structure Interaction in Civil Engineering, European Commission.

Prevost, J. and R. Popescu. 1996. "Constitutive Relations for Soil Materials." *Electronic Journal of Geotechnical Engineering*, November.

Roscoe, K.H. and J.B. Burland. 1968. "On the generalized stress-strain behavior of 'wet' clay." *Engineering Plasticity*. Cambridge: Cambridge University Press, 535-609.

Roscoe, K.H., A.N. Schofield, and C.P. Wroth. 1958. "On the yielding of soils." *Geotechnique*, vol. 8, no. 1:22-53.

Roscoe, K.H., A.N. Schofield, and A. Thurairajah. 1963. "Yielding of clays in states wetter than critical." *Geotechnique*, vol. 8, no. 1:211-240.

Schofield, A. and P. Wroth. 1968. Critical State Soil Mechanics. London: McGraw-Hill. Available at http://www.geotechnique.info/.

Smith, I. and D. Griffith. 1982. Programming the Finite Element Method 2nd edition. J. Wiley and Sons.

Smith, B. R. and W. S. Sanders. 2005. "Translating strategic vision into tactical implementation: interpretive vs. analytical thought in AFRL technology development." *Defense AT&L* magazine, vol. 35, no. 3:42-45.

Tingle, J. 2006. Phone call and follow-up electronic correspondence from Jeb Tingle to Brad Doudican, 16 June.

U.S. Army Corps of Engineers. 1990. *Engineering and Design Settlement Analysis*. Engineer Manual EM 1110-1-1904, Washington D.C.

Whitney, T. and G. Frank. 2005. "Analysis of Concepts for Airfield Matting Systems." Dayton: University of Dayton Research Institute, UDR-TR-2005-00108.

Whittle, A. J. and M. J. Kavvadas. 1994. "Formulation of MIT-E3 Constitutive Model for Overconsolidated Clays." *Journal of Geotechnical Engineering*, vol. 120, no. 1:173-198.

Wood, D. M. 2004. Geotechnical Modelling. New York: Spon Press.

Wood, D. M. 1990. Soil Behavior and Critical State Soil Mechanics. New York: Cambridge University Press.